

Environmental Effects on Late-Type Galaxies in Nearby Clusters

Alessandro Boselli¹

alessandro.boselli@oamp.fr

Laboratoire d'Astrophysique de Marseille, BP-8, Traverse du Siphon, F-13376 Marseille, France

Giuseppe Gavazzi²

giuseppe.gavazzi@mib.infn.it

Universit degli studi di Milano-Bicocca, Piazza delle scienze 3, 20126 Milano, Italy

ABSTRACT

The transformations taking place in late-type galaxies in the environment of rich clusters of galaxies at $z = 0$ are reviewed. From the handful of late-type galaxies that inhabit local clusters, whether they were formed in-situ and survived as such, avoiding transformation or even destruction or if they are newcomers that recently infall from outside, we can learn an important lesson on the latest stages of galaxy evolution. We start by reviewing the observational scenario, covering the broadest possible stretch of the electromagnetic spectrum, from the gas tracers (radio and optical), the star formation tracers (UV and optical), the old star tracers (Near-IR) and the dust (Far-IR). Strong emphasis is given to the three nearby, well studied clusters Virgo, A1367 and Coma, representative of different evolutionary stages, from unrelaxed, spiral rich (Virgo) to relaxed, spiral poor clusters (Coma). We continue by providing a review of models of galaxy interactions relevant to clusters of galaxies. Prototypes of various mechanisms and processes are discussed and their typical time-scales are given in an Appendix. Observations indicate the presence of healthy late-type galaxies falling into nearby clusters individually or belonging to massive groups. More rare are infalling galaxies belonging to compact groups where significant pre-processing might take place. Once entered the cluster, they loose their gas and quench their star formation activity, becoming anemics. Observations and theory agree in indicating that the interaction with the intergalactic medium is responsible for the gas depletion. This process, however, cannot be at the origin of the cluster lenticular galaxy population. Physical and statistical properties of S0 in nearby clusters and at higher redshift, indicate that they originate from spiral galaxies transformed by gravitational interactions.

Subject headings: Galaxies: general, Galaxies: clusters: individual: Virgo, A1367, Coma

1. Introduction

On scales < 100 Mpc, the size of the largest known coherent matter aggregates, the density of galaxies in the local universe spans from $\sim 0.2 \rho_0$ in voids to $\sim 5 \rho_0$ in superclusters and filaments, $\sim 100 \rho_0$ in the cores of rich clusters, up to $\sim 1000 \rho_0$ in compact groups, where ρ_0 is the average “field” density (Geller & Huchra 1989).

It has been known for decades (Hubble & Humason 1931) that galaxy Hubble type and local density are not independent quantities. In their analysis of nearby clusters, Dressler (1980) and Whitmore et al. (1993) agreed that the fraction of spiral galaxies decreases from 80% in the “field”, to 60% in the outskirts to virtually zero in the cores of rich clusters, compensated by an opposite increase of elliptical and S0 galaxies. Morphological segregation is perhaps the clearest signature of the environmental dependence of the processes that govern the formation and evolution of galaxies. Understanding the morphology segregation, i.e. the shaping of the Hubble sequence in the various environments, has challenged astronomers for years: “Nature or Nurture”? The issue is still hotly debated, as it involves many controversial fields of modern astrophysics, including observations, simulations and theories.

With the advent of 10m class telescopes we hope that galaxy evolution will be shortly disclosed observationally, much as in a rewound movie taken along the “fossil” sequence, from today’s fully evolved nearby galaxies to the early objects forming their first stars far away in space and time. Similarly we can imagine to shoot the movie of the morphology segregation by comparing frames of clusters taken at increasingly large z . Snapshots at $z = 0$ would show the fully formed and evolved clusters with their final mix of E/S0/S. Frames taken between $z = 0.2$ and 0.5 would show an unchanged fraction of E, with the action focused on increasingly active spirals (the Butcher-Oemler effect (Butcher & Oemler 1978, 1984)) and a decreasing fraction of S0 (Dressler et al. 1997; Dressler 2004). By $z = 0.5 - 1$ the scene would be on clusters under formation, when large groups of galaxies coalesce. Effective “pre-processing” is taking place in these low velocity-dispersion environments, where minor merging and tidal interactions among galaxies are shaping up the S0s (Mihos 2004; Fujita 2004). None has yet observed elliptical galaxies under formation at $z = 3$ and beyond. But there is general consent that they should have formed at these early epochs, very much from “nature” and little from “nurture”, even before clusters existed (Dressler 2004; Treu 2004; Nolan 2004; Franx 2004). Maybe in a decade from now, when the JWST will provide these last photographs, the full movie of the shaping of the Hubble sequence will be on view, as many groups of researchers are focusing large efforts on it (the Morphs group (Dressler et al. 1999), the CNOC1 group (Yee et al. 1996), the ACSCS team (Postman et al. 1996), the EDisCS group (Halliday et al. 2004) and the team of van Dokkum and collaborators (van Dokkum et al. 2000)).

This is perhaps somewhat optimistic, however. Pretending to understand galaxy evolution really means shooting a movie whose individual photographs are composed of SEDs, obtained combining best quality data taken over a large stretch of the electromagnetic spectrum, each individual band providing information on the evolution of a particular galaxy component. Restframe UV fluxes and Balmer emission line strengths are the best current, massive star-formation tracers. Optical bands provide the morphology, NIR bands trace the oldest stars, MIR and FIR the dust (and extinction);

the radio (continuum) tells about the nuclear activity, the supernova rate and the magnetic fields, and the 21 cm line the primordial gas reservoir and its dynamics.

The problem is that, as z increases, characteristic features become unobservable or more difficult to observe. By $z = 1$, for example, the $H\alpha$ line ends up in the H band, a noisy place to carry out observations. The peak of the dust emission falls in the sub-mm bands where the sensitivity of telescopes will remain poor until ALMA. The 21 cm line drops to lower sensitivity and angular resolution bands where line correlators do not yet exist (we are not aware of a single HI emission measurement taken beyond $z=0.15$). Furthermore, the movie’s linear resolution decreases with z , so that detailed morphological information quickly fades away. Most dramatic is the lost of sensitivity with increasing z . By $z < 0.2$ dwarf galaxies run completely out of the scene. Meaningful, high-resolution SEDs in the whole luminosity range covered by galaxies are obtainable only at $z = 0$, providing the boundary conditions to models and simulations of galaxy evolution.

The end point of the evolution is within the reach of modern telescopes. Significantly less evolved galaxies can only be observed, with lower resolution, if they are more luminous. Dwarf galaxies, Ims, BCDs and dEs, by far the most common types of galaxies in the universe, yet the less understood, can only be observed locally.

Since the rate of evolution of galaxies is found to correlate primarily with their dynamical mass (infrared luminosity) according to a remarkably anti-hierarchical scheme (Gavazzi (1993); Gavazzi & Scodéggi (1996); Gavazzi et al. (1996); Boselli et al. (2001); Gavazzi et al. (2002a); Scodéggi et al. (2002a)) that has been lately named “downsizing”, distant surveys might undersample low-luminosity, slowly evolving systems. This is why studying nearby clusters still is a worthwhile activity.

Another pro of local clusters is that they are ideal laboratories for studying interaction mechanisms at high resolution. Prototypes of all relevant mechanisms can be found in nearby clusters. Abell 1367, for example, contains perhaps the best known example of currently ongoing ram-pressure stripping (CGCG 97-073), a rare example of a merging system in a cluster (UGC 6697) and even a local prototype of infalling group where pre-processing occurs at the present cosmological epoch (see Section 4.10). Infall was much more effective, but unfortunately hard to observe, in the past ($z \sim 0.5$), when it contributed shaping the S0 galaxies (pre-processing).

So far we insisted on the importance of observing nearby clusters. Among them we have focused the present review on three specific ones: Virgo, Abell 1367 and Coma that are among the best studied in the universe. The variety of their conditions, e.g. spiral fraction, X-ray luminosity, kinematic properties, makes them suitable “laboratories” for comparing clusters in different evolutionary stages: near formation (Virgo), still significantly accreting (A1367), near virialization (Coma).

Honestly speaking, the present review was conceived while we were assembling “GOLDmine”, the galaxy database that we made available on the WEB (goldmine.mib.infn.it) (Gavazzi et al. 2003a). Two third of the galaxies contained in GOLDmine belong in fact to these three clusters and a significant fraction of them are among the best sampled SEDs. This does not mean that we haven’t tried to review the work of other groups. Certainly we haven’t done it as extensively as we should, and we apologize for that.

But why focusing the present review on late-type galaxies, that are less numerous, they evolve slower than the more intriguing S0s and Es? What can we learn from the handful late-type galaxies that still inhabit local clusters? There are several reasons for concentrating on them. One is that, due to the fragility of their stellar and gaseous disks, they are sensitive probes of their environment. Another is that, since their rate of evolution (star formation history) is mild and continuous, they provide a linear clock for evolution, as opposed to E whose action occurred suddenly in one brief and intense episode that occurred early in their life. Spirals are also interesting because significant infall of galaxies of this type has occurred and is still occurring (at decreasing rate due to the Λ dominated universe) onto clusters of galaxies. Will they sooner or later evolve into lenticulars? Can we use them as probes of the cluster environment? To help better focusing the addressed

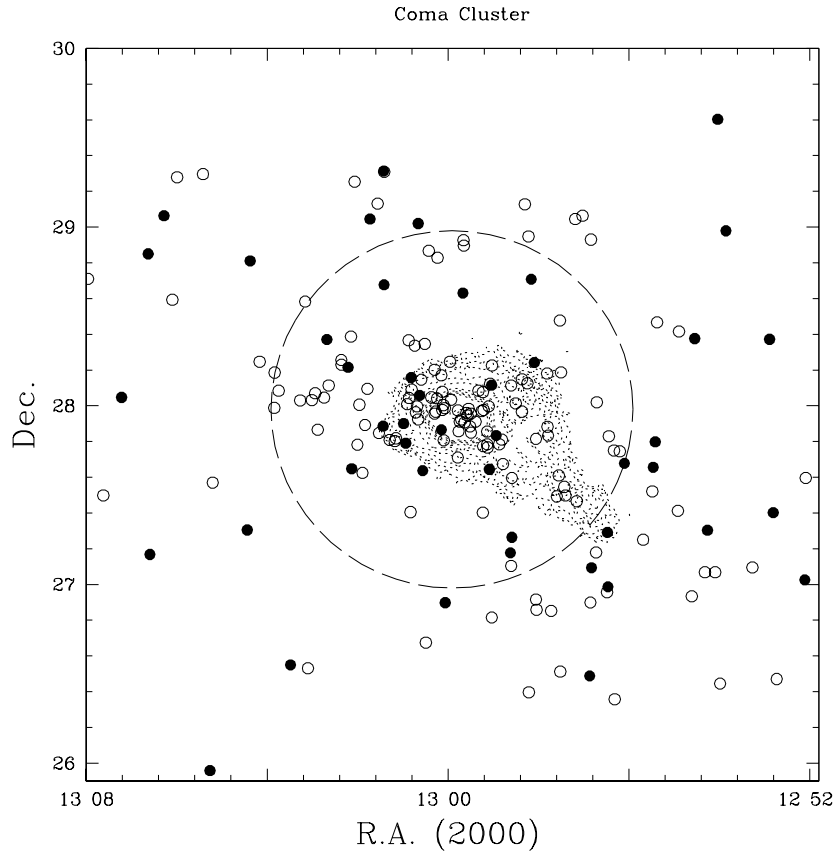


Fig. 1.— The celestial distribution of galaxies brighter than 15.7 from the CGCG catalogue, Zwicky et al. (1968) in a 4×4 deg 2 box around the Coma cluster. The 146 early-type (E+S0+S0a) galaxies (empty symbols) clearly mark the cluster density enhancement, whereas the 49 late-type (\geq Sa) objects (filled symbols, including 10 unclassified spirals) hardly trace the cluster. The circle of 1 degree radius is traced about the X-ray center. The X-ray contours from XMM are superposed.

issues, let's take a look at the Coma cluster whose bright galaxy distribution is shown in Figure

1. The early-type galaxies clearly mark the cluster density enhancement, whereas the late-type objects hardly trace the cluster at all, making Abell (1965) to doubt their very membership to the Coma cluster. The latter are very “healthy” objects, actively star forming, as witnessed by their average H α E.W. (equivalent width) of 35 Å (with peaks of 78 Å). This perhaps explains why Abell questioned their membership to Coma, because the majority of galaxies observed in clusters shows no signs of recent star formation activity. He didn’t know that some of these objects are not as in “good shape” as it looks at first glance, something that was realized 20 years later. The pioneering work of Giovanelli & Haynes (1985), continued by many other researchers, among them Gavazzi (1987, 1989), showed in fact that galaxies at projected distances < 1 Mpc from the center of Coma suffer from significant neutral hydrogen deficiency (see Section 2.1), having lost from 30 % to 90 % of their original HI content. The first resolved map of their HI distribution was obtained even more recently by Bravo-Alfaro et al. (2000). It shows that in most highly or moderately deficient objects the HI distribution is asymmetric or significantly displaced from the parent optical galaxy. This phenomenon occurs in objects projected within the X-ray emitting gas in the Coma cluster. For the interpretation of this observation, whether is due to ram-pressure stripping or to galaxy-galaxy or galaxy-cluster interactions, the reader is referred to the remaining of the discussion. However, generally speaking, a high HI deficiency represents perhaps the clearest signature of the interaction occurring to galaxies in the environment of rich clusters, in other words it gives a clear clue to their cluster membership. Abell was wrong! These are bona fide cluster members. What future is reserved to these galaxies? This is the type of issue addressed by the present review. The reader can find many excellent review papers in the literature that deal with the evolution of galaxies in the cluster environment (Haynes et al. 1984; Dressler 1984; Sarazin 1986; Dressler et al. 1997; Poggianti et al. 2001a; Driver & De Propris 2003; van Gorkom 2004) each focused on a particular aspect or wavelength domain. The most recent achievements in cluster research are collected in the proceedings of the Carnegie Observatories Astrophysics Series, Vol. 3: Clusters of Galaxies: Probes of Cosmological Structure and Galaxy Evolution (2004). With the present review we wish, for the first time, to consider together all aspects. The price we pay is that we must narrow down the reviewed interval of z , in practice to $z=0$. We start by reviewing the observational scenario (Sections 2, 3), covering the broadest possible stretch of the electromagnetic spectrum, from the gas tracers (radio and optical), the star formation tracers (UV and optical), the old star tracers (Near-IR) and the dust (Far-IR). We continue by providing a review of models of galaxy interactions relevant to clusters of galaxies (Section 4). We conclude with a discussion on what proposed model(s) better interprets various aspects of the observational scenario (Section 5), once again checking the models predictions on recent data on Virgo, Coma and A1367.

2. The constituents of late-type galaxies in nearby clusters: comparison with the “field”

2.1. The atomic hydrogen

The atomic gas is the principal component of the ISM in late-type galaxies, supplying the “fuel” that feeds the star formation. In normal, isolated galaxies the HI gas distribution outstands the optical disk: column densities of $\sim 10^{20}$ atoms cm^{-2} are observed at ~ 1.8 the optical diameter, with a relatively flat radial distribution, sometimes showing a central dip (Cayatte et al. 1994; Salpeter & Hoffman 1996; Broeils & Rhee 1997). The HI extension in the direction perpendicular to the disk is comparable to the optical thickness (Lee & Irwin 1997).

Because of its distribution the HI gas is weakly bound by the galaxy’s gravitational potential well, thus it can be easily removed. It is therefore obvious to expect that the HI content and distribution of galaxies in clusters differ from those of isolated galaxies (see the reviews by Haynes et al. (1984); van Gorkom (2004)). The first study of the atomic gas properties of galaxies in the Virgo cluster dates back to the sixties (Robinson & Koehler 1965). Since then, several HI surveys of this and other nearby clusters were carried out using single dish radiotelescopes (Giovanelli & Haynes 1985) and interferometers (Warmels 1988; Cayatte et al. 1990; Bravo-Alfaro et al. 2000). Owing to the survey of Hoffman et al. (1996) and to recent Arecibo observations (e.g. Gavazzi et al. (2005b)) HI data are available for the entire late-type galaxy population in the Virgo cluster, including dwarf irregulars and BCDs.

All works agree on the general conclusion that cluster galaxies have on average a lower atomic gas content than their isolated counterparts, as first noticed by Davies & Lewis (1973). A quantitative determination of this difference could however not be assessed before the systematic HI properties of isolated galaxies were known. This fundamental step was achieved by Haynes & Giovanelli (1984) who studied at Arecibo a reference sample selected from the Karachentseva (1973) catalogue of isolated galaxies. Haynes & Giovanelli (1984) defined the HI-deficiency parameter as the logarithmic difference between the observed HI mass and the expected value in isolated objects of similar morphological type and linear size. Galaxies with an HI-deficiency parameter ≤ 0.3 can be treated as unperturbed objects¹.

By comparing the statistical HI properties of galaxies in 9 nearby clusters with those of “field” objects of similar type and luminosity, Haynes et al. (1984) and Giovanelli & Haynes (1985) showed that clusters contain a large fraction of HI deficient galaxies, with the exception of unrelaxed, loose ones. This fraction is a strong function of the angular distance from the X-ray center (Gavazzi 1989; Boselli 1994).

Dressler (1986), by re-analyzing the Haynes & Giovanelli (1984) catalogue showed that the most deficient galaxies are generally early-type spirals in radial orbits, while gas-rich galaxies have isotropic or circular orbits (confirmed by Solanes et al. (2001)). Solanes et al. (2001), analyzing the HI prop-

¹The isolated sample by Haynes & Giovanelli (1984) is mainly composed of giant galaxies. The HI-deficiency parameter of dwarf objects is therefore poorly calibrated

erties of ~ 1900 galaxies in 18 nearby clusters, concluded that 2/3 of the clusters are composed of HI deficient galaxies inside the Abell radius R_A . The residuals of the deficiency parameter is related to the galaxy morphology and not to their optical size: early-type spirals and probably dwarfs are more deficient than Sbc-Sc at any radii inside $2R_A$. The deficiency increases toward the cluster center, being significant for $r < R_A$. They did not confirm the relationship between the fraction of HI-deficient galaxies and the cluster X-ray luminosity claimed by Giovanelli & Haynes (1985).

Gavazzi et al. (2005c) have completed the HI observations of late-type CGCG galaxies in the Coma supercluster. One important issue that they were able to address, given the completeness of their data-set, is on what scale the phenomenon of HI ablation holds. The HI deficiency parameter of individual galaxies is given in Fig.2 as a function of the projected linear separation from the X-ray center of the Coma cluster, out to 15 Mpc, along with average values taken in bins of 0.5° (from 0° to 2°) and in bins of 1° further out. It is apparent that significant HI deficiency occurs out to approximately 3 Mpc radius. Little above one virial radius (i.e. at 2.2 Mpc, Girardi et al. (1998)), the average HI content of the supercluster galaxies becomes indistinguishable from that of the field, in agreement with Solanes et al. (2001). We stress that the filaments constituting the "Homunculus legs" (de Lapparent et al. 1986), i.e. the groups/filaments in the immediate surrounding of the Coma cluster, perhaps infalling toward Coma (not shown in Fig.2), are made of galaxies retaining 100 % of their HI content, identical to unperturbed, isolated galaxies.

The HI survey of the Virgo cluster has also been completed by Gavazzi et al. (2005b), allowing to determine the radial distribution of the HI deficiency parameter of all spirals brighter than 18.0 mag (only $m_p < 13.0$ mag are plotted in Fig.2 for consistency with Coma). Unfortunately for Virgo the survey does not extend out in the low density region of the local supercluster as much as in Coma, but only out to 3.2 Mpc. We find that in Virgo there is a significant population of non-deficient galaxies at all radii, mixed with highly deficient (>1) ones. These exist within 2.2 Mpc, just above 1 virial radius (i.e. at 1.7 Mpc, Girardi et al. (1998)). Furthermore it is found that individual groups constituting the Virgo cluster (cloud N and S for example) contain less than 10 % highly deficient objects, compared to 33% in Cluster A (M87).

High resolution HI mapping of galaxies in the Virgo cluster with the Westerbork (Warmels 1988) and VLA (Cayatte et al. 1990) interferometers, and more recently in the Coma cluster (Bravo-Alfaro et al. 2000) revealed that cluster galaxies not only suffer from significant HI depletion, but that their HI distribution is less extended than isolated objects of similar morphological type and luminosity (Warmels 1988; Cayatte et al. 1994; Boselli et al. 2002).

While in normal isolated late-type galaxies the HI diameter (as measured at the 10^{20} atoms cm^{-2} isophote) is on average a factor of ~ 1.8 larger than the optical isophotal B band 25 mag arcsec^{-2} diameter (somewhat depending on the morphological type), in cluster objects the HI to optical diameter ratio strongly depends on the HI-deficiency parameter and on the distance from the cluster center (Warmels 1988; Cayatte et al. 1994). The most HI-deficient objects close to the X-ray center of Virgo have HI diameters up to ~ 5 times smaller than the optical ones (Cayatte et al. 1994). Anemic galaxies whose HI disks are slightly smaller than the optical ones, have significantly lower

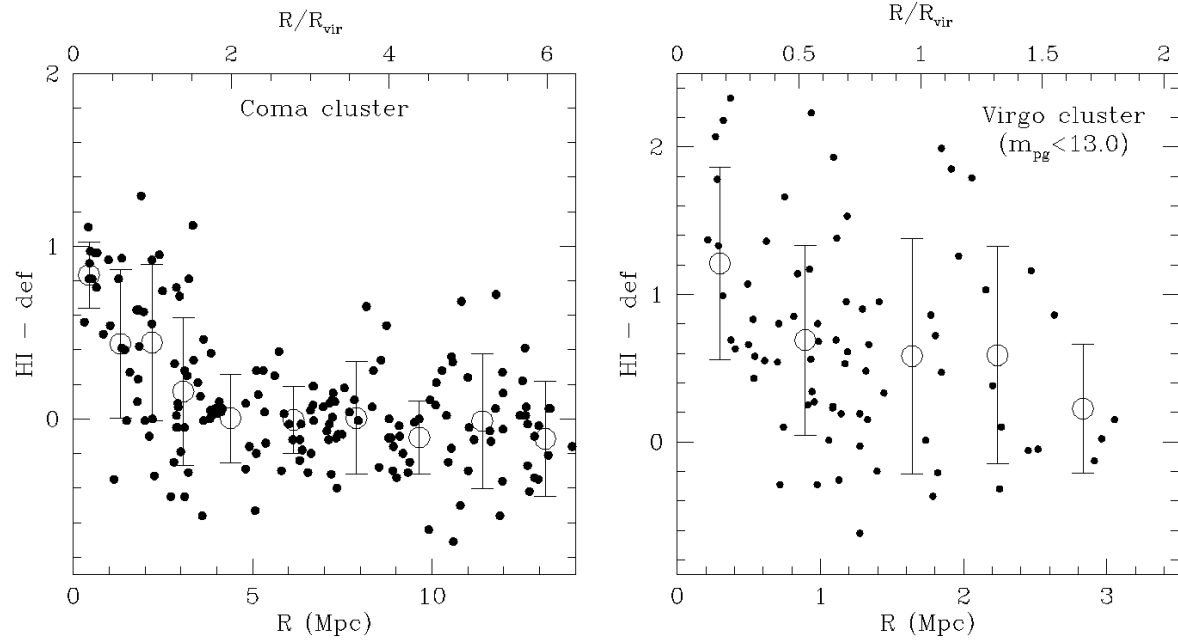


Fig. 2.— The projected distribution about the X-ray center of the HI deficiency of similar luminosity late-type members of the Coma (left) and Virgo clusters (right). Large circles represent averages with one σ uncertainties (adapted from Gavazzi et al. (2005c,b)).

HI column densities (by a factor of ~ 10) than normal, isolated objects of similar morphological type (Cayatte et al. 1994). The HI surface density correlates tightly with the HI-deficiency parameter (Boselli et al. 2002). Asymmetries in the HI distribution and displacements of the gas from the optical parent galaxies are frequently observed in moderately HI deficient objects (Gavazzi 1989; Cayatte et al. 1994; Bravo-Alfaro et al. 2000; Vogt et al. 2004).

The HI mass function of the Virgo cluster was found by Gavazzi et al. (2005b) to differ significantly from the one in the “field” due to the combined effect of morphology segregation and presence of HI-deficient objects. A similar result was recently obtained by Springob et al. (2005) who found, on average, a decrease of M_* and a flattening of the low-mass end of the HI mass function in high density environments.

The recently initiated Arecibo Legacy Fast ALFA (ALFALFA) survey aims to map ~ 7000 deg 2 of the high Galactic latitude sky visible from Arecibo (Giovanelli et al. 2005b). The survey will detect on the order of 20,000 extragalactic H I line sources out to $z \sim 0.06$ and enable a first wide-area blind search for local H I emitters. Environmental studies will greatly benefit from this survey.

2.2. The molecular hydrogen

The molecular gas phase, even if it represents only $\sim 15\%$ of the total gas reservoir in normal, late-type galaxies (Boselli et al. 2002), is the component of the ISM that takes direct part to the process of star formation. The HI gas has in fact to condense inside molecular clouds before collapsing to form stars. It is thus expected that any possible external perturbation induced by the environment on the molecular gas can have important consequences on the star formation activity, and thus on the evolution of late-type galaxies.

Early systematic works aimed at determining the molecular gas properties of late-type galaxies in clusters are the CO surveys of Virgo by Stark et al. (1986), Kenney & Young (1988a) and Boselli et al. (1995a) and that of Coma by Casoli et al. (1991). Using a *standard* conversion factor $X=n(H_2)/I(CO)$ between the intensity of the CO line and the column density of the molecular hydrogen calibrated on the Milky Way, these authors estimated the molecular hydrogen mass $M(H_2)$ of cluster galaxies. Their immediate conclusion was that cluster galaxies have a normal molecular gas content and the interpretation was that molecular gas, being more centrally peaked, deep inside the potential well of the galaxy, than the atomic gas, cannot be easily removed by any stripping mechanism (Kenney & Young 1989; Rengarajan & Iyengar 1992). Molecular gas removal could be effective only in low-mass galaxies with shallow potential wells, explaining the apparent CO deficiency of low-luminosity Virgo galaxies (Kenney & Young 1988b).

This result suffers however from several biases. It firstly resides on the hypothesis that the relation between the CO line intensity and the H_2 gas column density is universal. Boselli et al. (2002) showed however that X varies by more than a factor of 10 over the sampled range of UV radiation field, metallicity, morphological type and luminosity. The second limitation is the lack of a CO reference sample of isolated galaxies selected according to criteria similar to the cluster (Boselli et al. 1997a). For example the CO survey by Casoli et al. (1991) is mostly FIR selected, thus biased toward strong CO emitters (Boselli et al. 1995b).

To overcome these difficulties Boselli et al. (1997a) and Sauty et al. (2003) obtained CO observation of an optically selected sample of isolated galaxies. They applied a luminosity-dependent CO to H_2 conversion factor, calibrated on the nearby galaxies with an independent measure of X :

$$\log X = -0.38(\pm 0.06) \log L_H + 24.23(\pm 0.24) \quad (\text{mol cm}^{-2}(\text{K km s}^{-1})^{-1}) \quad (1)$$

From a H band luminosity- H_2 mass relation calibrated on the reference sample of isolated galaxies selected following similar criteria (Boselli et al. 2002):

$$\log M(H_2)_e = 3.28(\pm 0.39) + 0.51(\pm 0.05) \log L_H \quad (\text{in solar units}) \quad (2)$$

they obtained, in full analogy with the HI deficiency (Haynes & Giovanelli 1984) an H_2 deficiency parameter defined as:

$$Def_{H_2} = \log M(H_2)_e - \log M(H_2)_o \quad (3)$$

where $M(H_2)_e$ is the expected molecular gas mass of a galaxy of a given H luminosity as determined from eq. 2 and $M(H_2)_o$ is the observed molecular gas mass (Boselli et al. 2002).

The lack of relationship between the HI and the H₂ deficiency parameters confirms and extends to lower luminosities similar previous claims obtained in Coma (Boselli et al. 1997a; Casoli et al. 1991) and in Virgo (Kenney & Young 1989; Boselli 1994). The low luminosity, CO deficient spiral galaxies found in Virgo by Kenney & Young (1988b) are not necessarily deficient in molecular hydrogen since their H₂ mass was probably underestimated assuming a constant X conversion factor.

We conclude that cluster galaxies are significantly deficient in atomic hydrogen, but their molecular content is, on average, normal.

2.3. The metal content

Metals are produced and injected into the interstellar medium by massive stars through stellar winds and supernova explosions. They play a fundamental role in the process of star formation. Since they are produced by stars during their evolution, they can be used to constrain the star formation history of galaxies.

Skillman et al. (1996) analyzed the effects of the environment on the metal content of spiral galaxies by comparing the metallicity gradients observed in 9 objects in the Virgo cluster with similar measurements of isolated objects of equal type. The 9 galaxies were selected to span a large range in HI-deficiency and angular distance from the cluster center. HI-deficient galaxies in the center of Virgo have, on average, higher metallicity (0.3 to 0.5 dex in O/H) than HI normal galaxies at the periphery of the cluster or isolated objects with similar morphology and luminosity (Skillman et al. 1996; Pilyugin et al. 2002). Moreover Skillman et al. (1996) showed that HI deficient Virgo galaxies have shallower abundance gradients than normal objects. Gavazzi et al. (2006, in preparation) recently analyzed the HI-deficiency metallicity relation using integrated long slit spectra of a large sample of ~ 300 galaxies in the Virgo cluster and in the Coma/A1367 supercluster. Their analysis (Fig.3) shows that the most HI deficient galaxies have on average larger metallicities than similar objects with a normal gas content, confirming the results of Skillman et al. (1996)². A similar trend was also observed for the dwarfs, which, in dense environments, seem to have higher metallicities than isolated objects (Vilchez 1995). The unanimous interpretation of this finding is that metals in cluster galaxies are less diluted in the unpolluted gas, due to HI ablation.

2.4. The dust

Dust grains of different size and composition build up from metals produced by stars and injected into the ISM by stellar winds and supernovae explosions. Dust plays an important role in

²Remember however that the trend between metallicity residual and HI-deficiency is exclusively observed when metallicities are determined using the calibration of van Zee et al. (1998) which is based on [NII]/H α . Due to a bias, the other two methods, requiring the detection of [OIII], H β and [OII], cannot be applied to highly HI deficient galaxies because these lines are not detected in these objects.

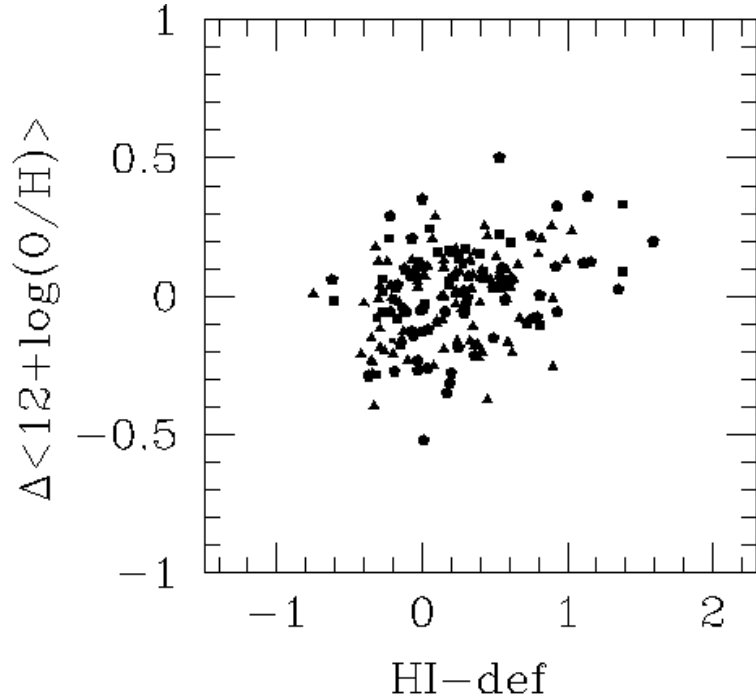


Fig. 3.— The relationship between the residual from the metallicity ($12+\log(O/H)$) vs. luminosity (L_V) relation and the HI deficiency parameter. The metallicity has been derived averaging the three calibrations of van Zee et al. (1998), Dopita et al. (2000) and Kobulnicky et al. (1999). Squares represent Sa-Sb, triangles Sbc-Scd, pentagons Sd-Im-BCD.

the process of star formation since atoms of hydrogen condense on dust grains to form H_2 molecules (Hollenbach et al. 1971). The interstellar dust is observable in absorption at ultraviolet and optical wavelengths and in emission in the mid- and far-IR, as the Infrared Astronomy Satellite (IRAS) dramatically revealed (Soifer et al. 1987). While most of the flux emitted by dust in normal galaxies is in the 60-200 μm domain (e.g. Boselli et al. (2003a)) (relatively warm, $T_{dust}=30$ K big grains), the bulk of the dust mass is colder ($T_{dust} \leq 15$ K), and it radiates in the sub-mm domain at $> 100\mu m$ (Bianchi et al. 1999). At intermediate wavelengths (15-60 μm) the emission is dominated by very small grains, while in the mid-IR (5-15 μm) it comes mostly from unidentified infrared bands (UIB), probably associated to planar molecules, called PAHs (Desert et al. 1990).

Dust is generally associated with the gaseous component: the dust to gas column density ratio is relatively well correlated to the metallicity of the ISM, and thus it varies with galaxy morphology and/or luminosity or, within a galaxy, it follows the metallicity gradient. It is thus expected that part of the dust associated with the atomic gas can be removed from cluster spirals and might contribute to the IGM pollution ³.

The mid-IR (5-18 μm) emission per unit galaxy mass of normal, late-type galaxies in the Virgo

³For a recent review on the infrared properties of clusters of galaxies observed by ISO see Metcalfe et al. (2005)

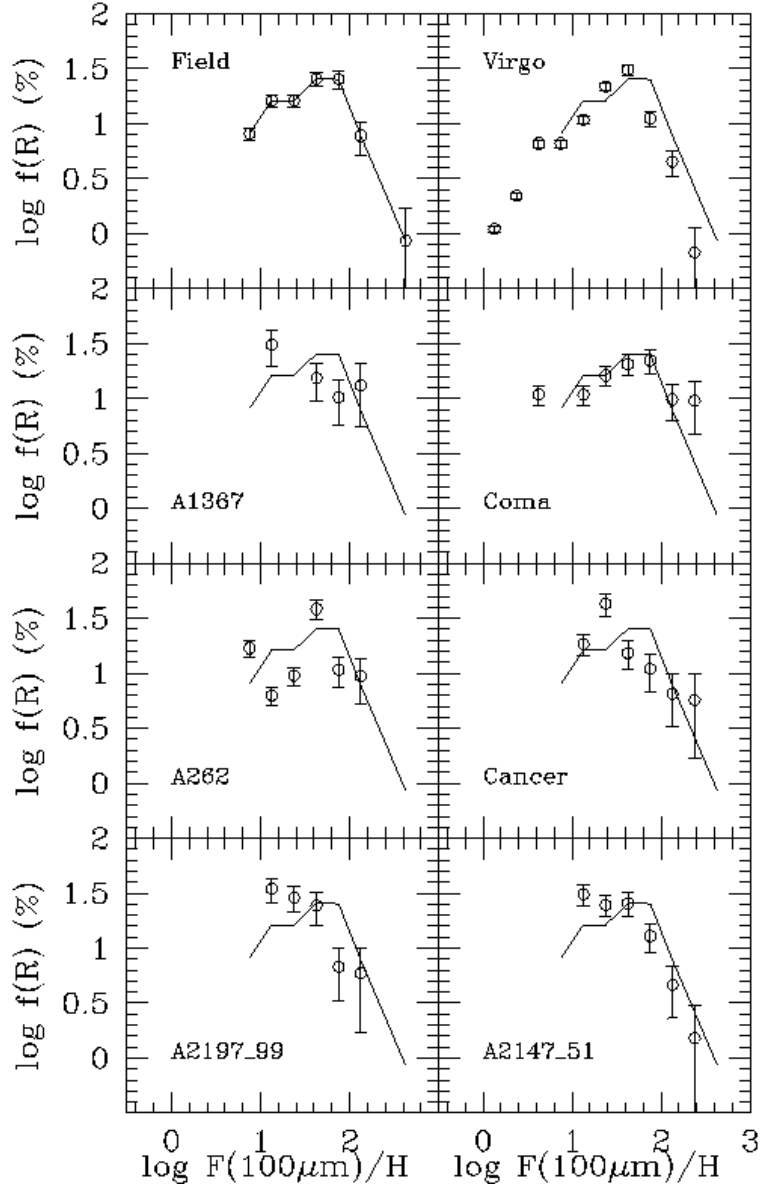


Fig. 4.— The differential far-IR to near-IR ($F(100 \mu\text{m})/H$) distribution in seven nearby clusters (dots) and in the reference sample of isolated galaxies (continuum line).

cluster does not depend on the distance from the cluster center (Boselli et al. 1998), thus it can be tentatively concluded that the carriers of the IR bands, dominating the emission at these wavelengths, are not affected by the cluster environment.

Using far-IR IRAS data for a sample of ~ 200 galaxies in 7 nearby clusters, Bicay & Giovanelli (1987) showed that optically selected cluster galaxies have a normal far-IR (60-100 μm) emission. There is however a lack of bright ($L_{\text{FIR}} > 10^{11} \text{ L}_\odot$) galaxies in clusters, and there is also a trend

between the dust temperature and the HI deficiency, with HI deficient objects having colder dust. This result was confirmed in the Virgo cluster by Doyon & Joseph (1989), who also found that HI-deficient galaxies have slightly lower 60 and 100 μm flux densities per unit optical area than HI normal galaxies.

Using far-IR flux densities normalized to the photographic magnitude, Gavazzi (1988) showed that the far-IR luminosity function of isolated and cluster galaxies are similar, except for the lack of objects with high far-IR to optical ratio, as claimed by Bicay & Giovanelli (1987).

Using the data on 9 nearby clusters and on the Great Wall (reference sample) obtained from GOLDmine we re-determined the far-IR luminosity distribution (see Fig. 4), but this time using far-IR (100 μm) normalized to H band flux densities⁴. As for the far-IR to optical luminosity

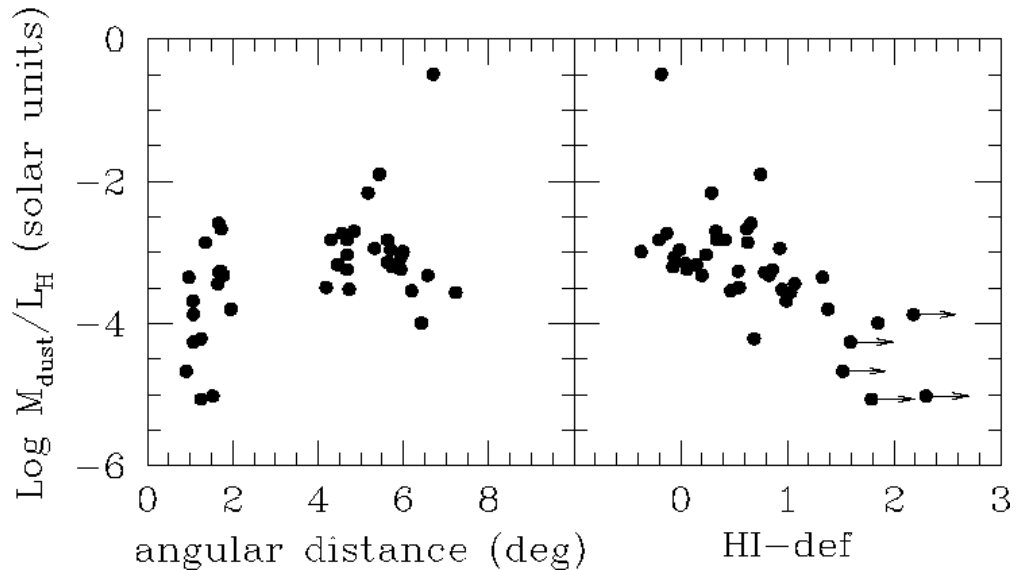


Fig. 5.— The relationship between the total dust mass normalized to the H band luminosity and a) the angular distance from the cluster center and b) the HI deficiency parameter for Virgo cluster galaxies observed at 170 μm with ISOPHOT. Filled dots are for HI detected galaxies, arrows for undetected objects (upper limits to the HI mass).

distribution, we do not observe any systematic difference between cluster and “field” galaxies. The emission of normal galaxies in the 60-100 μm range is however primarily dictated by the intensity of the UV and visible stellar radiation field, and only marginally by the dust mass. Therefore the above test is not sufficient to exclude dust removal in cluster galaxies.

The lack of homogeneously selected photometric data in the range 100 μm -1 mm for cluster and

⁴Normalizations are necessary to remove the first order dependences on luminosity (“bigger galaxies have more of everything”). As shown by Gavazzi et al. (1996), the proper normalization is the one obtained using the near-IR H band luminosity because this parameter traces the total dynamical mass of galaxies, it suffers from low internal extinction and it is not affected by recent events of star formation.

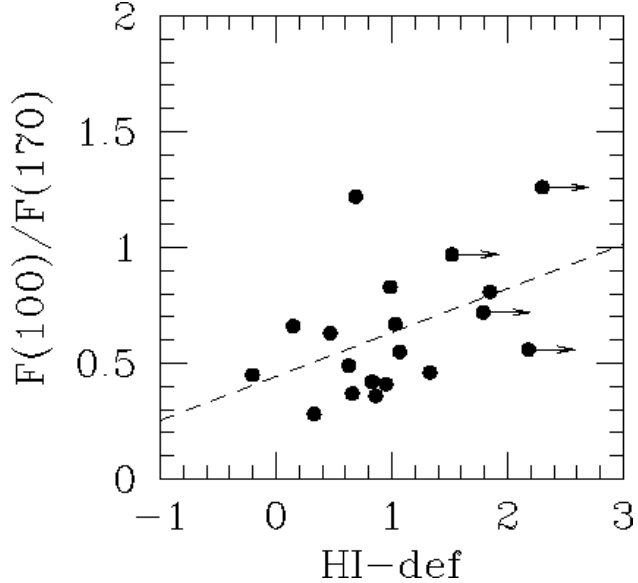


Fig. 6.— The relationship between the 100 to 170 μm flux density ratio and the HI deficiency parameter for Virgo cluster galaxies. Filled dots are for HI detected galaxies, arrows for HI undetected objects. The dashed line represents the best fit to the data.

isolated galaxies prevents us from studying the possible effects of the environment on the cold dust component using a similar statistical approach. At present the only systematic observations at this wavelength are the ISOPHOT 170 μm data of 63 late-type galaxies in the Virgo cluster by Tuffs et al. (2002). Using these data we show in Fig. 5 the relationship between the total dust mass (defined as the sum of the cold and warm dust masses given by Tuffs et al. (2002), normalized to the total galaxy mass, as traced by the H band luminosity) vs. the angular distance from the cluster center and vs. the HI-deficiency parameter. Both figures show an interesting trend of decreasing dust content with decreasing clustercentric distance and with increasing HI-deficiency, that could suggest dust removal in gas stripped galaxies. The reader should however take this result with some caution because it might be biased by a possible dust mass vs. morphology relation, an effect that remains to be confirmed when more far-IR data will be available, in particular of early-type spirals. A safer test is shown in Fig. 6 where the 100 to 170 μm flux density ratio (which gives a model independent dust temperature, thus is a tracer of the dust mass because $M_{\text{dust}} \propto T_{\text{dust}}^{-6}$, for a β emissivity parameter equal to 2, Bianchi et al. (1999)) is plotted against the HI-deficiency parameter. The sample has been limited to the massive spirals earlier than Scd. Figure 6 indicates a trend of the dust temperature (and thus an inverse trend of the dust mass) with the HI-deficiency, suggesting that the external cold dust might be swept together with the neutral hydrogen in stripped galaxies⁵.

⁵Notice that this trend is opposite to the one between the 60 to 100 μm flux density ratio and the HI-deficiency (decrease of temperature with the deficiency) found by Bicay & Giovanelli (1987)

Given the poor statistics and the aforementioned lack of a reference sample, dust depletion in cluster galaxies requires confirmation. The 60-170 μm all-sky survey that will be soon carried out by the Japanese satellite ASTRO-F (spring 2006) will help disclosing this issue.

2.5. The cosmic rays

The 1400 MHz (20 cm) radio continuum emission of normal, late-type galaxies is dominated by the synchrotron emission of cosmic ray electrons on magnetic fields. The contribution of thermal emission is negligible ($\leq 10\%$) in bright disk galaxies (Gioia et al. 1982; Klein 1990), but it can be relevant (up to 60-70%) in BCD galaxies (Klein et al. 1991). The tight relationship between the radio continuum and the H α emission observed in normal galaxies demonstrates that cosmic-ray electrons are accelerated by the young stellar population, probably in supernova remnants (Lequeux 1971; Kennicutt 1983a; Gavazzi et al. 1991a).

Gavazzi & Jaffe (1986) in their first systematic comparison of the radio continuum properties

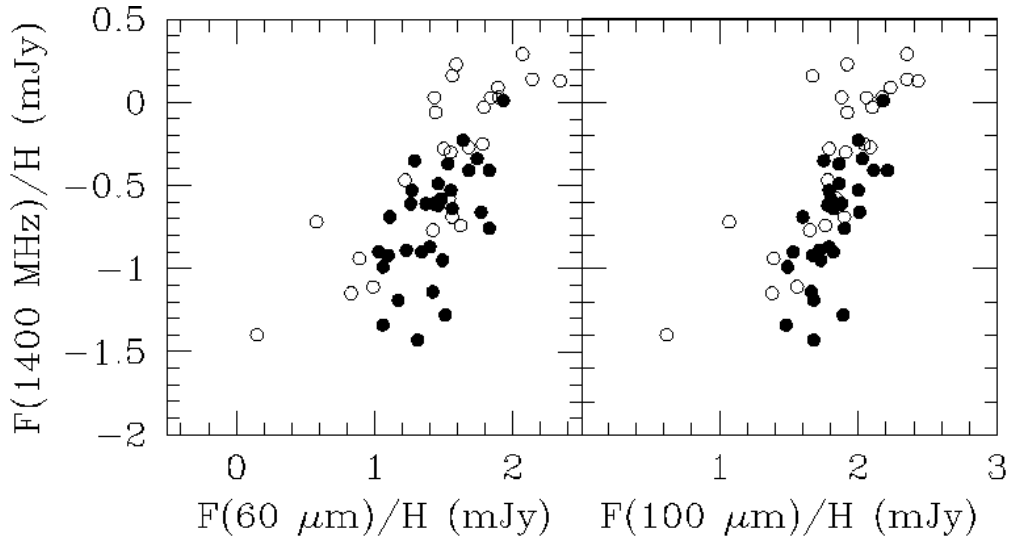


Fig. 7.— The relationship between radio continuum (at 1400 MHz) and the far-IR at 60 (left panel) and 100 (μm) emission (normalized to the H band luminosity) for galaxies in the two clusters Coma and A1367 (open symbols) and in the “field” (filled symbols).

of late-type galaxies in different density environments concluded that spiral galaxies in the Coma and A1367 clusters have their radio continuum emission enhanced by ~ 5 times with respect to isolated objects. This result was confirmed by Andersen & Owen (1995), Rengarajan et al. (1997) and Gavazzi & Boselli (1999). A marginal increase in the radio emissivity is observed in Virgo and A262, and none in loose clusters such as Cancer (Gavazzi & Boselli 1999).

Gavazzi et al. (1991a) showed that the far-IR radio correlation, shared by late-type galaxies in a huge luminosity interval, is different for cluster and isolated galaxies. The cluster objects have an

increased radio emissivity, at any given far-IR luminosity, with respect to “field” objects. This is shown in Fig. 7, where the normalized (to H) radio continuum emission at 20 cm is plotted versus the normalized (to H) far-IR (60 and 100 μm) emission for galaxies in the Coma and A1367 clusters (open symbols) and in the “field” (filled symbols). A similar increase has been observed at other frequencies (6.3 and 2.8 cm) in some galaxies close to the Virgo center by Niklas et al. (1995).

The synchrotron emissivity ϵ_ν is proportional to the density of relativistic electrons n_e and to the magnetic field density B as (Rybicki & Lightman 1979):

$$\epsilon_\nu \propto n_e \times B^{(1+\eta)/2} \times \nu^{-\alpha_r} \quad (\text{erg cm}^{-3}\text{s}^{-1}\text{str}^{-1}\text{Hz}^{-1}) \quad (4)$$

with typical spectral slope $\alpha_r=0.8$ (Klein 1990; Gioia et al. 1982). The density of relativistic electrons n_e , which are accelerated in supernova remnants, is proportional to the number of young stars, thus to the ongoing star formation rate. Since both the current star formation activity and the far-IR emission of cluster galaxies are comparable to, or lower than those of isolated objects (see Sections 2.4, 2.6), the observed increased radio emissivity and radio to far-IR ratio of cluster objects implies a factor of $\sim 2\text{-}3$ increase of the magnetic field density, possibly due to compression (Gavazzi & Boselli 1999) or most likely due to shock induced re-acceleration of relativistic electrons, as proposed by Völk & Xu (1994).

2.6. The star formation activity

The current star formation activity of galaxies can be studied using both direct and indirect tracers⁶. Any luminosity tracer of the young stellar population can be translated into a star formation rate (in $\text{M}_\odot \text{ yrs}^{-1}$) using stellar population synthesis models, provided that the star formation activity is constant over a time scale similar to the age of the emitting population. The $\text{H}\alpha$ emission of a galaxy is due to the hydrogen ionized in HII regions by massive ($> 8 \text{ M}_\odot$), young ($< 4 \text{ }10^6 \text{ yrs}$) OB stars (Kennicutt 1998). Once corrected for dust extinction (i.e. using the Balmer decrement), the $\text{H}\alpha$ luminosity is the most direct star formation tracer in normal galaxies. The UV luminosity is also a good tracer of young stars: at 2000 \AA , for instance, the emission of late-type galaxies is due to relatively young and massive (2-5 M_\odot) A stars (Boselli et al. 2001). The UV luminosity is proportional to the star formation rate provided that the star formation is constant over time scales of the order of $3 \text{ }10^8 \text{ yrs}$, which generally holds true in unperturbed disks. UV fluxes must however be corrected for dust extinction, using for example the method proposed by Buat et al. (2002), Boselli et al. (2003a) or Cortese et al. (2005a) based on the Far-IR to UV flux ratio.

The first attempt to study the star formation properties of galaxies in nearby clusters was carried out by Kennicutt (1983b). By comparing the $\text{H}\alpha$ equivalent width of 26 Virgo galaxies with that

⁶Indirect tracers of the star formation rate, such as the far-IR and radio continuum luminosities, should be used with caution for cluster galaxies because, as discussed in Sections 2.4 and 2.5, these quantities might not be reliable indicators of the star formation activity, due to dust removal or magnetic field compression

of isolated objects of similar Hubble type he showed that Virgo cluster galaxies have, on average, a lower star formation activity, redder colors and a lower HI gas content than their “field” counterparts. This pattern is fully confirmed by Gavazzi et al. (2002b) and more recently by Gavazzi et al. (2005a) who extended the $\text{H}\alpha$ imaging survey of galaxies in Virgo, Coma and A1367 to 545 cluster members, 95% complete at $m_{pg} \leq 18.0$ in Virgo and at $m_{pg} \leq 15.7$ in Coma. Their analysis showed that the current, massive star-formation rate per unit mass increases along the Hubble sequence from Sa to Scd, it decreases to a relative minimum for Im and it reaches the highest value for BCDs (see Figure 8). Within each Hubble type class, galaxies with normal HI content ($HI - def < 0.4$) have $\text{H}\alpha$ E.W. ⁷ systematically higher than their HI deficient ($HI - def > 0.4$) counterparts by a factor of two. Moreover the relative minimum found for Im galaxies is not due to a particularly high HI deficiency among these objects, but is a characteristic of objects in this Hubble class.

Both the SFR per unit mass and the birthrate parameter b , defined as the ratio between the present

⁷When we refer to $\text{H}\alpha$ E.W. we mean $\text{H}\alpha + [\text{NII}]$ E.W., since measurements are affected by the contamination of the [NII] lines bracketing $\text{H}\alpha$.

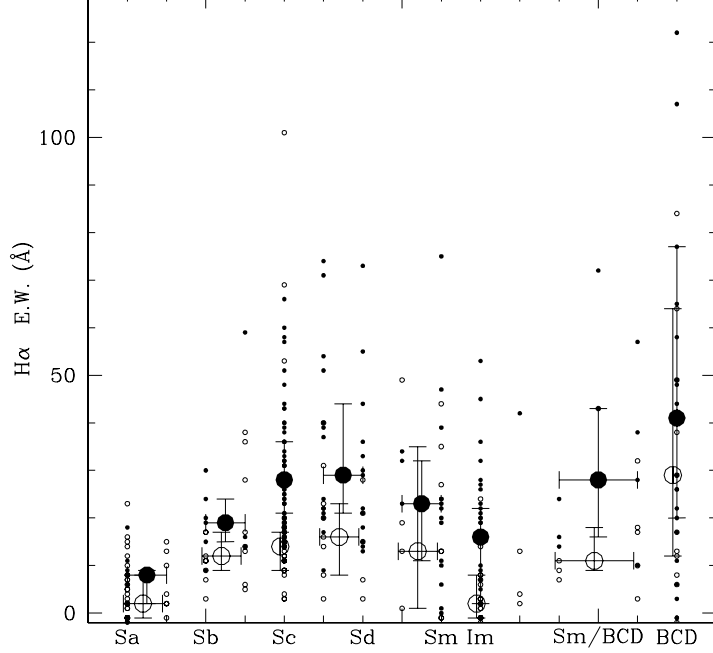


Fig. 8.— The distribution of the individual $\text{H}\alpha$ E.W. measurements in the Virgo cluster along the Hubble sequence (small dots) and of the median $\text{H}\alpha$ E.W. in bins of Hubble type. Error bars are drawn at the 25th and 75th percentile of the distribution. Filled symbols represent $HI - def \leq 0.4$ (unperturbed) objects and open symbols $HI - def > 0.4$ (HI deficient) galaxies.

day star formation rate and the star formation rate averaged over the entire life of the galaxy (Boselli et al. 2001), strongly depends on the total (HI plus H₂) gas deficiency parameter: gas deficient objects have a birthrate parameter significantly lower than that expected from their luminosity. This indicates that the present day star formation activity of cluster galaxies is regulated by the total (HI plus H₂) gas content, despite the fact that most of the total gas is located outside the optical star forming disks. The role of the molecular gas phase is thus probably dominant only on small scales (Boselli et al. 2001).

Mixed with the massive, passively evolving galaxies, however, there exist a population of low-mass cluster objects (Gavazzi et al. 1991a, 1998) with a surprisingly high fraction of actively star forming galaxies showing vigorous star formation activity, comparable to that of isolated galaxies, or even boosted by the dynamical interaction with the IGM (as in the case of CGCG 97073 and 97079 in A1367; see sect. 4.10.2) or by tidal interactions with nearby companions (as the Blue Infalling Group (BIG) in A1367; see sect. 4.10.3).

Beside the global star formation activity, the morphology of the star formation regions of galaxies in clusters has been studied in some details (Moss & Whittle 2000; Koopmann & Kenney 1998, 2004a,b; Knapen 2005), leading however to controversial results that derive from the intrinsic difficulty of classifying the (irregular and seeing dependent) H α morphology. One aspect is to find whether cluster disks show a truncation of the H α emission in their outer profiles, as expected in the ram-pressure scenario, or if significant star formation excess takes place in the circumnuclear regions, as expected if nuclear sinking of gas occurs due to tidal processes, including harassment (see Section 4) ⁸. Using an objective-prism survey of 320 galaxies in 8 nearby clusters, Moss et al. (1998) and Moss & Whittle (2000) found an excess of galaxies with circumnuclear H α emission, showing perturbed or peculiar H α morphologies. Their frequency increases with the local (and central) galaxy density, suggesting that they are produced by tidal (galaxy-galaxy or galaxy-cluster) interactions. We notice however that, because of the poor spatial resolution of their objective-prism data (4 kpc), what Moss et al. (1998) and Moss & Whittle (2000) attribute to circumnuclear H α emission corresponds in fact to a truncated disk.

Koopmann & Kenney (1998, 2004a,b); Koopmann et al. (2006), in their H α imaging survey of 55 Virgo cluster galaxies, found that a severe reduction of the star formation activity takes place only in the outer disks, producing truncated H α profiles, with normal or possibly enhanced activity in the inner disks. To illustrate this point we show in Figure 9 two galaxies: the normal VCC 92 (NGC 4192) (left) and the HI deficient, anemic, nucleated VCC 1690 (NGC 4569). On top of the continuum r band frames, contours of the HI column density are sketched (adapted from Cayatte et al. (1990)). In spite of their different gas deficiency, vigorous star formation takes place up to the HI radius. Among the deficient objects the H α morphology is always that of a truncated disk. Once the gas is radially removed (outside-in) by interactions of any kind, a radial truncation of the

⁸We remind however that ram pressure can induce an increase of the inner disk gas column density up to a factor of ~ 1.5 in galaxies moving edge-on close to the cluster center (~ 100 kpc; Vollmer et al. (2001b)), or the formation of an inner gas ring (Schulz & Struck 2001). The increase of the gas column density might induce an inner disk star formation and feed a nuclear activity (Schulz & Struck 2001)

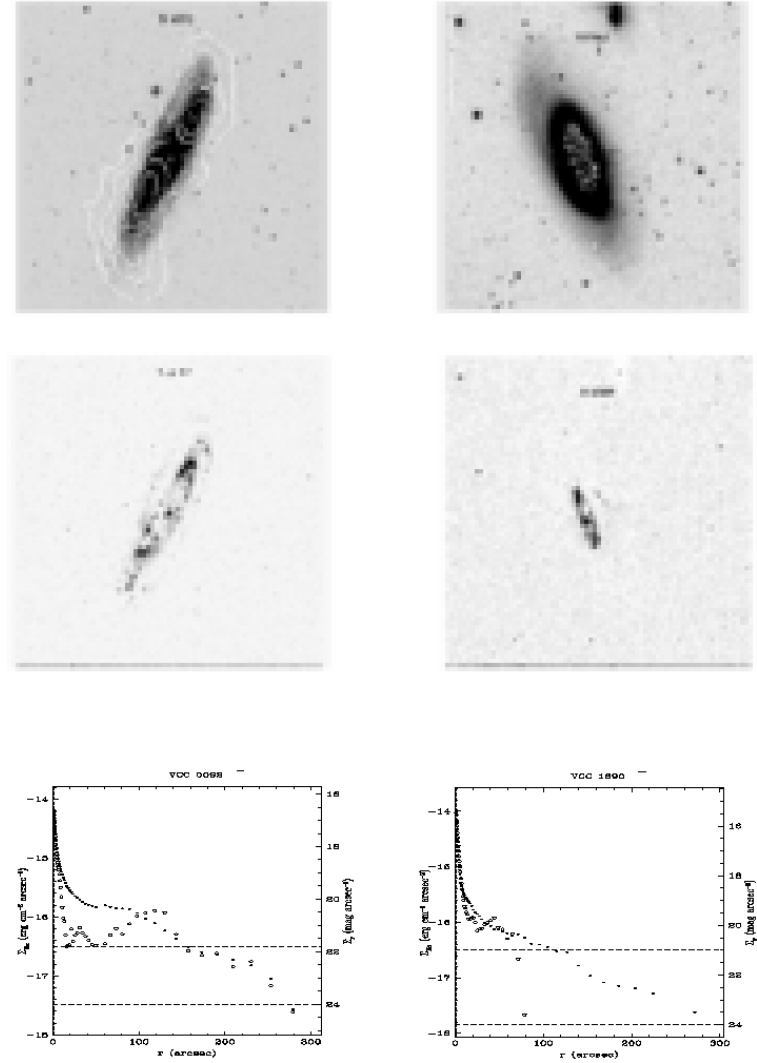


Fig. 9.— *r* band continuum images (upper panel) with superposed HI isophotal contours adapted from Cayatte et al. (1990); $\text{H}\alpha$ NET images (central panel); *r* (filled dots) and $\text{H}\alpha$ (NET; empty dots) surface brightness profiles (bottom panel) for two galaxies in the Virgo cluster: the normal VCC 92 (NGC 4192) and the deficient VCC 1690 (NGC 4569).

star formation activity, as well as a steepening of the stellar disk with decreasing wavelength and of the metallicity are expected to occur, as first claimed by Larson et al. (1980), and predicted by the chemo-spectrophotometric models of galaxy evolution of Boissier & Prantzos (2000). The radial

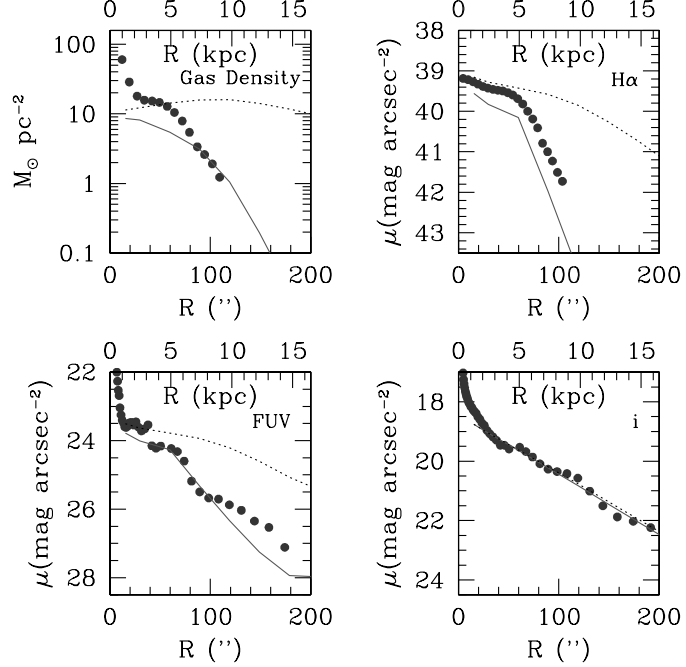


Fig. 10.— The radial profile of the observed (filled dots) total gas, H α , FUV (1530 \AA), and i surface brightness (corrected for dust extinction) of NGC 4569, compared to the multizone spectrophotometric model predictions for an unperturbed galaxy of similar total mass and velocity rotation curve (dotted line). The continuum line gives the radial profiles predicted by models after a 400 Myr old gas stripping event. Strong truncation occurs to the gas and to the H α , mild to the FUV and none to the i band. (adapted from Boselli et al. (2005b))

truncation of the star formation activity is in fact dictated by the Schmidt law, as the decrease of the total gas column density produces an instantaneous decrease of the star formation activity. Multi zone chemo-spectrophotometric models show a clean dependence of the disk truncation on wavelength, given that, depending on their age, different stellar populations contribute more to different wavelengths. By comparing model predictions with observed multifrequency radial profiles it is thus possible to date the stripping process. In the case of the anemic, HI-deficient Virgo cluster galaxy NGC 4569 (see Fig. 10) Boselli et al. (2005b) were able to reproduce the truncation of the total gas, of the star forming disk and of the various stellar populations assuming a ram-pressure stripping event that took place ~ 400 Myr ago. Gas stripping in cluster galaxies with truncated HI and H α disks but unperturbed stellar disks at long wavelengths ($\lambda \geq 6000 \text{ \AA}$) is thus a relatively recent event (some 10^8 yr), indicating that the perturbing interaction took place close to the cluster center (this time scale is in fact ~ 5 times smaller than the cluster crossing time).

Statistical evidence for a definite increasing trend of the ratio of the optical to H α radius ("trun-

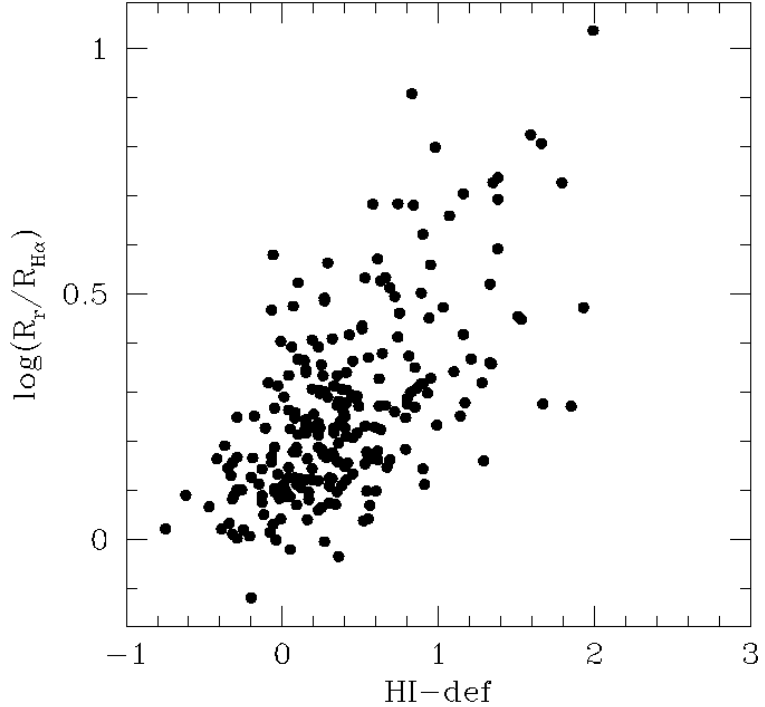


Fig. 11.— The ratio of the optical to H α radius versus the HI deficiency of late-type galaxies in the Virgo cluster. The H α isophotal radius is computed within $10^{-16.5}$ erg cm $^{-2}$ s $^{-1}$ \AA^{-1} arcsec $^{-2}$ and the r band isophotal radius is within 24th mag arcsec $^{-2}$ (adapted from Gavazzi et al., in preparation).

cation”) and the HI deficiency parameter (see Fig. 11) was found by Gavazzi et al. (2006, in preparation) in their recent analysis of the complete H α survey of disk galaxies in the Virgo cluster.

Another important issue is that the amount and the scale over which the current star formation rate is found quenched in nearby clusters of galaxies seems to depend significantly on luminosity. For the Virgo cluster the H α data-set analyzed by Gavazzi et al. (2005a) is 95% complete at $m_{pg} \leq 18.0$ ($M_{pg} \leq -13.0$) over the area covered by the VCC, i.e. up to approximately 2.5 virial radii from M87. Similar completeness (95%) at $m_{pg} \leq 15.7$ ($M_{pg} \leq -19.0$) is reached in Coma, but over a much larger area of the Great Wall, including the bridge between Coma and A1367.

In bright spiral galaxies⁹ the star formation rate per unit mass decreases from $\sim 20 - 30 \text{\AA}$ found at approximately 2 virial radii projected distance from Coma and Virgo, inward (see open circles in Fig.12) to virtually zero at the cluster center. An even more conspicuous decrease is observed in the redshift range $0.05 < z < 0.095$ by Gomez et al. (2003) using a sample of ~ 8500 galaxies from the SDSS, and by Lewis et al. (2002) on ~ 11000 galaxies from the 2dF. These surveys have shown

⁹We use two slightly different thresholds to discriminate bright from faint in Virgo and Coma. In Virgo we use the optical limit $M_{pg} \leq -19.0$ and in Coma the Near-Infrared limit $L_H = 10.5$

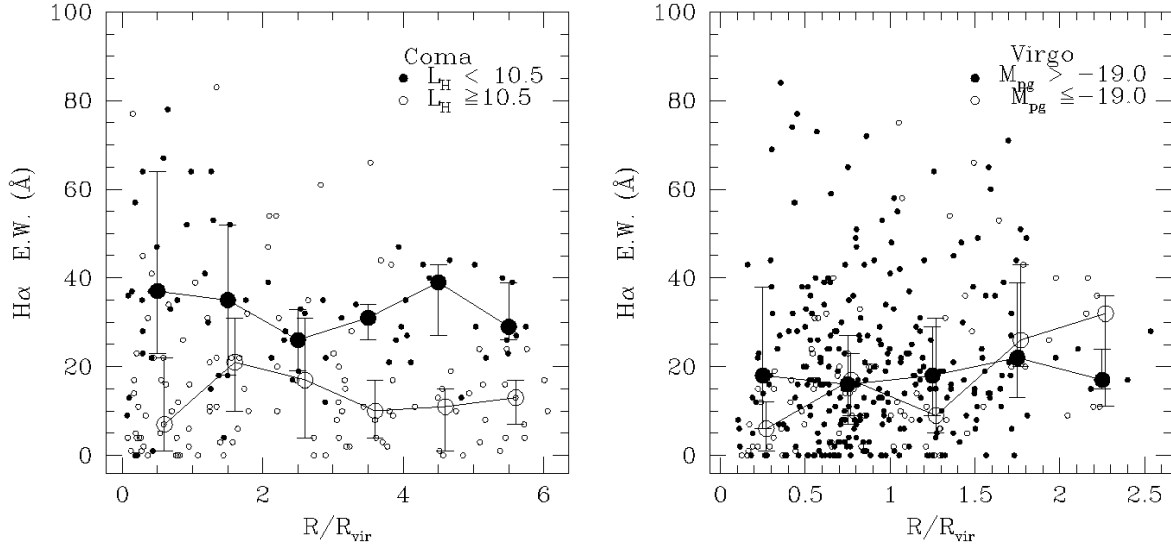


Fig. 12.— The clustercentric radial distribution of the individual H α E.W. measurements in the Virgo cluster (right) and in the Coma+A1367 clusters (left). High and low luminosity galaxies are given with open and filled dots respectively. Medians in bins of 0.5 (1) R/R_{vir} are given. Error bars mark the 25th and 75th percentile of the distribution.

that the star formation decreases above a characteristic galaxy projected density of $\sim 1 h_{75}^{-2} \text{Mpc}^{-2}$, corresponding to 1-2 virial radii (Gomez et al. 2003; Lewis et al. 2002; Tanaka et al. 2004; Nichol 2004), consistently with Figs.12 and with the clustercentric distribution of the HI (Fig.2).

The SDSS and 2dF surveys have the virtue of extending the study of the star formation activity in clusters to lower density environments and to extremely significant statistical samples. However, they are limited by the absence of reliable morphology indicators for the bulk of their objects (the morphological classification based only on light concentration and/or spectrophotometric parameters has been proved to be highly inaccurate (Scoville et al. 2002b)). They suffer from the difficulty of disentangling the radial dependence of the star formation activity in spiral galaxies from the morphology segregation effect itself.

What we found most surprising in Virgo and Coma is that galaxies less luminous than some threshold have their star formation rate per unit mass independent on the clustercentric radius (see the filled circles in Fig.12). This pattern could not be found neither in the SDSS nor in the 2dF because these surveys do not include such low luminosity objects. The sample of nearby clusters used by Gomez et al. (2003), for instance, is limited to $M_r \leq -20.5$, while that of Lewis et al. (2002) to $M_b \leq -19$.

The analysis of 60 clusters at $z < 0.11$ in the 2dF by De Propris et al. (2004) showed that the fraction of blue galaxies depends on the luminosity, clustercentric distance and galaxy density, but is insensitive to the Bautz-Morgan type, the velocity dispersion (mass), richness, presence of substructures and cluster concentration. Similarly, the 2dF analysis by Bower & Balogh (2004) shows that significant quenching of the SFR occurs above the local galaxy density threshold of \sim

1-2 $h_{75}^{-2} \text{Mpc}^{-2}$, but is insensitive to the radial clustercentric distance and to the velocity dispersion. These evidences indicate that significant suppression of the SFR takes place in the group environment, where tidal mechanisms, as opposed to ram pressure, are likely to take place. Summarizing, the present star formation rate in late-type cluster galaxies is significantly more quiescent than in their “field” counterparts and it is found to depend primarily on the residual HI content. The hydrodynamic interaction with the hot IGM is certainly responsible of significant HI ablation at the present cosmological epoch, thereby producing radial truncation in the birth of new stars, however tidal processes might have been dominant at suppressing the star formation during earlier preprocessing phases.

3. Other observational characteristics of cluster galaxies

3.1. Morphology segregation

As mentioned in the introduction, morphology segregation is at present the strongest observational signature of a different nature or nurture of cluster galaxies. In his seminal work based on photographic plates of 55 nearby clusters including ~ 6000 galaxies Dressler (1980) showed that the fraction of early-type galaxies (ellipticals and lenticulars) increases with the galaxy density and/or clustercentric radius (Whitmore et al. 1993). This relation appears universal, as it holds over 6 orders of magnitude, from rich clusters to loose groups (Postman & Geller 1984). Whitmore et al. (1993) claim that the morphology-radius relation is independent of the number density within the central 0.5 Mpc, of the X-ray luminosity or of the velocity dispersion of the cluster. The fraction of ellipticals in the outer parts of clusters is \sim constant (10 to 16 %) at a distance > 0.5 Mpc. This fraction increases to 60-70% in the cluster center. The fraction of lenticulars rises moderately up to the central 0.2 Mpc, then it drops sharply. On the other hand the fraction of spirals decreases continuously from the outskirts ($\sim 60\%$) to the cluster center, where it drops to virtually 0%. Furthermore, in the Coma cluster, the fraction of barred galaxies increases toward the cluster core (Thompson 1981).

Binggeli et al. (1990), Thuan et al. (1991) and Sabatini et al. (2005) showed that segregation also affects dwarf galaxies, i.e. dwarf ellipticals are more frequent in dense environments while dwarf irregulars are ubiquitous.

Vogt et al. (2004) showed that the spiral fraction depends inversely on the cluster X-ray temperature. They also found that, while the fraction of ellipticals is almost constant ($\sim 15\%$ regardless of the X-ray temperature or spiral fraction), there is a strong inverse correlation between the fraction of spirals and S0s constituting the remaining 85%, in other words the increase of the spiral fraction in the clusters outskirts compensates for the decrease of lenticulars. This effect holds in clusters of different richness, and extends beyond the virial radius. Both early- and late-type spirals are found in an envelope surrounding the cluster core, at a mean distance of $1.5 h^{-1} \text{Mpc}$, while ellipticals are at $\sim 0.85 h^{-1} \text{Mpc}$. Note that the morphology-density relation also affects distant ($z=0.5$), rich, centrally-concentrated clusters, while it seems to avoid irregular ones (Dressler et al. 1997). In

distant clusters the spiral fraction is larger, the elliptical fraction is \geq and the lenticular fraction is a factor of ~ 2 -3 smaller than in nearby clusters (Dressler et al. 1997; Fasano et al. 2000).

As mentioned in the introduction, morphology segregation is self-evident in the Coma cluster. Andreon (1996) showed however that, while spirals are homogeneously distributed over the cluster, the early-type component concentrates along the direction marked by the supercluster structure. Furthermore he showed evidence for velocity segregation, with ellipticals and lenticulars having significantly smaller dispersion (~ 700 km s $^{-1}$) than spirals (~ 1300 km s $^{-1}$) (see also Section 3.4). More recently Kashikawa et al. (1998), by analyzing CCD images covering more than 5 square degree of the Coma cluster, showed a strong luminosity segregation in the magnitude range $-20 \leq M_R \leq -16$. Galaxies with high central light concentration have a clustering strength significantly dependent on luminosity, while objects with a low central concentration show almost no luminosity segregation. Once again we remind that interpreting this evidence in terms of morphology is not straightforward since, as mentioned earlier, galaxy light profiles better correlate in shape with luminosity than with morphological type: both dE and low-luminosity late-type have exponential light profiles with low concentration indices (Gavazzi et al. 2000b).

The study of the galaxy morphology distribution in the Virgo cluster is made complex by projection effects due to the elongated 3-D structure of the cluster (see Section 3.4). Schindler et al. (1999) compared the distribution of galaxies cataloged in the VCC with that of the X-ray emitting gas from the ROSAT All Sky Survey, and found that the two components have a similar distributions. The cluster can be decomposed in three major substructures centered on M87, M49 and M86. They found no luminosity segregation and positive morphology segregation: spirals are more spread than early-types, while nucleated dwarf ellipticals are more concentrated toward the cluster center than their non-nucleated counterparts (see also Binggeli et al. (1987)).

The SDSS and 2dF surveys made it possible to extend the study of morphology segregation to regions of low density contrast with respect to the “field”. They confirm the increase of the fraction of the red, bulge-dominated galaxies with galaxy density and cluster-centric distance (Goto et al. 2003b; Hogg et al. 2003; Balogh et al. 2004; De Propris et al. 2004) that was known in rich nearby clusters.

3.2. The luminosity function

The determination of the luminosity function (LF) in distinct morphological classes (elliptical vs. spirals) is a difficult task both for the clusters and for the “field” because of the lack of high quality imaging material that is necessary for an accurate morphological classification. Let us then start reviewing the most recent determinations of the global (elliptical + spirals) LF, as derived from the extensive spectroscopic and imaging surveys carried on in the optical in the nearby Uni-

verse (POSS, SDSS, 2dF)¹⁰. Paolillo et al. (2001), by combining POSS-II data of 39 nearby Abell clusters, determined that the composite cluster luminosity function in the high-luminosity range ($-22 \leq M_R \leq -18.5$) has a Schechter parameter $\alpha \sim -1.1 \pm 0.2$, both at red and blue wavelengths. At fainter magnitudes, however, the slope becomes significantly steeper. Yagi et al. (2002), using R band CCD images of 10 nearby ($z \leq 0.076$) clusters, determined that the composite luminosity function in the range $-23.5 \leq M_R \leq -16$ has a slope $\alpha(R) \sim -1.31$. More recently, using the 2dF redshift survey of 60 nearby clusters ($z \leq 0.11$), De Propris et al. (2003) constructed a composite luminosity function in the b_J band. In the magnitude range $-22.5 \leq M_{b_J} \leq -15$ they derive a slope $\alpha(b_J) = -1.28$. These works indicate that the slope of the faint end of the optical luminosity function is steeper in clusters ($\alpha \sim -1.3$) than in the “field” ($\alpha \sim -1.2$; Blanton et al. (2001)). A steeper slope ($\alpha(R) \sim -1.6$) in the magnitude range $-17 \leq M_R \leq -14$ was found by Trentham et al. (2005), indicating that the steepening of the cluster luminosity function is due to the dwarf galaxy population.

De Propris et al. (2003) also showed that the cluster luminosity function has a characteristic magnitude $M_{b_J}^* \sim 0.3$ mag. brighter than the “field” one, that they tentatively attribute to an excess of very bright galaxies in the cluster cores. Furthermore the luminosity function is similar in clusters with high and low velocity dispersions, of different type and richness, with or without substructures. It was however noticed that the cluster luminosity function has a dip at $M_R \sim -18.5$ mostly due to the early-type component, whose presence generally correlates with the cluster velocity dispersion (Yagi et al. 2002).

In their effort to disentangle the contribution of early- and late-type galaxies to the LF, by dividing galaxies according to the shape of their radial light profiles, Yagi et al. (2002) showed that the composite cluster luminosity function of exponential disks has a faint end slope $\alpha(R) = -1.49$, significantly steeper than that of galaxies characterized by $r^{1/4}$ light profiles ($\alpha(R) = -1.08$). The interpretation of this finding in terms of morphology is however uncertain because it is well known that both early- and late-type low-luminosity systems are characterized by exponential disks, and both early- and late-type high luminosity, bulge dominated systems have $\sim r^{1/4}$ light profiles (Gavazzi et al. 2000b).

Using a spectral classification similar to the one used for the “field” by Madgwick et al. (2002), De Propris et al. (2003) showed that the luminosity function of cluster galaxies with early-type-like spectra is brighter and steeper than in the “field”, while that of objects with late-type-like spectra is similar. This suggests that the observed steepening of the cluster luminosity function is due to the early-type component. Once again, however one should use some caution since Gavazzi et al. (2004) showed that many bright cluster, late-type galaxies have spectra similar to ellipticals. These are systems devoid of gas with no star formation activity.

¹⁰For characterizing the luminosity function we will use in the following the Schechter (1976) formalism:

$$\phi(L)dL = \phi^* \left(\frac{L}{L^*}\right)^\alpha e^{-\left(\frac{L}{L^*}\right)} d\left(\frac{L}{L^*}\right) \quad (5)$$

For galaxies in the Virgo cluster, due to its proximity (17 Mpc), both the cluster membership, based on surface brightness criteria, and the morphological type separation are very accurate, even for the dwarf component. The B band LF, determined with high precision by Sandage et al. (1985), can be summarized as follows: the global LF has a faint end slope $\alpha(B)=-1.4$ up to $M_B \leq -13$, and even steeper at lower luminosities ($\alpha(B)=-1.6$ up to $M_B \leq -11$; Trentham & Hodgkin (2002)). Although Virgo is a spiral rich cluster, the steep rise of the luminosity function is primarily due to the dwarf elliptical component, which appears flatter in the “field” (Binggeli et al. 1990). The spirals (Sa-Sm) follow a Gaussian, peaked at $M_B=-17.7$, but when the fainter Im are added, which follow a Schechter function of slope $\alpha(B)=-0.25$, the combined late-type (Spiral + Im) galaxies have a slope $\alpha(B)=-0.80$.

A similarly accurate type separation is not yet achieved in the “field” because of the poorer morphological classification. Using a spectroscopic type classification, Madgwick et al. (2002) obtained slopes $\alpha(b_J) = -0.99, -1.24, -1.50$ for early-spirals, late-spirals and irregulars respectively. Consistent values are obtained by Heyl et al. (1997) with similar techniques ($\alpha(b_J) = -0.99, -1.25, -1.37, -1.36$ for Sab, Sbc, Scd, Sdm/Starburst respectively). Marzke et al. (1998), using a morphological classification based on plate material for 5404 galaxies, determined a type-dependent luminosity function of slope $\alpha(B) = -1.11$ for spirals and $\alpha(B) = -1.81$ for peculiars and irregulars. Despite the large uncertainty affecting these determination, it appears that, at least at optical wavelengths, the slope of the late-type galaxies luminosity function of Virgo is significantly flatter than that of the “field”.

For nearby clusters such as Coma, A1367 and Virgo it is possible to derive separate determinations of the LF, each for every frequency band relevant to the stellar emission, from $H\alpha$ and UV to near-IR. The comparison with the “field” is however possible only for the global (all types) LFs. In the spiral poor, relatively relaxed Coma cluster the slope α (in the visible) listed in the literature ranges between ~ -1.7 and ~ -1.2 , depending on the absolute magnitude range and on the cluster region included (Iglesias-Páramo et al. 2003). The slope α and the difference between the slope of the luminosity function in the “field” and in clusters are wavelength dependent, as shown in Fig. 13. While at $\lambda > 2000$ Å the slope of the Coma luminosity function is increasingly (with λ) steeper than that in the “field”, for $\lambda > 1500$ Å the reverse is true. At long wavelengths (near-IR) the luminosity is a tracer of the dynamical mass (Gavazzi et al. 1996), thus the luminosity function can be assumed as a mass function. Even though significantly steeper than in the “field” at near-IR, the cluster luminosity function ($\alpha \sim -1.5$; de Propris et al. (1998); Mobasher & Trentham (1998), Andreon & Pelló (2000), Balogh et al. (2001)) is still significantly flatter than the one predicted by CDM semi-analytical hierarchical models of galaxy formation (Somerville & Primack 1999). In any cosmology, CDM models predict slopes $\alpha \sim -2$ for the mass function. Assuming a mass to light ratio in agreement with the Tully-Fisher relation, it is at present impossible to obtain from these models the observed slope of the near-IR LF.

At wavelengths shorter than ≤ 2500 Å, where the emission of galaxies is dominated by the star

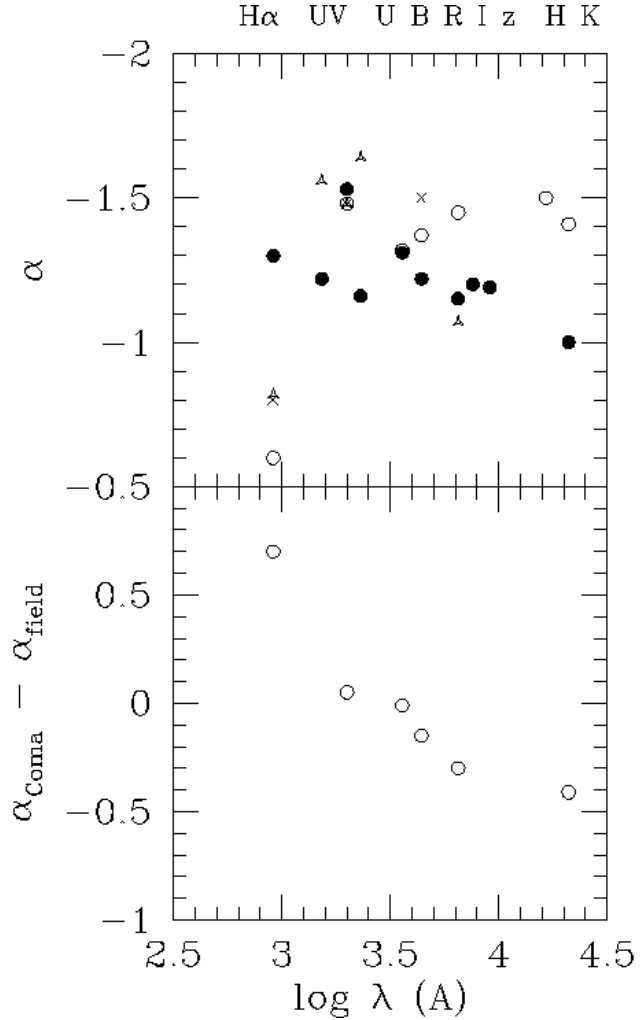


Fig. 13.— The wavelength dependence of the slope of the luminosity function for cluster and isolated galaxies (upper panel) and of the difference between α in Coma and in the “field” (lower panel). Filled symbols are for “field” galaxies, empty circles for Coma, triangles for A1367 and crosses for Virgo. For the clusters we took averages of the various luminosity functions available in the literature. For the “field” we used Blanton et al. (2001) in the visible, Gallego et al. (1995) in the $H\alpha$, Treyer (private communication) in the UV at 2000 Å and Wyder et al. (2005) in the UV GALEX bands. In the K band we averaged Cole et al. (2001) with Huang et al. (2003) and Kochanek et al. (2001).

formation activity ¹¹ the luminosity function is representative of the late-type galaxy population.

¹¹In elliptical galaxies the (faint) UV emission is not due to star formation, but to extreme Horizontal Branch stars and their progeny (O’Connell 1999): their contribution to the faint end slope of the UV luminosity function is significant because of the large number of E contributing at low luminosity (Cortese et al. 2003, 2005b)

Iglesias-Páramo et al. (2002) constructed the first $H\alpha$ luminosity function of cluster galaxies using a deep, wide field $H\alpha$ imaging survey of Coma and A1367 and compared it to that of Virgo. Despite their different nature (Coma is relaxed, spiral poor, A1367 relaxed spiral rich and Virgo unrelaxed spiral rich), the three clusters have a similar $H\alpha$ luminosity function with slope $\alpha(H\alpha) = -0.70 \pm 0.10$. In the bright luminosity range this slope is similar to that of the “field” determined by Gallego et al. (1995). At fainter luminosities it is significantly flatter than the poorly constrained ($\alpha(H\alpha) \sim -1.3$) found by Gallego et al. (1995).

The composite cluster UV luminosity function, obtained by combining balloon borne 1650-2000 Å data of Coma, A1367 and Virgo, has a slope $\alpha(UV) = -1.50 \pm 0.10$ (Cortese et al. 2003), consistent with the “field” one ($\alpha(UV) = -1.51$, Sullivan et al. (2000)). More recent results based on higher quality and deeper GALEX UV data of A1367 give a slope of the UV luminosity function ($\alpha(UV2310\text{\AA}) = -1.64 \pm 0.21$; $\alpha(UV1530\text{\AA}) = -1.56 \pm 0.19$; Cortese et al. (2005b)) significantly steeper than in the “field” ($\alpha(UV2310\text{\AA}) = -1.16 \pm 0.07$; $\alpha(UV1530\text{\AA}) = -1.22 \pm 0.07$; Wyder et al. (2005)). If limited to star forming galaxies, however, the cluster and “field” luminosity functions are similar (Cortese et al. 2005b).

We conclude that the cluster luminosity function is increasingly steeper than that in the “field” for $\lambda \geq 1500$ Å, and it is flatter for the ionizing radiation < 912 Å. The steepening of the cluster luminosity function with increasing λ is due to the increasing contribution of E-dEs toward longer wavelengths. The weight of E-dEs in the luminosity function is already significant in the UV bands while it vanishes only for $\lambda < 912$ Å.

3.3. Galactic kinematic disturbances

The presence of kinematic disturbances in late-type galaxies in clusters is controversial. Based on the analysis of long slit spectra, Rubin et al. (1988) and Whitmore et al. (1988) showed that the rotation curve of cluster galaxies strongly decline at outer radii, in particular in those galaxies located close to the cluster center, in contrast with the asymptotically flat or rising rotation curve of isolated objects. They also showed that most of the declining rotation curves are associated with HI-deficient galaxies (Rubin et al. 1988). This evidence was at that time interpreted as the result of stripping of the dark matter halo surrounding galaxies during galaxy-galaxy and/or galaxy-IGM interaction, or as the prevention of halo formation in the cluster environment (Whitmore et al. 1988).

This result was however questioned by Amram et al. (1993) who analyzed more accurate 2-D velocity fields of 21 cluster galaxies obtained with a Fabry-Perot spectrograph, finding flat (or smoothly declining) rotation curves.

More recently Rubin et al. (1999), in their analysis of long-slit rotation curves of 89 spiral galaxies in the Virgo cluster, reiterated that approximately one half of the Virgo galaxies show kinematic disturbances in their rotation curve (asymmetrical rotational velocities on the two sides of the major axis, falling outer velocities, inner velocity peculiarities, dips in the rotation velocities at intermediate radii, velocities near zero for the near nuclear gas). These disturbances are consistent

with recent (≤ 1 Gyr, the time necessary to re-distribute the mass within the disks in a few rotation cycles) tidal encounters or accretion events (see also Barton et al. (1999)). Disturbances are not correlated with Hubble type, luminosity, local galaxy density or HI deficiency. The authors claim that galaxies with perturbed rotation curves have a Gaussian velocity distribution peaked at the average cluster velocity, but they are often located at the cluster periphery, possibly on radial orbits.

Using a sample of 510 cluster galaxies with long slit spectroscopy, Dale et al. (2001) recently criticized this result. They maintained that the residual of the Tully-Fisher relation does not depend on the location of galaxies within clusters. They only observed that the rotation curve of galaxies in the periphery are more extended than in the galaxies close to the cluster core, consistent with their H α morphology. By analyzing the H α rotation curves of late-type galaxies in nearby clusters Vogt et al. (2004); Chemin et al. (2005) came to the similar conclusion that the distribution of HII regions along spiral disks is often truncated or asymmetric or perturbed. Asymmetric spirals are not observed beyond $1 h^{-1}\text{Mpc}$, and are found predominantly in the richest cluster cores. We conclude that, if any, mild differences exist between the kinematic properties of cluster and “field” galaxies.

3.4. Large scale velocity distributions, evidences for infall?

It is well known that the velocity distribution of cluster galaxies is type-dependent: while that of the early-type component is virialized, the one of late-types hardly follows a Gaussian distribution, being skewed toward highly deviating velocities (Biviano et al. 1997), probably because of their more elongated radial orbits, with higher elongations in late, star forming than in early-spirals (Biviano & Katgert 2004). By itself this provides an evidence for infall of late-type galaxies onto clusters (see e.g. Colless & Dunn (1996); Rines et al. (2003)).

Using the updated redshifts of Virgo (taken from GOLDmine) and new redshift determinations (Cortese et al. 2004) of galaxies in the central 1 deg regions of Coma and A1367 surveyed by Iglesias-Páramo et al. (2002, 2003) in the H α and r' band down to faint ($r' < 21$) magnitudes, we plot in Fig. 14 the velocity distributions of galaxies in these three clusters. For Virgo we divide early- from late-type galaxies according to the morphological classification given in the VCC. For Coma and A1367, where no such a reliable classification exists at this faint level, we use the H α line to discriminate between star forming and non star forming galaxies. It is apparent from the figure that in the three clusters the velocity distribution of the early type objects is Gaussian: $\langle V \rangle_{A1367} = 6347 \text{ km s}^{-1}$; $\delta V_{A1367} = 760 \text{ km s}^{-1}$, $\langle V \rangle_{Coma} = 6994 \text{ km s}^{-1}$; $\delta V_{Coma} = 1149 \text{ km s}^{-1}$, $\langle V \rangle_{Virgo} = 1202 \text{ km s}^{-1}$; $\delta V_{Virgo} = 753 \text{ km s}^{-1}$, while that of the late-type component is non-Gaussian, generally broader and with a significantly larger mean redshift. For this component a realistic estimate of the velocity dispersion is the one derived from the difference between the 25 and 75 percentiles of the redshift distribution: $\langle V \rangle_{A1367} = 7080 \text{ km s}^{-1}$; $\delta V_{A1367} = 1415 \text{ km s}^{-1}$, $\langle V \rangle_{Coma} = 7796 \text{ km s}^{-1}$; $\delta V_{Coma} = 1560 \text{ km s}^{-1}$, $\langle V \rangle_{Virgo} = 1340 \text{ km s}^{-1}$; $\delta V_{Virgo} = 1150 \text{ km s}^{-1}$. A consistent result for Virgo was obtained by Binggeli et al. (1987, 1993) and by Conselice

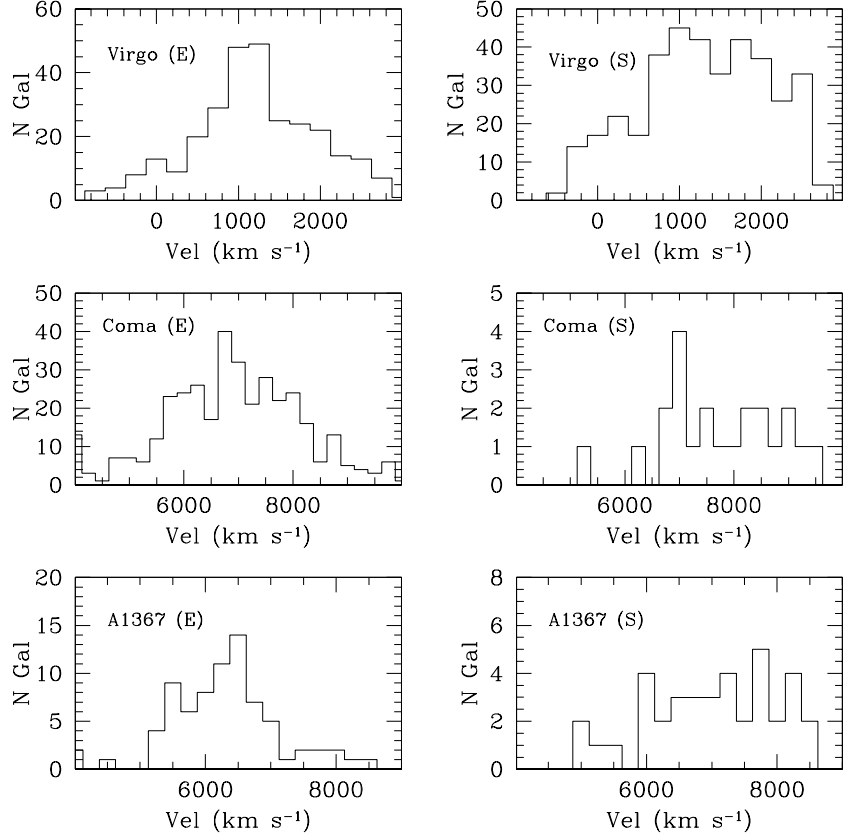


Fig. 14.— The velocity distribution of galaxies in the A1367, Coma and Virgo clusters, divided in early (left) and late-types (right).

et al. (2001) who also noticed that the velocity distribution of dE galaxies resembles more that of late-type galaxies than of Es. Similarly Colless & Dunn (1996) (see also Andreon (1996)) showed that the velocity dispersion of the late-type galaxies in the Coma cluster is $\sim \sqrt{2}$ that of the early type component, suggesting that spirals are free falling into the cluster core.

A direct proof of infall would require the knowledge of the galaxies trajectories in 3-D. Unfortunately the velocity component perpendicular to the line of sight cannot be measured, but, combining the line-of-sight component of the redshift with some independent distance estimate (e.g. from the Tully-Fisher or fundamental plane relation), the peculiar motions can be reconstructed (Tully & Shaya 1984)). Using these methods peculiar galaxy motions (up to 2000 km s⁻¹), induced by the cluster potential well, have been detected in several nearby clusters such as Virgo (Tully & Shaya 1984; Gavazzi et al. 1991b, 1999) and Coma (Gavazzi et al. 1991b).

The Coma cluster has been considered for a long time as the prototype of old, relaxed clusters. X-ray observations and dynamical studies (White et al. 1993; Colless & Dunn 1996; Briel et al. 2001), showed however that the structure of the cluster is formed by a massive main body centered

on the 2 cD galaxies NGC 4874 and 4889, and a less massive substructure centered on NGC 4839 infalling onto the main cluster. It is still unclear whether the NGC 4839 subgroup already crossed the cluster core or it is falling into it for the first time (Colless & Dunn 1996). The interaction between this substructure and the main cluster is probably the driver of the PSB galaxies observed by Caldwell et al. (1993) and Poggianti et al. (2004) (discussed in Section 3.5).

The dynamical study of A1367 (Cortese et al. 2004) revealed the presence of a relatively compact group with low velocity dispersion ($\sim 170 \text{ km s}^{-1}$) and composed of highly perturbed, star forming objects, falling into the main cluster at $\sim 1700 \text{ km s}^{-1}$ (see Sect. 4.10.3). There is also evidence of individual galaxies falling onto nearby clusters, such as CGCG 97-073 and CGCG 97-079 in A1367 (see sect. 4.10).

Because of its smaller distance (17 Mpc) and of its depth along the line of sight, the distance determination of galaxies within the Virgo cluster using the Tully-Fisher and the fundamental plane relation is sufficiently accurate to disentangle the 3-D structure of the cluster (Tully & Shaya 1984); directly proving the presence of infalling galaxies. Gavazzi et al. (1999) found that the distance of cluster A ($\mu_o = 30.78 \pm 0.07$), associated with M87, is consistent with the determination based on the Cepheid's method ($\mu_o = 31.0$). Cluster B, off-set to the south, is found at $\mu_o = 31.76 \pm 0.09$. This subcluster is falling onto A at about 500 km s^{-1} . Clouds W and M are at twice the distance of A. Their recessional velocity indicates that these clouds are in Hubble flow, thus little perturbed by the presence of Virgo. Galaxies on the North-West and South-East of the main cluster A belong to two clouds composed almost exclusively of spiral galaxies with distances consistent with A, but with significantly different velocity distributions, suggesting that they are falling onto cluster A at approximately 500 km s^{-1} from the far and near-side respectively. Moreover a significant fraction of gas "healthy" and currently star forming galaxies is unexpectedly found projected near the center of the Virgo cluster. Their average Tully-Fisher distance is found approximately one magnitude further away ($\mu_o = 31.77$) than that of their gas-deficient counterparts ($\mu_o = 30.85$). It is suggested that these gas healthy objects belong to a cloud that in fact lies a few Mpc behind Virgo, in the process of falling toward the Virgo cluster (Gavazzi et al. 2002b; Solanes et al. 2002). The velocity dispersion of each individual substructure is $\sim 500 \text{ km s}^{-1}$ (Binggeli et al. 1993; Gavazzi et al. 1999), resembling that of a formed cluster rather than a group.

3.5. The Spiral - S0 connection

When Van den Bergh discussed his morphology classification system, he pointed out the existence of "anemic" galaxies that might represent the missing link between normal spirals and lenticulars. They are characterized by an arm-interarm contrast less pronounced than normal spirals, they are gas-poor, with low star formation activity, redder colors than normal spirals with similar bulge to disk ratios. Their fraction is significantly larger in clusters such as Virgo than in the "field" (van den Bergh 1976). The "passive" spirals also inhabit several SDSS clusters at redshift $0.05 < z < 0.1$, but they are preferentially found outside the cluster's cores (Goto et al. 2003a). The

first interpretation of their existence was that, once the gas reservoir feeding the star formation is removed from cluster spirals, they become lenticulars (van den Bergh 1976). In a detailed analysis of the star forming properties of anemic galaxies, Elmegreen et al. (2002) concluded that their gas surface density is below the threshold for the star formation to take place. Because of the lack of supply of young stars with low velocity dispersion, the disk heats up, dumping spiral waves on time scales of a few revolutions (Sellwood & Carlberg 1984; Fuchs & von Linden 1998; Elmegreen et al. 2002). The anemic sequence would thus represent the intermediate phase between spirals and S0 (van den Bergh 1976). Koopmann & Kenney (1998) have quantitatively shown that the excess of early-type spiral galaxies in the Virgo cluster is partly due to misleading classifications of low-concentration (disk-dominated) systems with reduced star formation activity rather than to a systematic increase of the bulge to disk ratio with galaxy density. They interpreted this result as an evidence that these low-concentration early-type spirals were blue, star forming late-type spirals whose activity was quenched by gas removal induced by their interaction with the ICM. There exist, however, several observational evidences indicating that lenticular galaxies in nearby clusters are not gas stripped late-type galaxies. Dressler (1980) showed that the bulge size and the bulge-to-disk ratio of lenticulars are systematically larger than those of spirals in all density regimes. He thus concluded that “since the tightly bound inner bulges should be unaffected by ablation, the dissimilarity in the bulge and bulge/disk distributions in all density regimes is inconsistent with the idea that most S0 galaxies result from the removal of disk gas from a spiral by ram-pressure stripping or evaporation” (Dressler 1980; Burstein 1979; Gisler 1980).

We checked this conclusion using our near-IR survey of the Virgo cluster. These H -band imaging data, beside a better photometric quality due to the linear response of the NICMOS-3 detectors compared to the photographic plates of Dressler (1980), have the advantage of being free from dust obscuration and from relatively recent episodes of star formation which might alter the morphological properties of galaxies. The H band Kormendy relation between the effective surface brightness μ_e and the effective radii R_e (radii including half of the total light) for lenticulars and spirals of type Sa-Sb in the Virgo cluster is given in Fig. 15. Sa-Sbs have, on average 0.65 mag arcsec $^{-2}$ lower surface brightness and almost a factor of 2 larger effective radii than lenticulars. This confirms the results of Dressler (1980) and makes the formation of lenticulars through gas sweeping in spirals very unlikely. This conclusion was recently confirmed by Christlein & Zabludoff (2004) who found that the bulge to disk ratio increases in cluster galaxies because of the increase of the bulge luminosity (as expected in a tidal interaction scenario) and not because of the fading of the disk luminosity (as expected in a ICM-IGM interaction).

Spectroscopic observations of 125 early-type galaxies in the Coma cluster revealed the presence of a significant number of objects with signs of recent star formation, such as Balmer absorption and emission lines and negative CN/H8 indices (Caldwell et al. 1993). The spectroscopic characteristics of these galaxies are similar to those of post-starburst galaxies observed in intermediate-redshift clusters, the so called E+A galaxies (Caldwell et al. 1993). Interestingly most E+A galaxies were found in the south west periphery of the Coma cluster, probably associated with the NGC 4839

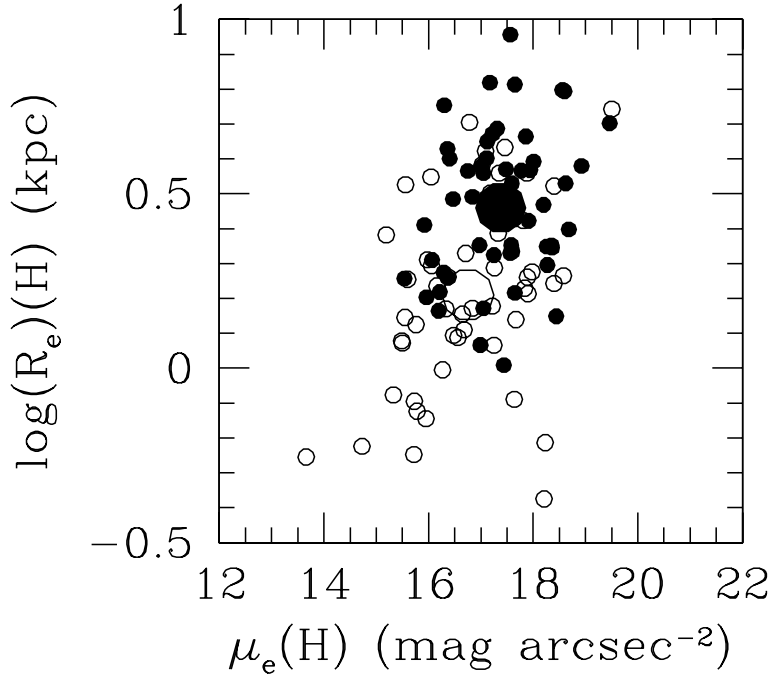


Fig. 15.— The relationship between the H band effective radius and effective surface brightness in the Virgo cluster. Open symbols are for S0 galaxies, filled symbols for Sa-Sb galaxies. Large symbols represents averages.

group, but with a larger velocity dispersion than the remaining early-type galaxies belonging to the same group (Caldwell et al. 1993).

HST images of some starburst or post-starburst galaxies in the Coma periphery revealed that they have exponential disks, some with an embedded central spiral, whereas kinematic data showed rotation curves typical of late-type galaxies (Caldwell et al. 1996, 1999).

The analysis of Poggianti et al. (2001a,b) of ~ 300 early-type galaxies in the Coma cluster confirmed most of the Caldwell et al. results. Using several spectral indices in the visible bands, these authors were able to discriminate between age and metallicity effects, and concluded that more than 40% of the low luminosity ($M_B > -19$) S0s in Coma undergone star formation episodes in the last ~ 5 Gyr, significantly later than elliptical galaxies.

Poggianti et al. (2004) found that $k+a/a+k$ galaxies (post starburst/post-star forming galaxies with no current star formation activity that were forming stars at a vigorous rate in the last 1.5 Gyrs, as indicated by their high Balmer absorption lines ($H\delta E.W. \geq 5 \text{ \AA}$)) in Coma are all low luminosity objects ($M_V > -18.5$), thus significantly different from the high luminosity ones ($M_V \leq -20$) observed in high redshift clusters. They have also shown that these post starburst/post-star forming galaxies spatially correlate with substructures in the hot IGM, as revealed by the XMM-Newton

data, are located in the central ~ 1.4 Mpc of the cluster and have radial velocities significantly higher than the cluster mean. These evidences were interpreted as an indication that the activity of this population of low-luminosity, post-star forming galaxies was quenched (and boosted) by the interaction with the dense ICM (Poggianti et al. 2004).

How does the star formation history of early-type (Sa-Sb) spiral galaxies compares with that of normal (non-PSB) S0? To try constraining their star formation histories by fitting the UV to near-IR SEDs with Bruzual & Charlot (1993) stellar population synthesis models (as outlined in Section 2.6) Gavazzi et al. (2002a) concluded that S0-S0a have on average slightly smaller τ_S than early-type spirals of similar luminosity, indicating that the bulk of the star formation activity in lenticulars is older than in spirals.

Kinematic studies of nearby cluster and “field” S0 argue for a different nature of spirals and lenticulars. The larger scatter and a small zero point offset in the Tully-Fisher relation observed in Virgo and Coma cluster S0 galaxies compared to spirals indicate that lenticulars can hardly be formed by simple gas removal from healthy spirals. On the contrary it is argued that S0s are formed during minor mergers, slow encounters, harassment, or some combination of these, making S0s an heterogeneous class of objects (Dressler & Sandage 1983; Neistein et al. 1999; Hinz et al. 2003). Other statistical considerations such as the extremely weak dependence of the morphology segregation effect on galaxy density (the fraction of spiral galaxies changes by a factor of ~ 2 over a change of ~ 1000 in galaxy space density) are hardly explained by a simple transformation of spirals into S0 through ram pressure stripping, as noticed by Dressler (1980) and Dressler (2004), but seem to indicate that the morphology of galaxies was settled shortly after their birth, before the dense cluster environment was even formed.

In conclusion, while lenticular and quiescent early-type spirals have nearly indistinguishable stellar populations, significant differences in their structural and kinematic properties as well as statistical considerations argue against the origin of high mass S0s in nearby clusters from gas removal of spiral disks. On the contrary, low-luminosity disk-dominated S0 might be the result of ram-pressure stripping in late-type galaxies.

4. The physical processes acting in clusters

The analysis presented so far has shown that late-type galaxies in nearby clusters differ systematically from their field counterparts mainly in two respects: they are significantly HI-deficient and are characterized by a lower activity of star formation, with truncated HI and star forming disks. Other less clearcut differences are their molecular gas content, metallicity, cold dust content, kinematical perturbations and radio-continuum synchrotron emission. While in massive spirals the HI-deficiency and suppression of the star formation depend on the distance from the cluster center (provided that they are within 1-2 virial radii), in dwarf irregulars they depend primarily on the galaxy luminosity and very little on the clustercentric position.

Which are the physical processes that produced such differences? Are the physical conditions in today’s high density environments similar to the ones prevailing in the young universe when the

Table 1: The adopted parameters of clusters Coma, A1367 and Virgo.

<i>Cluster</i>	$\langle V \rangle$ km s $^{-1}$	$\delta V_{cluster}$ km s $^{-1}$	<i>ref</i>	ρ_{IGM} atom cm $^{-3}$	<i>ref</i>	T_{IGM} keV	<i>ref</i>	R_c kpc	<i>ref</i>	R_{vir} Mpc	<i>ref</i>	$M_{cluster}$ M \odot	<i>ref</i>
<i>Coma</i>	6960	880 (1560) ^a	1	$3.12 \cdot 10^{-3}$	3	8.2	3	257	3	2.19	7	$1.2 \cdot 10^{15}$	2
<i>A1367</i>	6420	822 (1415) ^a	1	$1.25 \cdot 10^{-3}$	3	3.5	3	240	3	2.13	7	$6.9 \cdot 10^{14}$	7
<i>Virgo</i>	951	886 (1150) ^a	4	$2.00 \cdot 10^{-3}$	5	2.3	8	130	5	1.68	7	$2.5 \cdot 10^{14}$	6

References: 1: Struble & Rood (1991); 2: Briel et al. (1992); 3: Mohr et al. (1999); 4: Binggeli et al. (1993) (spirals in the core of cluster A); 5: Böhringer, private communication; 6: Schindler et al. (1999) (the total mass is here calculated as the sum of the M87, M49 and M86 total extended masses); 7: Girardi et al. (1998); 8: Böhringer et al. (1994)

a: the velocity dispersion of the cluster as a whole and of the late-type component alone (in parenthesis), from this work.

morphology segregation was shaped? In other words, are the processes that transformed late-type galaxies into quiescent lenticulars in the past still able to modify the late-type galaxies that are currently infalling nearby clusters? Trying to answer these questions we now briefly review the physical processes that are believed to describe the interaction of galaxies in high density environments. The comparison of model predictions with observations is particularly well suited in the nearby Universe where the multifrequency observations have high spatial resolution.

Two broad classes of models are here considered: first the gravitational ones, including all sorts of tidal interactions (galaxy-galaxy, galaxy-cluster, harassment), then the hydrodynamical interactions taking place between the galaxy's ISM and the hot intergalactic medium (ram-pressure, viscous stripping, thermal evaporation). We also briefly review two hybrid processes: "starvation" (removal of the gas feeding the star formation) and "pre-processing" (taking place in groups of galaxies falling into clusters) that combine gravitational with hydrodynamic mechanisms.

4.1. Tidal interactions among galaxies

Tidal interactions among galaxy pairs act on gas, dust and stars, as well as on dark matter, with an efficiency depending on the gravitational bounding of the various components. This produces selective morphological transformations. Since tidal forces act as M/R^3 , if the typical galaxy radii are not too small compared to the average separation between galaxies, tidal interactions can be quite efficient at removing matter from galactic halos (Spitzer & Baade 1951; Richstone 1976; Farouki & Shapiro 1981; Icke 1985; Merritt 1983). As shown by the numerical simulations of Valluri & Jog (1990), tidal interactions are more efficient in perturbing the loose peripheral or extra-planar HI gas, than the molecular gas, located in the inner potential well. For what concerns the star formation, both observations (Keel et al. 1985; Kennicutt et al. 1987; Hummel et al. 1990; Condon et al. 1982) and simulations (Mihos et al. 1992; Iono et al. 2004) of interacting pairs show a major

increase of the nuclear activity and a milder (if any) in the disk.

It is intuitive that tidal interactions among galaxies are boosted in the dense cores of rich clusters of galaxies. However, due to the high relative velocities, tidal interactions among cluster galaxies, although more frequent, have significantly shorter duration than in the “field” ($t_{enc} \sim 10^8$ yr, see Appendix), thus the effects of the perturbation are less severe. For instance, the formation of bars, that is expected to take place in slow encounters, should be relatively rare in clusters (Mihos 2004). The simulations of Byrd & Valtonen (1990) (applied to spiral galaxies in clusters) show that tidal interactions produce enough gas inflow from the disk to the circumnuclear regions, provided that the perturbation parameter:

$$P_{gg} = (M_{comp}/M_{gal})/(d/r_{gal})^3 \quad (6)$$

is $P_{gg} \geq 0.006\text{-}0.1$ (depending on the halo to disk mass ratio), where M_{comp} is the companion mass, M_{gal} and r_{gal} are the mass and the visible disk radius of the spiral galaxy respectively and d is the separation between the two galaxies. A typical perturbation parameter P_{gg} for ~ 10 kpc radii galaxies in clusters can be roughly estimated assuming $M_{comp} \simeq M_{gal}$ and an average galaxy separation $\simeq 200$ kpc inside a cluster of 2 Mpc radius including ~ 1000 objects. The resulting $P_{gg} \simeq 10^{-4}$ is significantly smaller than the critical P_{gg} necessary for producing significant gas infall into the nucleus. This simple estimate is confirmed by Fujita (1998), who claims that the typical perturbation induced by a single high-speed encounter among cluster galaxies is too small to significantly affect the star formation rate. His model incorporates a more realistic modeling of the star formation process based on clouds collisions, than the simple nuclear infall treated by Byrd & Valtonen (1990). Furthermore, as discussed by Merritt (1984) and by Byrd & Valtonen (1990), the frequency of galaxy-galaxy encounters in rich clusters, as measured by the inverse of the relaxation time $t_{relax} \sim$ some 10^{10} years (see Table 2 and section 6), comparable to the age of the Universe, is negligibly small (see however Valluri & Jog (1990)).

Okamoto & Nagashima (2001) and Diaferio et al. (2001) with their hybrid N -body simulation and semi-analytical models, tried to reproduce the cluster morphology-density or morphology-radius relations observed by Whitmore et al. (1993). They concluded that, while the distribution of elliptical galaxies in clusters can be obtained with major merging, this is not the case for the lenticular galaxies with intermediate bulge to disk ratios. Bulges can be formed by the merging of two equal mass galaxies, while the subsequent gas cooling can form disks (Diaferio et al. 2001) by unequal mass mergers of disk galaxies, where disk destruction is not complete and some rotation is retained, or minor mergers between spirals and their companions (the disk is heated but not destroyed). The morphology segregation is qualitatively well reproduced by the semi-analytical simulation of Springel et al. (2001). Okamoto & Nagashima (2003), however, remarked that this result is very sensitive to the assumed bulge to disk ratio of lenticular galaxies.

Typical examples of cluster galaxies which recently underwent a gravitational interaction are NGC 4438 and NGC 4435 in Virgo (see sect. 4.10). Tidally interacting objects in clusters are relatively difficult to identify since tidal tracers are very short-lived: while in the field most of the ejected material in tidal tails remains bounded to the main galaxy, in clusters the tidal field strips the unbound material, maybe originating the diffuse intergalactic light (Mihos 2004).

4.2. Tidal interaction between galaxies and the cluster potential well

Given the large mass of clusters, exceeding 10^{14} M_\odot , tidal interactions between galaxies and the whole cluster potential well can effectively perturb cluster galaxies, inducing gas inflow, bar formation, nuclear and perhaps disk star formation (Merritt 1984; Miller 1986; Byrd & Valtonen 1990). Depending on the impact parameter, the disk structure can be perturbed, forming a spiral pattern (if the disk is parallel to the orbital plane), or developing a bulge (disk perpendicular or inclined with respect to the orbital plane, (Valluri 1993)). In any case the thickness of the disk is expected to increase slightly (Valluri 1993). Tidally perturbed disk galaxies in clusters, due to the increased non-circular velocities of stars can produce declining rotation curves at large radii (Valluri 1994).

The models of Fujita (1998), Valluri (1993) and Henriksen & Byrd (1996) show that tidal forces by the cluster potential well can accelerate molecular clouds of disk galaxies falling toward the cluster center. The rise of the kinetic pressure in the interstellar medium induces star formation (Elmegreen & Efremov 1997).

The efficiency of the interaction can be quantified by the perturbation parameter P_{gc} defined as (Byrd & Valtonen 1990)¹²:

$$P_{gc} = (M_{\text{cluster}}/M_{\text{gal}}) \times (R/r_{\text{gal}})^{-3} \quad (7)$$

where R is the distance of the galaxy from the cluster center. When the perturbation parameter becomes critical ($P_{gc} \sim 0.006\text{--}0.1$), the gas in the disk is driven toward the center of the galaxy on time scales of $2\text{--}3 \times 10^8 \text{ yr}$, triggering nuclear activity (Byrd & Valtonen 1990).

For a perturbation parameter close to the critical value, however, the interaction is unable to remove the outer gas producing the observed HI-deficiency of cluster galaxies (Byrd & Valtonen 1990). Byrd & Valtonen (1990) and Henriksen & Byrd (1996) speculate that the poorly gravitationally bound HI would be ejected from the galactic plane by supernova winds driven by the enhanced star formation activity. The effects of the interaction on the inner gaseous component are less clear. The molecular gas, shielded deeper inside the galaxy potential well would not be ejected, but consumed by star formation events on longer time scales.

The perturbation parameter for Coma, A1367 and Virgo galaxies can be derived using the empirical mass vs. diameter relation:

$$\text{Log}(M_{\text{gal}}) \text{ (M}_\odot\text{)} = 8.46 + 2.37 \times \text{Log}(r_{\text{gal}}) \quad (\text{kpc})$$

For the largest galaxies ($r_{\text{gal}}=30 \text{ kpc}$) we find on average $P_{gc}=0.28$ for Coma, 0.16 for A1367 and 0.06 for Virgo, at a typical distance of $R=500 \text{ kpc}$ from the cluster center. Figure 16 shows that

¹² P_{gc} as determined using eq. 7 and r_{tidal} given by eq. 8 must be considered as indicative since both equations are based on the hypothesis that the cluster potential is dominated by a unique dark matter halo and do not account for perturbations by the halos of individual galaxies. A more accurate estimate of both parameters requires N-body simulations to account for these non-linear effects.

the perturbation parameter becomes critical ($P_{gc} \sim 0.1$) first for large galaxies passing within few hundred kpc of the cluster center. Notice also that the perturbation parameter, at any given distance from the cluster center increases with the galaxy size (luminosity). Since the local tidal

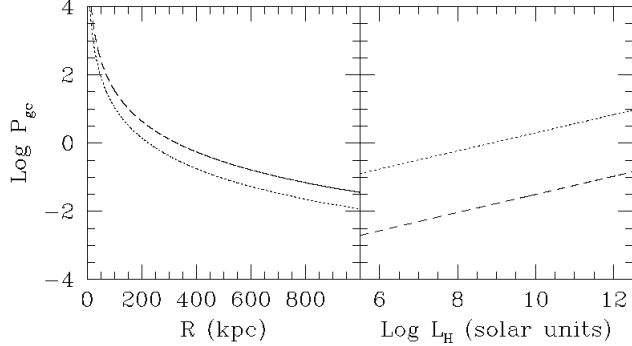


Fig. 16.— The logarithm of the perturbation parameter, defined in eq. 7, is plotted as a function of the distance from the cluster center (left panel) for Coma galaxies of linear radius 30 and 5 kpc respectively (top to bottom) and as a function of the H band luminosity (right panel) for Coma galaxies at 200 and 800 kpc (top to bottom) from the cluster center.

field varies as the inverse cube of the separation, and since this quantity is much larger than the typical size of spiral galaxies, disturbances are expected to be symmetric, contrary to galaxy-galaxy interactions (Byrd & Valtonen 1990).

Gas removal can take place only outside the tidal radius r_{tidal} (the galactocentric distance up to which the perturbation is effective in removing material) which can be estimated for galaxies near the core radius R_c ¹³ of the Coma, A1367 and Virgo clusters using the cluster parameters listed in Table 1 and (Merritt 1984):

$$r_{tidal}/R_c \sim 0.5 \times \Delta V_{gal}/\delta V_{cluster} \quad (8)$$

where ΔV_{gal} and $\delta V_{cluster}$ are the rotational velocity of the galaxy and the cluster velocity dispersion respectively. Using an empirical relationship between the optical radius and the rotational velocity:

$$\Delta V_{gal} = 21.55 \times r_{gal} \text{ (kpc)} + 50.00 \quad (\text{km s}^{-1})$$

we can estimate the tidal radius r_{tidal} at the core radii of the three clusters as a function of the galaxy optical radii:

$r_{tidal}(\text{Coma}) = 3.15 r_{gal} + 7.30$ kpc, $r_{tidal}(\text{A1367}) = 3.15 r_{gal} + 7.30$ kpc and $r_{tidal}(\text{Virgo}) = 1.58 r_{gal} + 3.67$ kpc. The truncation radius of galaxies in Coma and A1367 is thus significantly larger than the optical and even of the HI radius (which is ~ 1.8 times larger than the optical one, Cayatte et al. (1994)), while it is comparable to the HI radius in Virgo.

In conclusion, tidal interactions with the cluster potential can induce an increase of the nuclear

¹³The lowest values for the tidal radius are expected close to the core radius (Merritt 1984)

activity of cluster galaxies and, eventually, a decrease of the total gas amount consumed through star formation events. On the other hand, gas can be hardly removed directly by the interaction.

4.3. Galaxy harassment

Moore et al. (1996, 1998, 1999) proposed that the evolution of cluster galaxies is governed by the combined effect of multiple high speed galaxy-galaxy close (~ 50 kpc) encounters with the interaction with the potential of the cluster as a whole, a process that they named “galaxy harassment”. Harassment depends on the collisional frequency, on the strength of the individual collisions, on the cluster’s tidal field and on the distribution of the potential within galaxies.

Moore et al. simulations show that, at a fixed mean orbital radius, galaxies on elongated orbits experience greater harassment than objects on circular orbits. The multiple encounters heat the stellar component increasing the velocity dispersion and decreasing the angular momentum, meanwhile they make the gas to sink toward the galaxy center (Moore et al. 1996).

Because of their different potential distribution, massive and dwarf galaxies react differently to galaxy harassment. N-body (both pure gravitational and hydro-dynamical) simulations of low-mass ($L_*/5$ and $L_*/20$) spirals (represented by rotating exponential disks) in a Coma-like cluster show that, at any given galaxy radius, dark matter is more easily stripped than stars because of the different orbital distribution of the two components. At early stages a large fraction (up to 50%) of the stars are removed; the subsequent increase of binding energy, caused by the increase of the central density, makes further star stripping less efficient. The obtained stellar profiles are exponentials, when only stars are included in the initial conditions, and nucleated exponentials when the gas is added (Moore et al. 1998). All these properties, including the observed increase of the velocity dispersion, mimic those of cluster spheroidals. The simulations also show that the smallest spheroidals are destroyed in the inner (half of the virial radius) cluster. Only the densest and/or the nucleated objects would survive longer. Another model prediction is that nucleated objects have higher velocity dispersion than normal spheroidals¹⁴.

The evolution of bright disk galaxies ($\sim L_*$) in clusters differs from that of low-mass systems, as it depends primarily on the depth of their potential wells and on the disk scale length. High surface brightness galaxies, those with central steeply rising rotation curves, are found relatively stable to galaxy harassment. Beside minor star losses, the effect of the interaction is a small (0.5 mag arcsec^{-2}) increase of the central surface brightness, an increase of the disk scale height (by a factor of 2-4) and of the central velocity dispersion, with the fading of spiral features (Moore et al. 1999). These structural and kinematic properties resemble those of bright lenticulars.

Low surface brightness galaxies, because of their low mass concentration (flat rotation curves and large disk scale lengths), are strongly perturbed by the interaction. They are expected to loose

¹⁴The velocity dispersion of normal dwarf ellipticals and spheroidals in Virgo cluster A is slightly ($\sim 10\%$) smaller than that of their nucleated counterparts

most (up to 50-90 %) of their stars (the progenitors of the diffuse cluster light?), to increase their central velocity dispersion and consequently their central surface brightness by ~ 2 mag arcsec $^{-2}$ (Moore et al. 1999). Their resulting kinematic and structural properties resemble those of dE/dS0. An increased star formation activity is expected because of the central accumulation of gas and of the heating of molecular clouds, increasing the probability of cloud-cloud encounters, as shown by the models of Fujita (1998).

The recent simulations of Virgo like clusters by Gnedin (2003) adopting various cosmologies ($\Omega_0=1$, 0.4 with and without Λ) show that tidal heating is more effective in low- Ω_0 clusters. The maximum of the tidal forces do not always happen close to the cluster center, but during the encounters with massive galaxies or with unvirialized remnants of infalling groups of galaxies. These simulations also show that the collision rate of galaxies increases by 10-50% in the presence of substructures. In conclusion, galaxy harassment can effectively perturb low-luminosity galaxies because of their low-density cores and slowly rising rotation curves, thus contributing to the formation of cluster dwarf ellipticals (Moore et al. 1998), to the fueling of low-luminosity AGNs (Lake et al. 1998) and to the destruction of low surface brightness galaxies in clusters (Moore et al. 1999). The effects on massive objects should be less pronounced, with a minor increase of the disk star formation activity (Mihos 2004) and an increase of the velocity dispersion in the bulge (Moore et al. 1996).

4.4. Ram-pressure

Gunn & Gott (1972) first proposed that the ISM could be removed from galaxies moving at ~ 1000 km s $^{-1}$ through the hot ($\sim 10^7$ - 10^8 K) and dense ($\sim 10^{-3}$ - 10^{-4} atoms cm $^{-3}$) intergalactic medium by the ram-pressure mechanism. The interpretation of head-tail radio galaxies (Miley et al. 1972) in the ram-pressure scenario brought to the prediction of a dense IGM in clusters of galaxies before X-ray observations actually detected it (Gursky et al. 1972).

Ram-pressure can effectively remove the ISM if it overcomes the gravitational pressure anchoring the gas to the disk:

$$\rho_{IGM} V_{gal}^2 \geq 2\pi G \Sigma_{star} \Sigma_{gas} \quad (9)$$

where ρ_{IGM} is the density of the IGM, V_{gal} the galaxy velocity inside the cluster, Σ_{star} is the star surface density and Σ_{gas} the gas surface density.

A plethora of N-body and SPH simulations exists in the literature trying to investigate the role of ram-pressure on gas stripping of both cluster early- and late-type galaxies, and on the possible transformation of spiral into lenticular galaxies, or of dwarf irregulars into dSph.

The various models (SPH, N-body) differ in the way they account for the cluster gas distribution (density profile), the galaxy orbits within the cluster (radial, circular, galaxy inclination with respect to the orbit), the potential distribution within the galaxy (disk vs. bulge, with or without dark matter), the star formation (gas consumption and replenishment by recycled gas), the contribution of viscosity and/or thermal evaporation. In spite of these differences, assuming typical IGM densities and velocity dispersions observed in nearby clusters, all variations of the model concur at

establishing that ram-pressure is sufficient to remove part of the ISM from galaxies on time scales comparable with their cluster crossing time (a few 10^9 yr, see Sect. 6).

Radial orbits are more efficient because of the higher velocity, closer crossing to the cluster core (Abadi et al. 1999; Quilis et al. 2000; Vollmer et al. 2001b). The efficiency of removal depends on the inclination of the galaxy disk with respect to the trajectory, with face-on interactions more efficient than edge-on or inclined encounters (Abadi et al. 1999; Quilis et al. 2000; Vollmer et al. 2001b). However spiral galaxies on radial orbits should end up stripped because their interaction with the cluster IGM will sooner or later become face-on since the orientation of the galaxy rotation axis is conserved (Quilis et al. 2000). Because of their shallower potential well, gas removal is expected to act more efficiently on dwarf irregular galaxies than on giant spirals (Mori & Burkert 2000; Marcolini et al. 2003). Models indicate that the ram-pressure efficiency is higher if the galaxy ISM has a multiphase structure, containing bubbles, shells and holes ranging in size from a few parsec to a kiloparsec, and if it is taken into account that HI disks are centrally depleted even in isolated galaxies (Quilis et al. 2000).

Before leading to a complete gas ablation, ram-pressure produces significant compression ahead of the galaxy, with the possible formation of a bow-shock and of a low density gaseous tail behind, giving to the galaxy a cometary shape (Balsara et al. 1994; Stevens et al. 1999; Murakami & Babul 1999; Quilis et al. 2000; Mori & Burkert 2000). When the interaction is close to edge-on the central gas density can increase by a factor of ~ 1.5 (Vollmer et al. 2001b), because the outer HI is captured by the inner disk. The distribution of the HI gas can be very asymmetric, depending on the impact parameters (Vollmer et al. 2001b). Only clouds with a surface density $< 4 \cdot 10^{-3} \text{ g cm}^{-2}$ can be swept out of the galaxy. Since molecular clouds have surface densities of the order of $10^{-2} \text{ g cm}^{-2}$, they are mostly unaffected by the interaction (Quilis et al. 2000), although the gas compression can facilitate the collapse of molecular clouds, thereby increasing the star formation rate (Bekki & Couch 2003).

Tosa (1994) shows that ram-pressure generates a single-armed spiral structure in the galactic gas, with the spiral pattern having a retrograde rotation, while ring-like features can form in the inner disk (Sofue & Wakamatsu 1993; Schulz & Struck 2001). The models of Schulz & Struck (2001) also show that the displacement of the gas with respect to the disk can trigger gravitational instabilities, with the formation of flocculent spirals. These spiral arms transport angular momentum outward, compressing the inner disk and forming a prominent gas ring. Inclined galaxies experience less gas removal but a larger angular momentum loss than face-on events (Schulz & Struck 2001).

Gas can be accreted from the downstream side into the core (Balsara et al. 1994; Vollmer et al. 2001b; Schulz & Struck 2001), in particular in retrograde encounters, where the loss of angular momentum can create a galactic disk (Sofue & Wakamatsu 1993). In the case of edge-on stripping more than 50% of the stripped gas can be re-accreted, whereas in face-on encounters the fraction of re-accreted gas is significantly smaller (Vollmer et al. 2001b). This re-accreted gas might temporarily increase the disk surface density (Vollmer et al. 2001b).

The hydrodynamic interaction between the hot IGM and the cold ISM leads to an increase of the external pressure, the formation of bow-shocks, thermal instabilities and turbulent motions within

the disk of the galaxy. All these phenomena increase cloud-cloud collisions, cloud collapse, and can thus be responsible for an enhanced star formation activity of cluster galaxies (Evrard 1991; Bekki & Couch 2003). By modeling pressure variations of the ISM due to ram-pressure, combined with HI to H₂ gas transformation (molecular cloud formation and destruction) and HI sweeping, Fujita (1998) and Fujita & Nagashima (1999) quantified the variations of the star formation activity following the formalism of Elmegreen & Efremov (1997). Their models show that on short time scales ($\sim 10^8$ yr) in high density, rich clusters the star formation activity can increase up to a factor of 2 at most. On longer timescales, however, the removal of the HI gas reservoir leads to a decrease of the fuel feeding the star formation, and galaxies become quiescent (Fujita 1998; Fujita & Nagashima 1999; Okamoto & Nagashima 2001). This mild increase of the star formation activity is however not observed in models with low gas density and shallow potential clusters.

A decrease of the molecular gas content of cluster disk galaxies (up to $\sim 80\%$) is expected from the gas consumption due to the increase of star formation activity (from 0.1 to 0.5 $M_\odot \text{ yr}^{-1}$ 8 Myr after the cloud collapse; Bekki & Couch (2003)) and not from gas removal during the interaction. It is interesting to note that in clusters with typical gas temperature and velocity dispersion, the increase of star formation is higher during the transit in the cluster outskirts, where the IGM density is lower, than near the cluster center where gas removal by ram-pressure suppresses the star formation (Bekki & Couch 2003).

The old stellar component is unperturbed during ram-pressure interactions (Quilis et al. 2000). For face-on interactions, however, the gas escaping from the plane can induce tidal forces on the galaxy stellar disk shallowing the potential well on time scales comparable with the time scale for gas stripping (\sim some 10^8 yr). These forces can increase the velocity dispersion perpendicular to the disk, thickening the stellar disk. The N-body simulations of Farouki & Shapiro (1980) showed that the thickening of the disk is possible only in the outer disk since only there the gas is removed, leaving the inner disk unaffected. It is thus unlikely that ram-pressure formed the thick and large bulges of S0s (Farouki & Shapiro 1980). Schulz & Struck (2001) speculated however that successive crossing of the cluster can produce cycles of annealing, which might form the prominent bulges typical of S0s.

If ram-pressure is responsible for the HI ablation in clusters we would expect from Eq. 9 a correlation between the HI-deficiency parameter and $\rho_{IGM} V_{gal}^2 / 2\pi G \Sigma_{star} \Sigma_{gas}$. Let's check the calculation for 3 nearby clusters, Coma, A1367 and Virgo (as usual using data from GOLDmine). We assume $\delta V_{cluster}$ (for the late-type component) and ρ_{IGM} from Table 1 and let $V_{gal} = \sqrt{3\delta V_{cluster}^2}$. The stellar surface density within the optical diameter (in units of g cm^{-2}) can be estimated from the *H* band luminosity, assuming a mass to light ratio of 4.6 (Gavazzi et al. 1996):

$$\Sigma_{star} = \frac{4.6 L_H}{\pi (a/2)^2} \quad (10)$$

where L_H is the *H* band luminosity and a is the optical major diameter. The estimate of Σ_{star} is simply an average over the entire galaxy, without assuming a realistic stellar distribution. As shown in Fig. 17, the stellar surface density correlates with the total galaxy mass, as traced by the *H* band luminosity: $\text{Log} \Sigma_{star} = -4.310 + 0.296 \text{ Log} L_H$ (g cm^{-2}).

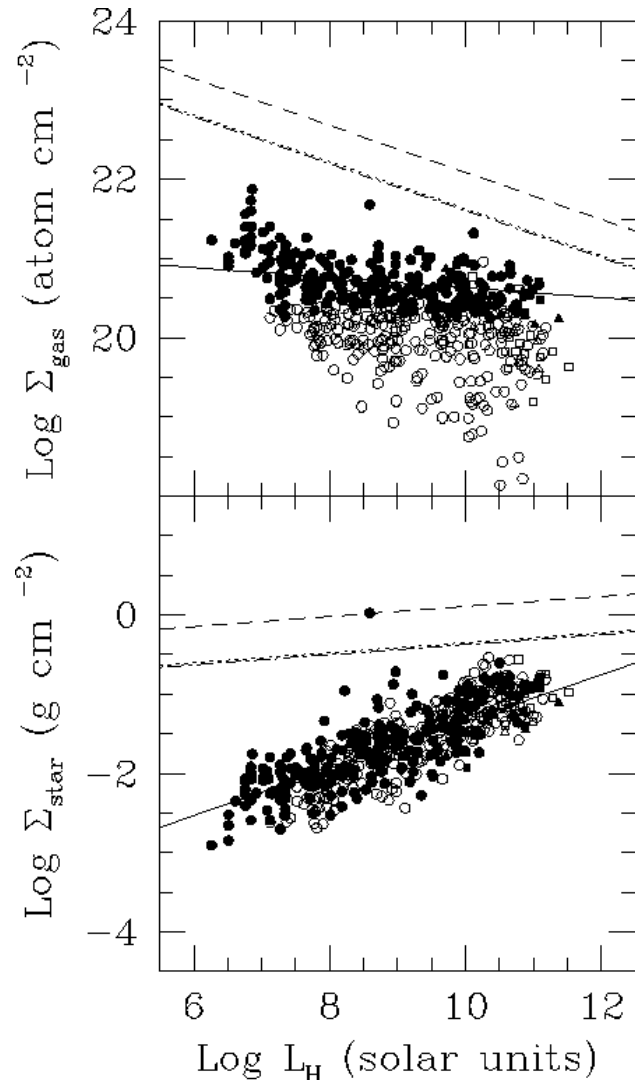


Fig. 17.— The relationship between the logarithm of the gas surface density (upper panel), the stellar surface density (lower panel) and the logarithm of the H band luminosity. Filled symbols are for galaxies with a normal HI content (HI deficiency ≤ 0.3), empty symbols for deficient objects (HI deficiency > 0.3). Squares are for Coma, triangles for A1367 and circles for Virgo objects. The continuum line represents the best fit to the data (for the gas surface density only non-deficient galaxies are fitted). The dashed, dot-dashed and dotted lines indicate the upper limits to the gas and stellar densities for an efficient ram-pressure stripping for Coma, A1367 and Virgo respectively.

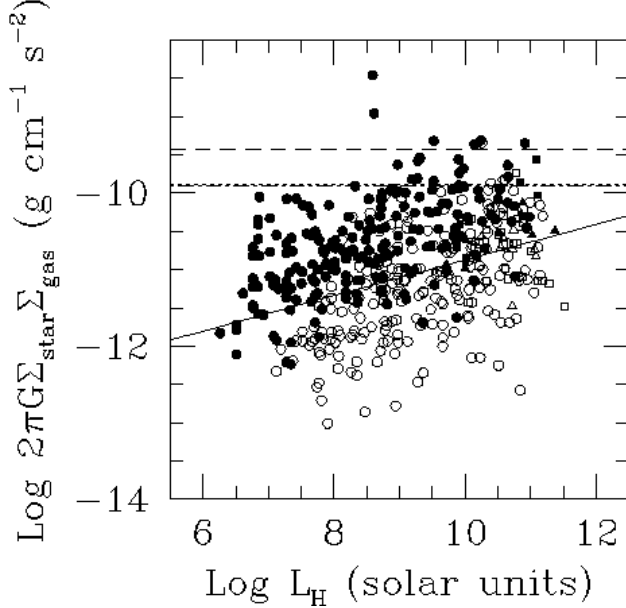


Fig. 18.— The relationship between the gravitational forces per unit area and the H band luminosity. Filled symbols are for galaxies with a normal HI content (HI deficiency ≤ 0.3), empty symbols for deficient objects (HI deficiency > 0.3), with squares for Coma, triangles for A1367 and circles for Virgo. The dashed, dotted-dashed and dotted lines indicate the upper limit to the gravitational pressure for an efficient ram-pressure stripping for Coma, A1367 and Virgo cluster galaxies respectively. The continuum line gives the fit to the data obtained by combining the best fits in Fig. 17.

The gas surface density Σ_{gas} (in units of cm^{-2}) involved in Eq. 9 can be determined adding the HI and H_2 mass estimates (when H_2 is available from Boselli et al. (2002), or assuming that H_2 is on average 15% of the total HI gas), and assuming that the HI gas diameter is ~ 1.8 times larger than the optical one¹⁵:

$$\Sigma_{gas} = \frac{M(\text{HI}) + M(\text{H}_2)}{\pi(1.8a/2)^2} \quad (11)$$

The derived gas surface density Σ_{gas} is a weakly decreasing function of the H band luminosity when galaxies with a normal HI gas content (HI deficiency ≤ 0.3) are considered: $\text{Log}\Sigma_{gas}=21.264-0.063\text{Log}L_H$ (atom cm^{-2}), as shown in Fig. 17 (filled dots).

The reader should not be surprised by the (mild) anti-correlation between $\text{Log}\Sigma_{gas}$ and $\text{Log}L_H$ since it is known that the gaseous mass fraction decreases with increasing mass (Boselli et al. 2001).

At this stage we can estimate an empirical relationship between the gravitational potential $2\pi G$

¹⁵Since deficient galaxies have the HI gas mostly removed from the outskirts, the gas surface density is underestimated in galaxies with an HI deficiency parameter ≥ 0.3 .

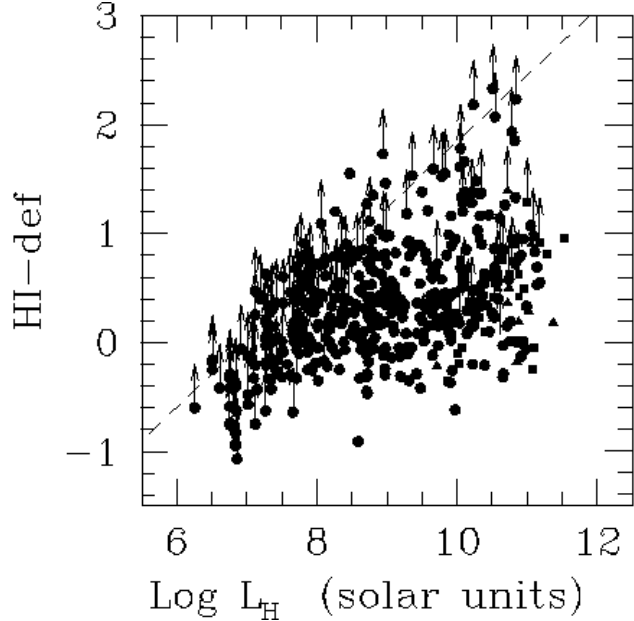


Fig. 19.— The relationship between the HI-deficiency parameter and the H band luminosity (in logarithmic scale) for Coma (squares), A1367 (triangles) and Virgo (circles) galaxies. Filled dots are for HI-detected galaxies, arrows for HI-undetected objects. The dotted line indicates the region inaccessible to the observations with a sensitivity of 1 mJy per channel for galaxies at the distance of Virgo.

Σ_{star} Σ_{gas} and the H -band luminosity and check if this potential is sufficient to prevent the gas to be swept away from stars by ram-pressure, as a function of H luminosity (see Fig. 18). It turns out that in the three clusters ram-pressure can effectively remove the atomic HI from any object with velocity similar or larger than the average cluster velocity dispersion¹⁶. This result is consistent with Vollmer et al. (2001b), who were able to reproduce the observed radial truncation of the HI disks in Virgo cluster galaxies. Given the dependence of the gravitational potential from the total H band luminosity, ram-pressure is expected to be more efficient at removing gas from low-mass objects than from massive spirals. This seems not confirmed observationally in Fig. 19 where the expected inverse relationship between the HI-deficiency parameter and the total mass of galaxies is not seen. This, however, is due to an observational bias because, at any given HI sensitivity, galaxies with larger HI deficiencies are more difficult to detect at low mass. In order to detect high HI deficiencies in dwarf galaxies it would be important to push the Arecibo observations of Virgo dwarf galaxies to very low limits¹⁷, beyond those reached by Hoffman et al. (1996) or Gavazzi et al.

¹⁶The efficiency of ram-pressure may be overestimated assuming the cluster central gas density ρ_{IGM} , as we did. However this should not represent a severe problem for most galaxies in radial orbits that will soon or later pass near the cluster center.

¹⁷This is in fact a high-priority project for the ALFA multi-beam system at Arecibo (Giovanelli et al. 2005a).

(2005b) and to better calibrate the HI deficiency parameter for dwarf systems, as attempted by Lee et al. (2003).

Examples of galaxies showing clear signs of undergoing ram-pressure stripping are CGCG 97-073 and 97-079 in A1367, NGC 4848 in Coma, NGC 4522 and 4654 in Virgo (see sect. 4.10).

4.5. Viscous stripping

Nulsen (1982) proposed viscous stripping as a possible mechanism capable of dragging gas out of galaxies in clusters. If a galaxy (of radius r_{gal}), carrying its cold and dense ISM, travels at speed V_{gal} across the hot (T_{IGM}) and tenuous (ρ_{IGM}) intergalactic medium, the outer layers of its ISM experience a viscosity momentum transfer sufficient for dragging out gas at some rate depending on whether the flux is laminar or turbulent.

If the flow is laminar, i.e if the Reynolds number:

$$Re = 2.8 \left(\frac{r_{gal}}{\lambda_{IGM}} \right) \times \left(\frac{V_{gal}}{c_{IGM}} \right) \leq 30$$

and if the mean free path of the ions in the hot gas is sufficiently small for the classical viscosity to apply:

$$\lambda_{IGM} [kpc] \simeq 11 \left(\frac{T_{IGM} [K]}{10^8} \right)^2 \times \left(\frac{10^{-3}}{\rho_{IGM} [cm^{-3}]} \right) \leq r_{gal}$$

(where $c_{IGM} = \sqrt{k_B T_{IGM} / m_H}$ is the sound speed in the IGM, k_B is the Boltzmann constant and m_H is the proton mass), then the mass loss rate is given by:

$$\dot{M}_{laminar} \simeq F_{laminar} / V_{gal} = \pi r_{gal}^2 \rho_{IGM} V_{gal} \times (12/Re) = 4.3 \pi r_{gal} \rho_{IGM} \lambda_{IGM} c_{IGM} \quad (12)$$

where $F_{laminar}$ is the drag force. If the flow is turbulent ($Re \geq 30$), then:

$$\dot{M}_{turbulent} \simeq F_{turbulent} / V_{gal} = \pi r_{gal}^2 \rho_{IGM} V_{gal} \quad (13)$$

In the turbulent case the drag force acting on the ISM is proportional to $\rho_{IGM} V_{gal}^2$, as in the case of ram-pressure.

In the case of the Coma, A1367 and Virgo clusters (whose properties are listed in Table 1), galaxies are subject to turbulent stripping whenever their linear sizes $r_{gal} \geq 10, 6$ and 15 kpc in the three clusters respectively¹⁸. Smaller objects experience laminar viscosity¹⁹.

As remarked by Nulsen (1982), if the flow velocity V_{gal} exceeds the adiabatic sound speed in the hot gas $\sqrt{5/3} c_{IGM}$ (1450, 970, 730 km s⁻¹ for Coma, A1367 and Virgo respectively) a shock will form ahead of the ISM. The stripping will occur preferentially on the front side of the galaxy, producing

¹⁸These values have to be taken as upper limits since λ_{IGM} might significantly decrease in the presence of weak tangled magnetic fields

¹⁹The condition $\lambda_{IGM} \leq r_{gal}$ is satisfied for $r_{gal} \geq 3.2, 1.4$ and 0.4 kpc in Coma, A1367 and Virgo respectively

an asymmetric gas distribution even on galaxies moving edge-on inside the IGM.

The time scales for complete gas stripping are relatively short: for both large (20 kpc; $5 \cdot 10^9 M_\odot$) and small (5 kpc; $5 \cdot 10^8 M_\odot$) galaxies in the Coma cluster, the time needed to completely remove the atomic gas is $\sim 4 \cdot 10^7$ yr. Longer times are needed in A1367 and Virgo: $\sim 10^8$ yr for large galaxies, from 4 (A1367) to 10 (Virgo) times longer for smaller objects.

The signature of viscous stripping on the structural, kinematic properties, molecular gas content and star formation activity of galaxies is expected to be similar to that of ram-pressure.

UGC 6697, proposed by Nulsen (1982) as the prototype of a galaxy ongoing turbulent viscous stripping, is in fact a merging galaxy (see sect. 4.10).

4.6. Thermal evaporation

As shown by Cowie & Songaila (1977) thermal evaporation can efficiently remove gas in cluster galaxies. If the IGM temperature is high compared to the galaxy velocity dispersion, at the interface between the hot IGM and the cold ISM the temperature of the ISM rises rapidly, the gas evaporates and is not retained by the gravitational field.

The mass loss rate can be estimated using the relation:

$$\dot{M}_{\text{evaporation}} = \pi r_{\text{gal}}^2 \rho_{\text{IGM}} c_{\text{IGM}} 4 \phi_s F(\sigma_o) \quad (14)$$

with $\phi_s \simeq 1$, $\sigma_o = 1.84 \lambda_{\text{IGM}} / (r_{\text{gal}} \phi_s)$ and $F(\sigma_o) = 2\sigma_o$ for $\sigma_o \leq 1$ (Nulsen 1982) (λ_{IGM} is defined in section 4.5). Given the properties of the three considered clusters, $\sigma_o \leq 1$ holds true for all galaxies, thus we can assume $F(\sigma_o) = 2\sigma_o$, and eq. 14 reduces to:

$$\dot{M}_{\text{evaporation}} \simeq 14.7 \pi r_{\text{gal}} \rho_{\text{IGM}} c_{\text{IGM}} \lambda_{\text{IGM}} \quad (15)$$

where c_{IGM} is defined in section 4.5.

Thermal evaporation is a sensitive function of the IGM temperature and of the magnetic field, and to a lesser extent of the density (Cowie & Songaila 1977); its efficiency can be reduced in presence of magnetic fields (Vikhlinin et al. 1997). A typical galaxy of radius 15 kpc and $5 \cdot 10^9 M_\odot$ of atomic gas can be completely stripped (assuming no magnetic fields) in $\sim 4 \cdot 10^7$ yr in Coma, $3 \cdot 10^8$ yr in A1367 and $\sim 10^9$ yr in Virgo.

As for the viscous stripping, the effects of the thermal evaporation on the kinematic and structural properties of cluster galaxies, as well as on the molecular gas content and star formation activity are difficult to quantify.

4.7. Starvation

Galaxy "starvation" or "strangulation", a process proposed more than 20 years ago by Larson et al. (1980) to explain the transformation of spirals into lenticulars, has been recently invoked to

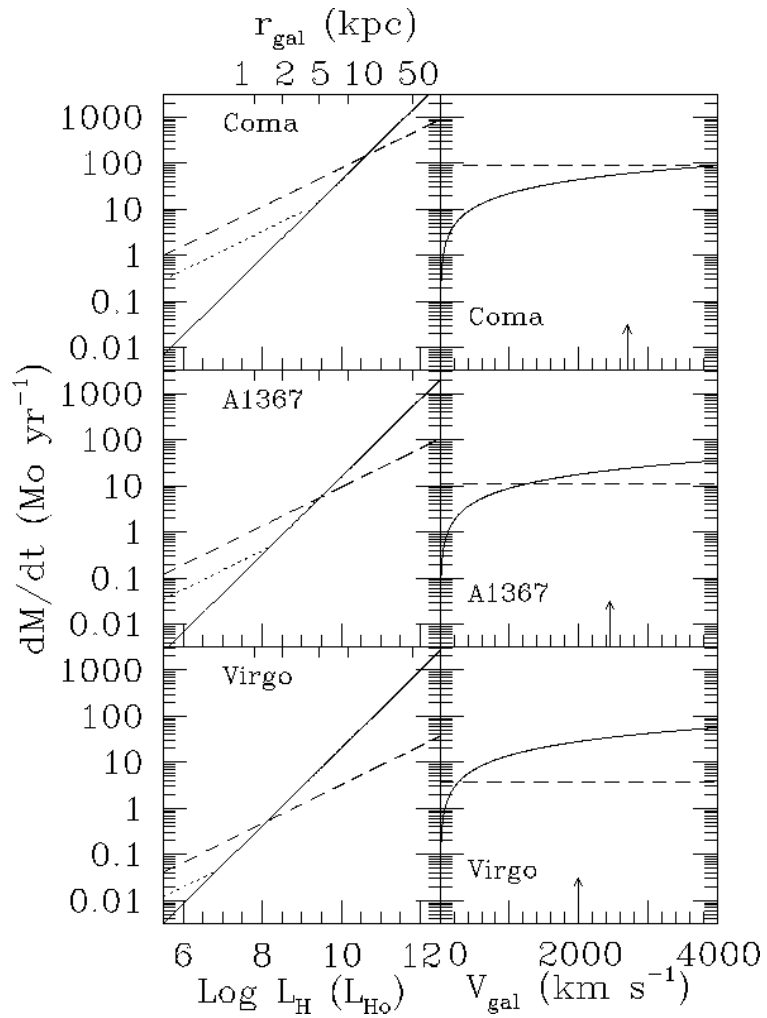


Fig. 20.— The mass loss rate for thermal evaporation (without magnetic fields: dashed line) and ram-pressure (or turbulent viscous stripping) for galaxies in Coma, A1367 and Virgo with radii > 10 , 4 and 1 kpc respectively (continuum line) and laminar viscous stripping (dotted line) are given as a function of the H band luminosity (linear size on the top axis) in the left panel. The galaxy velocity within the cluster is assumed $V_{\text{gal}} = \sqrt{3\delta V_{\text{cluster}}^2}$. Right panel: the comparison between the mass loss rates for thermal evaporation for galaxies of 10 kpc radii (dashed line) and ram-pressure (or turbulent viscous stripping) (continuum line) as a function of the galaxy velocity within the cluster. The vertical arrow indicates $V_{\text{gal}} = \sqrt{3\delta V_{\text{cluster}}^2}$ for the late-type component.

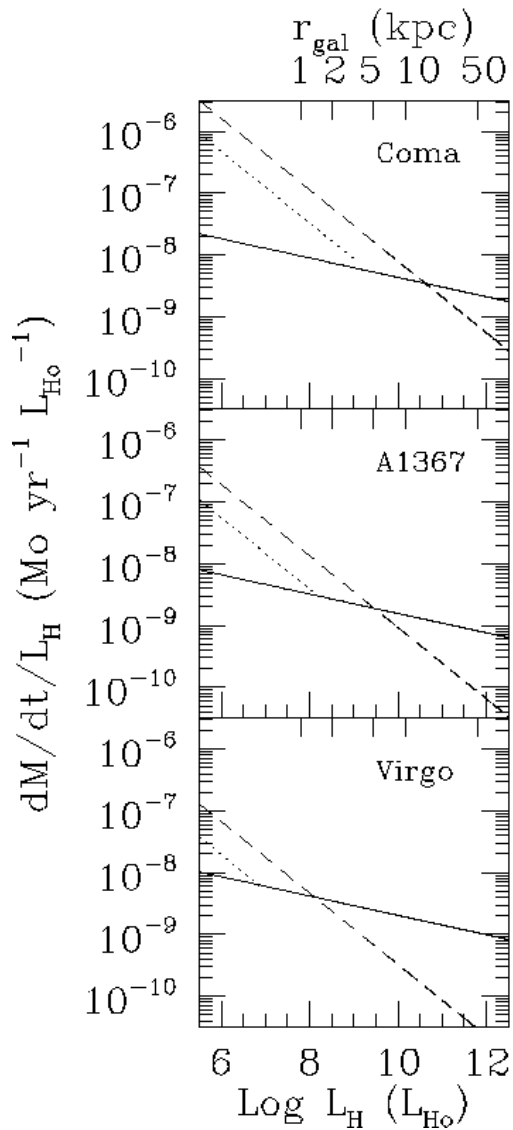


Fig. 21.— The mass loss rate per unit mass as a function of the H band luminosity. Same layout as in Fig. 20 (left panel)

explain the mild gradient in the morphology fraction found outside one virial radius in a cluster at $z=0.4$ (Treu et al. 2003). Emphasis is put on the large scale on which such a mechanism might be effective, contrary to other mechanisms previously described that, except galaxy harassment, are supposed to work on smaller scales (Treu et al. 2003; Balogh et al. 2000). Since in normal galaxies the gas that feeds the star formation (on time scales as long as the Hubble time) comes from infall of an extended gas reservoir, the effect of removing the outer galaxy halo would be that of preventing further infall of gas into the disk. On time scales of a few Gyr the star formation would thus exhaust the available gas, quenching further star formation activity.

The seminal idea of Larson et al. (1980) has been elaborated by Bekki et al. (2002). Their numerical simulations showed that even if a spiral orbits a cluster with a pericenter distance of ~ 3 core radii, $\sim 80\%$ of its halo is stripped within a few Gyr by the hydrodynamical interaction with the ICM plus the global tidal field of the cluster, preventing gas accretion into the disk, and consequently suppressing the star formation. In the end the spiral structure becomes less pronounced, and galaxies progressively becomes anemic, disk-dominated lenticulars. They might coincide with the small percentage of passive, anemic galaxies found in the SDSS by Goto et al. (2003a) at large clustercentric distances. Starvation, with its long time-scale, was invoked by Balogh et al. (2000) to explain the smooth transition in the star formation activity observed radially around density enhancements in the 2dF.

4.8. Preprocessing

According to the hierarchical scenario for the formation of large scale structures, groups of galaxies infalling onto clusters of galaxies represent the building blocks of today rich clusters of galaxies. Substructures seen in the X-rays and in kinematical studies of clusters of galaxies are the strongest evidence in favor of this cluster formation mechanism (Kodama et al. 2005). Galaxy groups may therefore represent natural sites for a *preprocessing* stage in the evolution of cluster galaxies (Mihos 2004; Fujita 2004; Dressler 2004) through tidal interactions, otherwise ineffective in high velocity dispersion environments. Meanwhile ram-pressure, starvation and evaporation might be already effective in these groups at $z \sim 0.5$, as shown by the simulations of Fujita (2004). Preprocessing might represent the ideal circumstance for the formation of lenticulars through unequal-mass mergers or minor mergers in spirals (Kodama & Smail 2001). These relatively violent events, as opposed to starvation, are able to heat up the disks, thus producing high bulge to disk lenticulars, as those observed in clusters. Since preprocessing occurs well outside the core of rich clusters, this mechanism has been invoked to explain why the atomic gas content and the star formation activity are found suppressed at large clustercentric distances (~ 1 virial radius) (Kodama et al. 2001). Although preprocessing might be at the origin of the post-starburst galaxy population in the SW extension of the Coma cluster (Caldwell et al. 1993), this mechanism is rare in nearby clusters, because in Λ cosmologies the rate of accretion of small groups on clusters has decreased at the present epoch. As remarked by Dressler (2004), the peak of groups in the building of cluster should happen at $z \sim 0.5$. In the Virgo cluster, for instance, the substructures that are now collapsing into

the main cluster have already grown massive enough to prevent preprocessing. There exist however an example of ongoing preprocessing taking place in A1367 (see Sect. 4.10.3). It should also be emphasized that local clusters contain significant examples of healthy spiral galaxies that made it to the inner cluster regions without being "wounded" by preprocessing and that are receiving their first and fatal kick directly from ram-pressure. Two are CGCG 97-073 and 079 in A1367 that are just as actively star forming as isolated objects and many other HI and H α healthy galaxies that lie between the virial and the core cluster radii.

4.9. Comparison between the various processes

We conclude that the relative importance of the processes considered above in nearby clusters depends on parameters that are difficult to quantify for individual galaxies, primarily depending on their 3-D position with respect the cluster center. Some general conclusions can however be summarized as follows:

1) Effects of the perturbation:

a) Gravitational interactions (galaxy-galaxy, galaxy-cluster, harassment) can induce nuclear gas infall that can be at the origin of nuclear activity. They can also contribute to heating up stellar disks and thus increasing the bulge to disk ratio (while retaining some bulge rotation). These processes are more efficient in low-luminosity and low-surface brightness galaxies, which might be easily transformed into dE. Gravitational interactions are thus able to transform spirals into lenticulars.

Tidal interactions with the cluster as a whole can hardly remove the outer HI disks since the truncation radius is larger than the HI disk radius. Thus they cannot be at the origin of the HI-deficient galaxy population in nearby clusters.

b) Interactions with the hot ICM can efficiently remove the outer disk gas and quench the star formation (directly by gas removal or via starvation) but they can hardly increase the bulge to disk ratio, as requested to explain the morphology segregation.

2) Time scales and probabilities:

Given the high velocity dispersion in clusters, the probability that spiral galaxies are perturbed by tidal interactions with nearby companions is extremely low. The time scale for tidal interactions (relaxation time) is some 10^{10} yr. Times scales for ram-pressure gas stripping (\sim one crossing time, 10^9 yr) are shorter than for harassment (several crossing times), where multiple encounters are necessary. In relaxed, gas rich clusters such as Coma, the time scale for gas removal for thermal evaporation or viscous stripping are very short (less than 10^8 yr), while some 10^8 yr in unrelaxed, gas poor clusters such as A1367 or Virgo. Models indicate that the time scale for galaxy starvation are of the order of some Gyr.

3) Efficiency as a function of the clustercentric distance:

The galaxy - cluster IGM interactions are most efficient close to the cluster center where the density and the temperature of the IGM (as well as the velocity of galaxies) reach their maxima. The perturbations induced by the cluster potential are also most efficient in the cluster center since the cluster tidal field is maximum at the core radius. Although the duration of the interaction might be shorter (because of the high relative velocity) than in the cluster outskirts, the frequency of galaxy-galaxy interactions reaches the maximum in the densest central regions. These processes seems thus confined to the inner part of the cluster, inside the virial radius.

Because of the combined action of galaxy-galaxy and galaxy-cluster gravitational interactions, galaxy harassment might be effective also at the cluster periphery. For similar reasons starvation and pre-processing might be effective well outside the cluster core and even outside the virial radius.

4) Relative importance of hydrodynamical mechanisms:

The relative importance of the three interactions between galaxies and the cluster IGM: viscous stripping, thermal evaporation and ram-pressure can be quantified. The mass loss rates $\dot{M} \simeq F/v_{gal}$ are comparable for turbulent viscous and ram-pressure stripping, both being proportional to $\pi r^2 \rho_{IGM} V_{gal}$. The laminar viscous stripping and the thermal evaporation have the same analytical dependence on the cluster and galaxy parameters, but the thermal evaporation is about three times more effective than the laminar viscous stripping.

At any given impact angle, position and transit velocity through the cluster (which are statistically known quantities), ram-pressure and viscous stripping dominate over thermal evaporation for large and fast galaxies. For small (dwarf) galaxies $\dot{M}_{evap} > \dot{M}_{lam} > \dot{M}_{ram}$ while for the giants it depends on the cluster: in Virgo \dot{M}_{ram} dominates over the other processes, in Coma thermal evaporation dominates over ram-pressure. Because of its higher IGM density and temperature, mass losses are on average 10 times larger in the Coma than in the Virgo cluster.

4.10. Prototypes of environmental disturbances

We briefly review a few nearby, well studied objects that may be considered as representatives of specific perturbation mechanisms.

4.10.1. Tidal interactions

Galaxies showing evident signs of an ongoing tidal interaction are relatively rare in nearby clusters. In Virgo for example, where the morphological classification is excellent owing to the available du Pont plates (Binggeli et al. 1985), only NGC 4438 out of 1802 galaxies classified as cluster members has clear tidal tails or other signs of ongoing tidal interactions.

The peculiar Sb galaxy NGC 4438 has recently undergone a high velocity, off-center (~ 900 km s $^{-1}$) encounter with the nearby (22 kpc projected separation) SB0 galaxy NGC 4435. NGC 4438 shows strong and extended tidal tails in both the optical (Arp 1966), near-IR (Boselli et al. 1997b) and UV (Boselli et al. 2005a). Both the atomic and molecular gas are displaced by ~ 5 kpc, toward the companion (Combes et al. 1988; Cayatte et al. 1990; Kenney et al. 1995), coinciding in position with the peak of the X-ray and radio continuum emission. The galaxy, with a mild nuclear activity, shows nuclear star formation and filaments of ionized gas originating from the plane of the disk (Kenney et al. 1995; Kenney & Yale 2002), and has a perturbed H α rotation curve (Kenney et al. 1995; Chemin et al. 2005). Whether some cold dust frozen into the ISM was removed during the interaction is hard to tell: no 6.75 nor 15 μ m emission is detected in mid-IR ISOCAM images at the level of a few μ Jy arcsec $^{-2}$ neither associated with the HI/CO peaks nor along the tidal tails (Boselli et al. 2003b). By combining multifrequency spectro-photometric data with population synthesis and galaxy evolution models Boselli et al. (2005a) showed that the galaxy recently (~ 10 Myr) underwent an instantaneous burst of star formation, significantly younger than the tidal interaction with NGC 4435, dated by dynamical models at ~ 100 Myr ago (Combes et al. 1988; Vollmer et al. 2005). It is interesting that the fraction of stellar mass produced by this starburst is <0.1 % of the total galaxy stellar mass, extremely small even in such a violent interaction.

Another example of ongoing, although in a more advanced stage, dynamical interaction in clusters is the merging galaxy UGC 6697 in A1367. This galaxy was originally taken as prototype of ongoing turbulent viscous stripping by Nulsen (1982) or of ram-pressure by Gavazzi et al. (1984; 1995b) because of its strong asymmetric HI (Gavazzi 1989; Dickey & Gavazzi 1991) and radio continuum morphology (Gavazzi & Jaffe 1987; Gavazzi et al. 1995), and its strong star formation activity (Gavazzi et al. 1995). Recent X-ray observations with Chandra (Sun & Vikhlinin 2005) reinforce the ram-pressure interpretation. An accurate kinematic study using both long slit and Fabry-Perot 2-D spectra suggests however the presence of two merging galaxies (Gavazzi et al. 2001c).

The presence of long filaments and plumes of ionized gas in the center and in the periphery of M87 (NGC 4486), the dominant Virgo galaxy, indicate a recent swallowing of a nearby gas rich object; the consequent matter infall is the most likely feeder of nuclear activity in this radio galaxy (Sparks et al. 1993; Gavazzi et al. 2000a).

M49 (NGC 4472), the other giant elliptical dominating the Virgo subcluster B, is in tidal interaction with the dwarf irregular galaxy UGC 7636 (Patterson & Thuan 1992; Henning et al. 1993; McNamara et al. 1994; Irwin & Sarazin 1996). Most of the HI gas of the dwarf irregular galaxy is found at a location intermediate between the dwarf irregular and the giant elliptical. Spatially coincident with the HI cloud Lee et al. (2000) detected an HII region whose metallicity is similar to that of UGC 7636. It is likely that tides from M49 first loosened the HI gas, then ram-pressure completed the gas removal from UGC 7636.

NGC 4698 (Bertola et al. 1999) and NGC 4772 (Haynes et al. 2000), two Sa galaxies in the Virgo cluster appear regular in their morphology, but in fact they show signs of a past merging event, as revealed by the geometric and kinematic decoupling of their disk and gas components. It is worth stressing that the information on evolved merging systems lacks completeness, as it requires ad-hoc

high-resolution kinematic observations.

4.10.2. *Ram-pressure*

The prototype of strong ongoing ram-pressure stripping is the galaxy CGCG 97-073 in A1367 (Fig. 22). This galaxy, located at the N-W periphery of this spiral rich cluster, is characterized by an asymmetric radio morphology, with 75 kpc long radio continuum tails in the direction opposite to the cluster center, similar to head-tail radio galaxies, and a steep gradient facing the cluster center (Gavazzi & Jaffe 1987; Gavazzi et al. 1995). The galaxy has also an asymmetric morphology in H α and at short optical wavelengths (both tracing the young stellar population) with a bow-shock structure in the direction of the cluster center and a low surface brightness tail in the opposite direction (coincident with the direction of the radio continuum tail), while it is quite symmetric in the near-IR (old stellar population) (Gavazzi et al. 1995). The HI gas, unresolved by the available VLA observations, is displaced toward the low surface brightness tail (Dickey & Gavazzi 1991), while the molecular gas is symmetrically distributed (Boselli et al. 1994). This galaxy has the radio to far-IR ratio higher than normal spiral galaxies, as well as an enhanced star formation activity per unit mass (as traced by its H α E.W.) compared to galaxies of similar type and luminosity (Gavazzi et al. 1995). Deep H α observations revealed the presence of long (75 kpc) tails of ionized gas associated to the radio continuum tail (Gavazzi et al. 2001a). All observational evidences indicate that this galaxy is undergoing ram-pressure stripping while entering the cluster for the first time. The interaction removes the HI gas while leaving the molecular gas unaffected, enhancing the star formation in the region facing the interaction with the cluster ICM and forming the radio continuum and H α trails (Gavazzi et al. 1995, 2001a; Boselli et al. 1994; Cortese et al. 2004). The ongoing interaction produced a weak starburst in the galaxy a few 10^7 years ago, as shown by the excess H α to UV ratio (Iglesias-Páramo et al. 2004), and triggered a shock compressing the magnetic field in the leading side of the galaxy.

The edge-on galaxy CGCG 97-079 is physically and morphologically similar to its near companion CGCG 97-073 (long radio continuum (Gavazzi et al. 1995) and ionized gas (Gavazzi et al. 2001a) tails, asymmetric HI profile (Dickey & Gavazzi 1991), unperturbed CO distribution (Boselli et al. 1994), enhanced star formation activity and radio to far-IR ratio (Gavazzi et al. 1995)). It is worth mentioning that these two objects are at ~ 0.4 virial radii from the cluster center, indicating that ram-pressure is effective not only in the highest density central regions.

Another candidate for currently ongoing ram-pressure stripping is NGC 4848 in the Coma cluster. Its HI and H α distributions are highly asymmetric (Gavazzi 1989; Bravo-Alfaro et al. 2001; Vollmer et al. 2001a). Some of the HI gas removed during the interaction might be falling back into the galaxy from the downstream side, as claimed by Vollmer et al. (2001a).

Well studied ram-pressure candidates in the Virgo cluster are NGC 4654, NGC 4522, NGC 4548, NGC 4569, NGC 4388 and NGC 4402. The morphological asymmetries and the kinematical structure of NGC 4654, however, can be explained only by a combined action of ram-pressure stripping (able to reproduce the extended gas) and tidal interaction with the nearby NGC 4639 (responsible

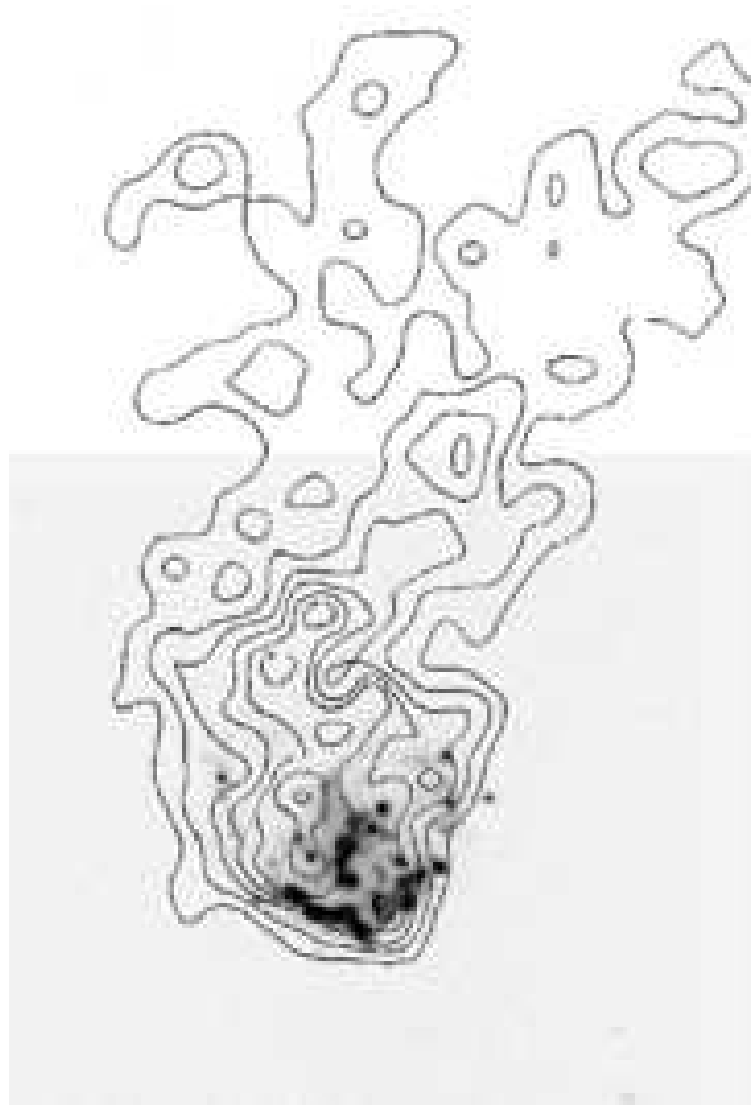


Fig. 22.— Contours of the radio continuum emission at 1400 MHz of CGCG 97-073 superposed to the H α frame, showing the head-tail morphology of the extended component (adapted from Gavazzi et al. (1995)).

for the asymmetric stellar distribution) (Vollmer 2003). NGC 4522 has an H α , HI, radio continuum and kinematical properties indicating an ongoing ram-pressure event (Kenney & Koopmann 1999; Vollmer et al. 2000, 2004b; Kenney et al. 2004). The comparison of model predictions with multifrequency observations made Vollmer et al. (2000) to conclude that the galaxy passed through the cluster center $\sim 6.5 \cdot 10^8$ yrs ago. Its perturbed H α morphology indicates that some recent star formation has been induced by the extraplanar atomic gas, probably displaced by ram-pressure stripping, falling back into the galaxy from the downstream side of its cometary trail (Vollmer et al. 2000). NGC 4548 is similar to NGC 4522, except that its face-on orientation makes the observation of the extraplanar gas more indirect (Vollmer et al. 1999). The kinematic analysis of the anemic galaxy NGC 4569 in the center of Virgo has shown that its strong HI-deficiency is probably due to a ram-pressure stripping event occurred ~ 300 Myr ago (Vollmer et al. 2004a). This result is in agreement with our recent analysis based on the comparison of multifrequency 2-D images with chemo-spectrophotometric models of galaxy evolution (Boselli et al. 2005b). The complex kinematic of the inner kiloparsec brought however Jogee et al. (2005) to conclude that NGC 4569 is also in an early stage of bar-driven/tidally driven gas inflow able to perturb the central star formation activity.

In the Seyfert 2 Virgo galaxy NGC 4388, the ram-pressure stripped gas, seen in the form of extended HI filaments, is ionized by the UV radiation field of the active galactic nucleus, producing strong optical emission lines (Yoshida et al. 2004; Veilleux et al. 1999). An extended (110 \times 25 kpc) HI gas cloud of $3.4 \cdot 10^8 M_\odot$ has been recently discovered at the north-east of NGC 4388 by Oosterloo & van Gorkom (2005). The authors claim that this gas has been removed by the ram-pressure exerted by the halo of the nearby M86. Another potential candidate for ram-pressure is NGC 4402, whose H α and HI morphology is similar to NGC 4522 (Crowl et al. 2005). Claims for ram-pressure stripping in early-type galaxies in Virgo, such as M86 (NGC 4406) are in Rangarajan et al. (1995); White et al. (1991); Nulsen & Carter (1987) (see however Elmegreen et al. (2000)).

Another issue that we wish to stress is that several galaxies that can be considered prototypes of the ram-pressure mechanism, either because their morphology indicates it or because they were successfully modeled by Vollmer et al. (2000, 2004a,b); Kenney et al. (2004) as being subject to ram-pressure stripping are found between 0.3 and 0.75 projected virial radii, i.e. at rather large clustercentric distances. Even though the mechanism itself operates at least up to 0.4 virial radii, its effects can last sufficiently to affect galaxies that have moved up to ~ 1 virial radius.

4.10.3. *Pre-processing*

The Blue Infalling Group in A1367 independently discovered by Sakai et al. (2002) and by Gavazzi et al. (2003b) and recently studied in depth by Cortese et al. (2006) is a typical (and to our knowledge unique) example of a pre-processing event in the nearby Universe (see Fig. 23). This group is composed of two $\sim M^*$ galaxies (CGCG 97-114 and 97-125) and several star forming dwarfs and extragalactic HII regions, all forming stars at a prodigious rate. The group has a small velocity dispersion (~ 170 kms $^{-1}$) and dynamical considerations indicate that it is falling at high velocity

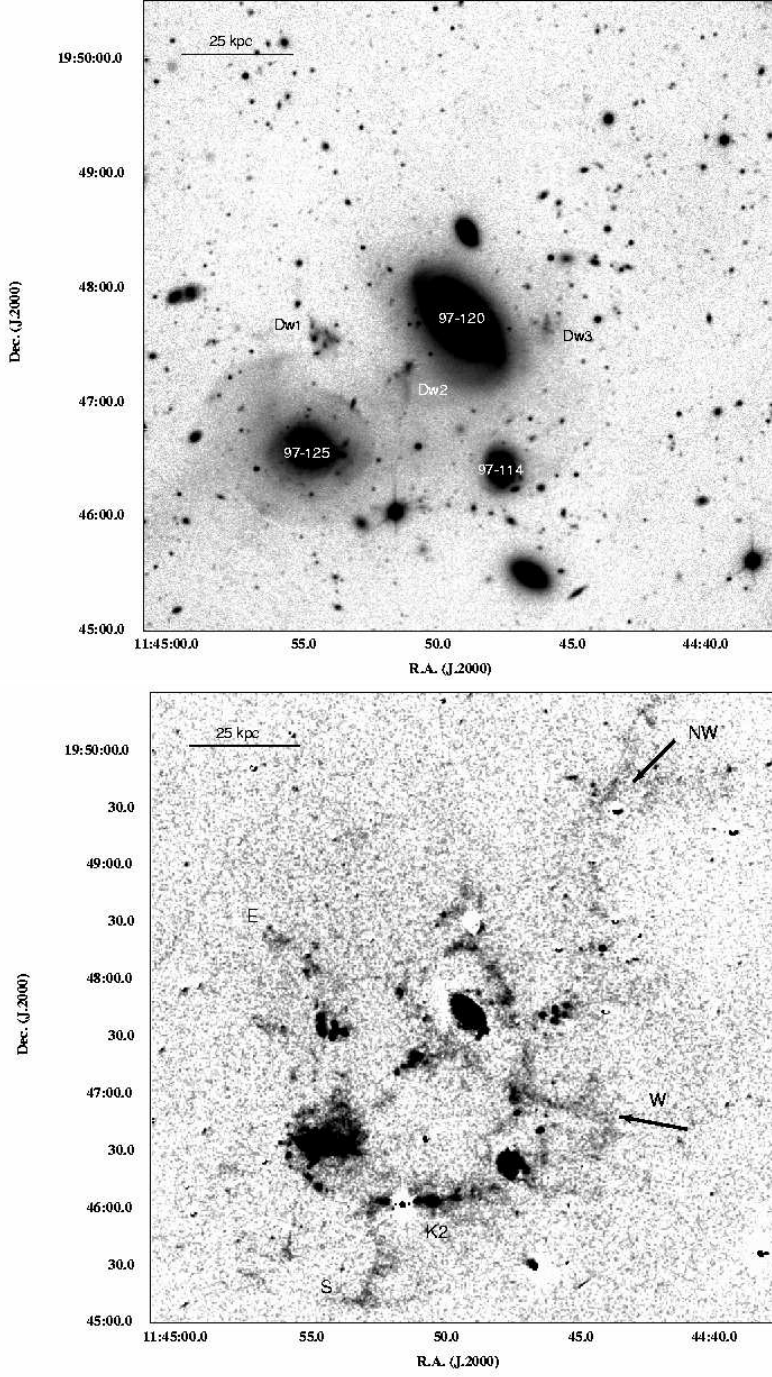


Fig. 23.— r band continuum (top) and H α net (bottom) images of the Blue Infalling Group in A1367. Notice the large-scale filamentary trails detected in the H α line (adapted from Cortese et al. (2006)).

(~ 1700 km s^{-1}) into the cluster A1367 (Gavazzi et al. 2003b; Cortese et al. 2004). All members show perturbed morphologies and enhanced star formation activity that seem produced by ongoing tidal interactions. High metallicity is determined in the group dwarfs and extragalactic HII regions, suggesting that they were produced by the violent tidal interaction between the two massive galaxies (Sakai et al. 2002), contrary to what it would be expected if they were independently evolved dwarfs. More evidence for gravitational interactions among the group members is offered by the early-type galaxy CGCG 97-125 (see Fig. 23) whose evident stellar shells witness a recent merging event. Cortese et al. (2006) discovered long (~ 150 kpc) $\text{H}\alpha$ trails associated with this group that are interpreted as due to ram-pressure stripping exerted by the cluster ICM on the ISM of the high velocity infalling galaxies. The thermal energy in the IGM is invoked to keep the gaseous trails ionized for a time much longer (10^8 yr) than the recombination time (10^7 yr).

5. Discussion and conclusion

Conclusive evidence built up in the last 25 years that, beside the morphological segregation effect, late-type galaxies belonging to rich nearby clusters differ significantly from their “field” counterparts. Primarily they are found deficient in atomic gas with respect to isolated galaxies (see sect. 2.1). Large HI deficiency parameters provide the clearest signature of their cluster membership. Because of the lack of gas, their star formation is significantly quenched (see sect. 2.6), despite the fact that the molecular gas component seems little perturbed (see sect. 2.2). Additional, but less clear-cut differences are: an excess of radio continuum activity, a higher metallicity and possibly a lower dust mass content of galaxies in high density environments. Kinematic properties instead (i.e. rotation curves), witnessing the dark matter distribution, seem little affected in clusters (see sect. 2 and 3).

Which physical processes, among the ones reviewed in sect. 4, are affecting the evolution of late-type galaxies falling on today’s clusters? The gravitational perturbations seem unlikely. Tidal interactions among galaxies are ineffective simply because in today’s high velocity dispersion clusters they are too short-lived to produce severe disturbances (sect. 4 and 6). The gravitational interaction with the cluster potential might induce some nuclear gas infall, but it can hardly remove the outer disk HI and thus originate the cluster HI-deficient galaxy population (sect. 4.2). Gas stripping in HI-deficient galaxies seems too a recent event (some 10^8 yr) for being produced by galaxy harassment, whose time scale is \sim ten times longer (sect. 4.3).

In today’s universe the interactions with the IGM are likely to be dominant. Among interactions with the cluster IGM, evaporation is effective in hot Coma-like clusters, especially for small galaxies, unless they are shielded by relevant magnetic fields (sect. 4.6). Ram pressure seems however the most relevant process whenever the gas is not too hot (A1367, Virgo) and provided that the cluster crossing velocity is high (see sect. 4.4). This condition seems satisfied since the orbits of spirals in nearby clusters are predominantly radial, as indicated by their non-Gaussian velocity distribution (see sect. 3.4). Dynamical simulations confirm this picture also for the young, unrelaxed Virgo

cluster, whose IGM density is not particularly high. Gas stripping might be locally more effective if the IGM has a non-uniform, clumpy distribution. Considering that the effects of ram-pressure, thermal evaporation and viscous stripping are probably additive, on time scales comparable to a crossing time, any late-type galaxy infalling into a rich cluster is expected to loose most of its atomic gas reservoir, in particular the weakly gravitationally bound one located in the outer disk. Observations corroborate the idea that galaxy - IGM interactions are the dominant phenomena affecting the evolution of late-type cluster galaxies in nearby clusters. The location of most severely HI-deficient late-type galaxies, with the smallest HI disks near the peaks of the IGM gas density argues in favor of the hydrodynamic scenario (sect. 2.1). There is also evidence that spirals in the

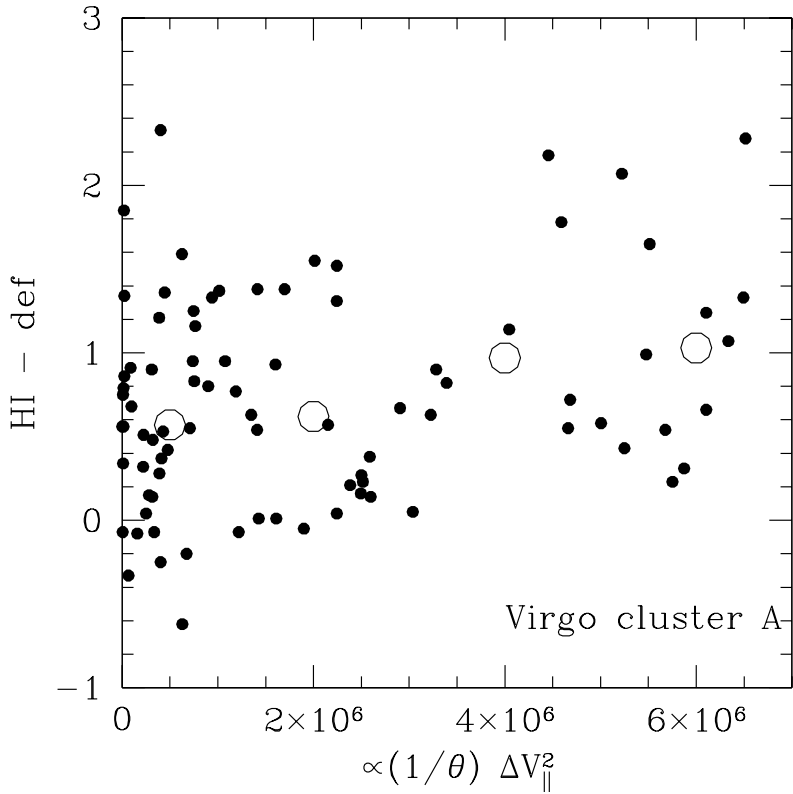


Fig. 24.— The correlation between the HI deficiency parameter and the square of the velocity deviation along the line of sight, divided by the angular distance from the center of cluster A in Virgo. Empty dots give averages in regularly spaced bins.

Virgo main cluster A show a weak correlation (see Fig. 24) between the HI deficiency parameter

and the quantity $(1/\theta) \times \Delta V_{\parallel}^2$, proportional to the square of the velocity along the line of sight divided by the angular distance from the cluster center (a quantity that is expected to increase with the ram-pressure ρV^2), arguing in favor of the ram-pressure hypothesis (notice that V^2 is very poorly determined from the observable component of the velocity parallel to the line of sight). Certainly this evidence does not support the tidal interaction scenario where $HI - def$ should rather decrease with ΔV_{\parallel} .

The truncation of the star forming disk in cluster HI-deficient spirals (see sect. 2.6) can also be explained in the ram-pressure scenario because the star formation is progressively suppressed once the gas is removed from the outer disk, as in NGC 4569. The interaction with the cluster IGM might sometime increase, on short time scales and in specific configurations, the total star formation activity of galaxies, as observed (i.e. CGCG 97-073 in A1367) and predicted by models (sect. 4.4), but on long timescales the galaxy global activity should however decrease.

On the contrary gravitational interactions are expected to trigger star formation, in particular in the nuclei (sect. 4.1), while the observations have unambiguously shown that on average the star formation activity of giant late-type galaxies decreases towards the cluster center. There are also evidences that cluster galaxies did not undergo strong bursts of star formation, as their constant H α to UV flux ratio implies, and that not all cluster galaxies with a truncated gas or young stellar disk have enhanced nuclear activity (gravitational interactions are expected first to trigger nuclear gas infall and only in the strongest cases to produce disk truncation) (see sect. 2.6).

Several prototypical galaxies provide convincing cases that the interactions with the cluster IGM are predominant in the nearby universe. NGC 4569, the typical HI-deficient, anemic galaxy in the Virgo cluster has kinematic and spectro-photometric disk properties that mimic a recent (300-400 Myr) ram-pressure stripping event (see sect. 4.10). We cannot exclude that some nuclear gas infall has been induced by the gravitational interaction with the potential of the cluster. Broadly speaking, the fact that most of the HI-deficient galaxies have truncated HI and H α disks, but not at longer wavelengths confirms that in most cases the interaction responsible for the gas depletion is relatively recent ($\leq 5 \times 10^8$ yr), as in NGC 4569. The existence of several marginally HI-deficient cluster spirals with asymmetric HI-profiles provides further evidence that the galaxy-IGM interaction is a recent event. The long, ionized trails behind CGCG 97-073 and CGCG 97-079 impose even stronger time constraints, indicating that in a few cases the interaction is still undergoing (sect. 4.10 and sect. 6).

The hydrodynamical galaxy - IGM interaction scenario poses some problems that might however only be apparent. It has been claimed that observing the threshold in the star formation activity at \sim one virial radius, i.e. at clustercentric distances where the IGM gas density is low (Treu et al. 2003), argues against the ram-pressure stripping scenario. This argument has been used in favor of other processes dominating the evolution of cluster gas-rich galaxies, such as pre-processing and starvation (Balogh et al. 2000; Lewis et al. 2002; Bower & Balogh 2004; Dressler 2004; Nichol 2004). First of all this result is based on wide field surveys, such as SDSS and 2dF, where HI data are unavailable and the optical galaxy classification is based on light profiles and/or spectra, without direct plate inspection. The threshold in the mean star formation activity of late-type cluster galaxies might be contaminated by the morphology segregation effect.

Furthermore we have stressed that the evidence offered by CGCG 97-079 and 97-073 in A1367 that ram-pressure is active at least up to ~ 0.8 Mpc (0.4 virial radius) combined with other examples showing that the effects of stripping might last until ~ 1 virial radius, reduces the necessity of invoking other processes such as pre-processing or starvation acting in the outskirt of clusters at $z=0$. Compact groups accreting on clusters, such as the Blue Infalling Group in A1367 (sect. 4.10), where effective pre-processing might take place, are extremely rare at $z=0$. We have in fact evidence that galaxies infall as individuals (CGCG 97-073 and CGCG 97-079), or belonging to extended sub structures with velocity dispersion comparable to already formed clusters (≥ 500 km s $^{-1}$, sect. 3.4).

A unified picture that combines near and far, present and past can be drawn coherently if one takes into account that the environmental conditions and the physical properties of galaxies have evolved significantly during the cosmic time, making the ranking of the mechanism that prevailed in shaping the Hubble sequence to change with time. The number of low velocity dispersion infalling groups, where pre-processing is effective, increased with z ; the density of the IGM and its temperature decreased with z . The gas fraction and the activity of star formation of galaxies, independently of their environmental conditions, increased significantly from $z=0$ at least up to $z=1$.

Given that the interaction with the cluster IGM cannot easily thicken the disk of a spiral galaxy and transform it into an S0 (sect. 3.5)²⁰, the formation of bulges is obtained straightforwardly from disk heating (perturbing or even stopping the rotation) during gravitational interactions with nearby companions and/or with the cluster potential (galaxy harassment) (sect. 4.1, 4.2, 4.3). The observed kinematical, structural and spectrophotometrical properties of bright lenticulars in nearby clusters are consistent with this interpretation. For low-luminosity lenticulars, however, as stated by Poggianti et al. (2004), there are some evidences that the suppression of the star formation was due to their interaction with the IGM (sect. 3.5). These considerations have induced groups of researchers working on clusters at high z to identify in gravitational pre-processing the most likely mechanism at the origin of the morphological segregation (Dressler 2004), although others invoked smoother processes such as starvation (Balogh et al. 2000). We refer the reader to several papers that appeared in the Carnegie Observatories Astrophysics Series, Vol. 3: Clusters of Galaxies: Probes of Cosmological Structure and Galaxy Evolution (2004) elaborating on this idea.

Several problems concerning the evolution of galaxies in clusters remain unsolved in this unified scenario. One deals for example with the origin of dwarf galaxies. Although the strong HI-deficiency of cluster dwarf irregulars expected in the hydrodynamical interaction scenario cannot be proved because of the lack of sensitive HI observations (sect. 2.1), there is evidence that their star formation activity does not decrease with clustercentric distances as for massive objects (sect. 2.6), maybe due

²⁰In the ram-pressure scenario bulges can form only under particular conditions, such as through the triggering of cycles of annealing after several crossings of the cluster (Schulz & Struck 2001) or edge-on stripping, when up to 50% of the gas can be re-accreted by the disk (Vollmer et al. 2001b) (see sect. 4.4)

to continuous replenishment of gas-rich dwarfs from outside, or maybe because dwarf irregulars, after gas removal, quickly fade into dEs, thus they drop out of late-type surveys. A close link between dIs and dEs, first proposed by Lin & Faber (1983), is strengthened by the existence of rotationally supported dEs (van Zee et al. 2004a,b), by the residual/past star formation activity of dEs observed in UV (Boselli et al. 2005c) or in optical spectra (i.e. VCC1499, Gavazzi et al. (2001b); Conselice et al. (2003a)), by the existence of dEs not totally devoid of gas (Conselice et al. 2003b), by the shape of the faint end of the cluster luminosity functions (Conselice 2002) and by the velocity distribution as broad as that of dwarf irregulars (Conselice et al. 2001).

It seems fair to conclude that gravitational perturbations in infalling groups are at the origin of local lenticular galaxies. However the process dominating the evolution of gas-rich, late-type galaxies falling-in at the present epoch is the interaction with the hot and dense IGM. The fate of late-type galaxies will be slightly different from what it would have been a Gyr ago: they will become HI-deficient, anemic, rotationally-supported spirals. On long timescales (several crossing times), because of the lack of gas supply, they will lose angular momentum, somewhat heating their stellar disks. They will probably become disk dominated, quiescent systems (3.5), but they will never make it to become real S0s.

If this evolutionary picture is correct, we still have to understand at which epoch and under what environmental conditions the hydrodynamical and the gravitational processes interchanged their prevailing role and, among other things, compare it with the inset of the Buchler-Oemler effect. These observational goals are within the reach of last generation ground based optical telescopes and of the HST. However we must wait another decade before neutral hydrogen measurements of galaxies at significant z with SKA will shade the final light on the evolutionary processes that took place in clusters of galaxies.

6. Appendix: Characteristic time scales

The age and the duration of certain interactions, their probability and their frequency can be relatively well quantified from the observations. In this appendix we summarize some time scales relevant to the processes acting on nearby clusters of galaxies:

6.1. Galaxy revolution time scale: t_{rev}

The time required by a galaxy to make a complete revolution around the rotation axis, t_{rev} , is given by the relation:

$$t_{rev} = 2\pi r_{gal}/\Delta V_{gal} \quad (16)$$

For normal late-type galaxies, with typical luminosities in the range $8 < \log L_H < 12$ ($L_{H\odot}$) t_{rev} ranges between 5×10^7 and 3×10^8 yr.

Some cluster galaxies have asymmetric HI distributions, with most of the gas located on one side of the galaxy, as observed using both interferometers and single dish radiotelescopes²¹. Whenever the atomic gas is partly removed from the disk of the galaxy, the resulting asymmetric HI distribution lasts for a few times t_{rev} . On longer time scales differential rotation re-distributes uniformly the gas over the disk. Thus observing an HI asymmetry implies that the gas removing mechanism has been acting since a very short time, or that gas sweeping is an ongoing process: whatever the interaction is, it ended no more than t_{rev} years ago. Typical galaxies with an asymmetric HI distribution are NGC 4654 (Phookun & Mundy 1995) and NGC 4438 (Cayatte et al. 1990) in Virgo, NGC 4848 (CGCG 160-055), NGC 4921 (CGCG 160-096) in Coma (Gavazzi 1989; Bravo-Alfaro et al. 2001), UGC 6697 (CGCG 97-087) and CGCG 97-079 in A1367 (Gavazzi 1989; Dickey & Gavazzi 1991). These are marginally HI-deficient galaxies: the ongoing interaction did not have enough time yet to remove the majority of the atomic gas.

6.2. Cluster crossing time: t_{cross}

It is more difficult to date the stripping epoch of HI-deficient galaxies (HI deficiency ≥ 0.3) since several processes can be responsible for gas removal. Ram-pressure, for instance, has a time scale comparable with the cluster crossing time t_{cross} .

²¹The HI profiles of asymmetric galaxies with an inclination larger than ≥ 30 degrees are “one-horned” instead of “two-horned” as observed in isolated unperturbed galaxies (Gavazzi 1989)

The cluster crossing time t_{cross} at the virialization radius R_{vir} is given by the relation:

$$t_{cross} = 2 \times R_{vir}/V_{gal} \simeq 2 \times R_{vir}/\sqrt{3}\delta V_{cluster} \quad (17)$$

Typical crossing times for galaxies in the clusters Coma, A1367 and Virgo range between 2 and 3 $\times 10^9$ yr (see Table 2).

6.3. Duration of tidal encounters: t_{enc}

Tidal encounters have shorter timescales, of the order of $t_{enc} \sim 10^8$ years, the time during which two galaxies moving at high speed in the potential well of the cluster remain close enough to get tidally perturbed. The time scale defining the effective duration of high velocity encounters t_{enc} such as galaxy-galaxy tidal interactions can be estimated using the relation (Binney & Tremaine 1987):

$$t_{enc} \simeq \max(r(1)_{gal}, r(2)_{gal}, b)/\Delta V \quad (18)$$

where $r(1)_{gal}$ and $r(2)_{gal}$ are the radii of the two galaxies, b their separation at the closest approach and ΔV the relative speed. For galaxies belonging to the three clusters listed in Table 1, for $\Delta V \simeq \delta V_{cluster}$, $t_{enc} \sim 10^8$ yr. Another very short time-scale.

6.4. Relaxation time: t_{relax}

The frequency of encounters, however, is significantly smaller ($\sim 1/t_{relax}$). The relaxation time t_{relax} , the time necessary for a galaxy to have its orbit perturbed by a tidal interaction, is given by the relation:

$$t_{relax} = 0.1 \times (D_{cluster}/\delta V_{cluster}) \times (N_{gal}/\ln(N_{gal})) = 0.2 \times (R_{vir}/\delta V_{cluster}) \times (N_{gal}/\ln(N_{gal})) \quad (19)$$

where $D_{cluster}$ is the size and $\delta V_{cluster}$ the velocity dispersion of the cluster, and N_{gal} the number of members (Binney & Tremaine 1987; Byrd & Valtonen 1990). The typical relaxation time for the three clusters analyzed in this work can be estimated using the data listed in Table 1 and using a rough estimate of $N_{gal} \sim 1000$. They are $\sim 5 \times 10^{10}$ yr, comparable to the age of the Universe (see Table 2).

6.5. Merging time: t_{mer}

Makino & Hut (1997) studied the merging rate of galaxies of similar mass in clusters. Merging processes are relatively rare in rich clusters since the probability of a merger is significantly higher

in low speed encounters. If N_{gal} is the number of galaxies randomly distributed in a cluster of radius $D_{cluster}$, r_h is the half-mass radius of the galaxy, ΔV_{gal} and $\delta V_{cluster}$ the galaxy and cluster velocity dispersions, the merging time t_{mer} is given by the relation (Makino & Hut 1997):

$$t_{mer} \sim \frac{2000}{N_{gal}^2} \left(\frac{D_{cluster}}{1Mpc} \right)^3 \left(\frac{0.1Mpc}{r_h} \right)^2 \left(\frac{100km s^{-1}}{\Delta V_{gal}} \right)^4 \left(\frac{\delta V_{cluster}}{300km s^{-1}} \right)^3 Gyr \quad (20)$$

As shown in Table 2 the time scales for merging of L^* galaxies inside the cluster virial radius are relatively high in Coma, A1367 and Virgo. Given the short length of time of t_{enc} and the low frequency of encounters ($\sim 1/t_{relax}$), it is not surprising that in the whole Virgo cluster only NGC 4438 shows clear evidence for ongoing tidal interactions. t_{merg} must have been much shorter in the past because of the strong dependence $\sim (1+z)^3$ of the density on z .

6.6. Recombination time: t_{rec}

The presence of asymmetric radio continuum tails, such as those observed in CGCG 97-073 and CGCG 97-079 in A1367 (Gavazzi et al. 1995), indicate that the interaction is still ongoing. These galaxies also present long (~ 75 kpc) ionized gas tails Gavazzi et al. (2001a). The recombination time t_{rec} is given by the relation (Osterbrock 1989):

$$t_{rec} = 1/(n_e * \alpha_A) \quad (21)$$

where n_e is the electron density and $\alpha_A = 4.2 \cdot 10^{-13} \text{ cm}^3 \text{ s}^{-1}$. If the gas density is known, and in the hypothesis that the gas is not ionized in situ, this relation can be used, combined with the tail length and the galaxy speed within the cluster, to estimate a lower limit to the first interaction responsible for the formation of the ionized tails. Gavazzi et al. (2001a) estimate that this time scale is a few times 10^7 yrs.

Table 2: The typical time scales for galaxies in the Coma, A1367 and Virgo clusters.

<i>Cluster</i>	t_{cross}	t_{relax}	$t_{merging}$
	<i>yr</i>	<i>yr</i>	<i>yr</i>
<i>Coma</i>	$1.6 \cdot 10^9$	$2.4 \cdot 10^{11}$	$6.9 \cdot 10^{11}$
<i>A1367</i>	$1.7 \cdot 10^9$	$7.2 \cdot 10^{10}$	$1.7 \cdot 10^{12}$
<i>Virgo</i>	$1.7 \cdot 10^9$	$3.6 \cdot 10^{10}$	$3.4 \cdot 10^{11}$

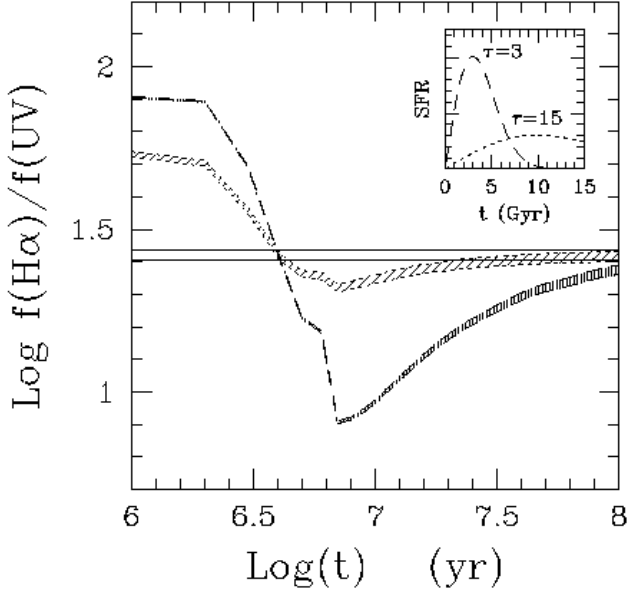


Fig. 25.— The time behavior of the $H\alpha$ to UV flux ratio after an instantaneous burst of star formation that occurred at $t = 0$ of intensity 100 (thick shaded region) and 10 (thin shaded region) times higher than the continuum formation activity, adapted from Iglesias-Páramo et al. (2004).

6.7. Dating recent starbursts: $t_{starburst}$

Beside fitting the SED's continuum from the UV to the near-IR with population synthesis models (Gavazzi et al. 2002a), several spectral features, combined with population synthesis models, are used to estimate the age of the underlying stellar population (see Worthey (1994); Poggianti & Barbaro (1996); Bruzual & Charlot (2003)). The debated issue here is which combination of indexes should be used to break the age-metallicity degeneracy.

Many applications of these methods are found in the literature aimed at estimating the age of galaxies in distant clusters. A local application to Coma PSB galaxies is the one by Poggianti et al. (2004). Spectral indices can be used to date the age of starbursts. The most generally used are the Balmer emission and underlying absorption lines. The draw-back of these methods is that the results are strongly dependent on the assumed star formation history: significant age difference arise from the same index if one or more instantaneous or continuum starbursts are assumed.

A promising clock for dating recent bursts of star formation comes from the $H\alpha$ to UV flux ratio, assuming that the IMF is universal. The emission at these wavelengths is associated with young stars. However, the stars producing the ionizing photons responsible of the $H\alpha$ emission are O-B stars, younger ($t < 4 \times 10^6$ yr) and more massive ($m > 10 M_\odot$) than the A stars ($m \sim 2-5 M_\odot$; $t \sim 3 \times 10^8$ yr) emitting in the UV (Boselli et al. 2001). After an instantaneous starburst the $H\alpha$ to UV ratio would thus increase on a time scale comparable to the life time of the O-B stars ($0 < t_{starburst} \simeq 4 \times 10^6$ yr) and decrease on timescales comparable to the age of the UV emitting stars ($10^7 < t_{starburst} \simeq 3 \times 10^8$ yr), as shown in Fig. 25 (adapted from Iglesias-Páramo et al. (2004)). However,

the variation of the H α to UV flux ratio is significant only for intense starbursts, where the star formation activity increases by at least a factor of 10 with respect to the standard activity. This promising technique needs high quality UV and H α photometric data, as well as Balmer decrement measurements and far-IR data necessary for an accurate dust extinction correction (Iglesias-Páramo et al. 2004).

We wish to thank J.M. Deharveng for encouraging us to write this review. C. Adami, H. Böhringer, S. Boissier, L. Cortese, J. Iglesias, C. Mendes de Oliveira, H. Wozniak, A. Zaccardo for their contributions. M. Colpi, L. Cortese, J.M. Deharveng, M. Haynes, R. Kennicutt, J. Lequeux, B. Poggianti and H. Wozniak for discussions and comments. We want to thank an anonymous referee whose comments and suggestions were precious for improving the present manuscript.

REFERENCES

Abadi, M. G., Moore, B., & Bower, R. G. 1999, MNRAS, 308, 947

Abell, G. O. 1965, ARA&A, 3, 1

Amram, P., Sullivan, W. T., Balkowski, C., Marcellin, M., & Cayatte, V. 1993, ApJ, 403, L59

Andersen, V. & Owen, F. N. 1995, AJ, 109, 1582

Andreon, S. 1996, A&A, 314, 763

Andreon, S. & Pelló, R. 2000, A&A, 353, 479

Arp, H. 1966, *Atlas of peculiar galaxies* (Pasadena: California Inst. Technology, 1966)

Balogh, M. L., Baldry, I. K., Nichol, R., Miller, C., Bower, R., & Glazebrook, K. 2004, ApJ, 615, L101

Balogh, M. L., Christlein, D., Zabludoff, A. I., & Zaritsky, D. 2001, ApJ, 557, 117

Balogh, M. L., Navarro, J. F., & Morris, S. L. 2000, ApJ, 540, 113

Balsara, D., Livio, M., & O'Dea, C. P. 1994, ApJ, 437, 83

Barton, E. J., Bromley, B. C., & Geller, M. J. 1999, ApJ, 511, L25

Bekki, K. & Couch, W. J. 2003, ApJ, 596, L13

Bekki, K., Couch, W. J., & Shioya, Y. 2002, ApJ, 577, 651

Bertola, F., Corsini, E. M., Vega Beltrán, J. C., Pizzella, A., Sarzi, M., Cappellari, M., & Funes, J. G. 1999, ApJ, 519, L127

Bianchi, S., Davies, J. I., & Alton, P. B. 1999, A&A, 344, L1

Bicay, M. D. & Giovanelli, R. 1987, ApJ, 321, 645

Binggeli, B., Popescu, C. C., & Tammann, G. A. 1993, A&AS, 98, 275

Binggeli, B., Sandage, A., & Tammann, G. A. 1985, AJ, 90, 1681

Binggeli, B., Tammann, G. A., & Sandage, A. 1987, AJ, 94, 251

Binggeli, B., Tarenghi, M., & Sandage, A. 1990, A&A, 228, 42

Binney, J. & Tremaine, S. 1987, *Galactic dynamics* (Princeton, NJ, Princeton University Press, 1987, 747 p.)

Biviano, A. & Katgert, P. 2004, A&A, 424, 779

Biviano, A., Katgert, P., Mazure, A., Moles, M., den Hartog, R., Perea, J., & Focardi, P. 1997, *A&A*, 321, 84

Blanton, M. R., Dalcanton, J., Eisenstein, D., Loveday, J., Strauss, M. A., SubbaRao, M., Weinberg, D. H., Anderson, J. E., Annis, J., Bahcall, N. A., Bernardi, M., Brinkmann, J., Brunner, R. J., Burles, S., Carey, L., Castander, F. J., Connolly, A. J., Csabai, I., Doi, M., Finkbeiner, D., Friedman, S., Frieman, J. A., Fukugita, M., Gunn, J. E., Hennessy, G. S., Hindsley, R. B., Hogg, D. W., Ichikawa, T., Ivezić, Ž., Kent, S., Knapp, G. R., Lamb, D. Q., Leger, R. F., Long, D. C., Lupton, R. H., McKay, T. A., Meiksin, A., Merelli, A., Munn, J. A., Narayanan, V., Newcomb, M., Nichol, R. C., Okamura, S., Owen, R., Pier, J. R., Pope, A., Postman, M., Quinn, T., Rockosi, C. M., Schlegel, D. J., Schneider, D. P., Shimasaku, K., Siegmund, W. A., Smee, S., Snir, Y., Stoughton, C., Stubbs, C., Szalay, A. S., Szokoly, G. P., Thakar, A. R., Tremonti, C., Tucker, D. L., Uomoto, A., Vanden Berk, D., Vogeley, M. S., Waddell, P., Yanny, B., Yasuda, N., & York, D. G. 2001, *AJ*, 121, 2358

Bohringer, H., Briel, U. G., Schwarz, R. A., Voges, W., Hartner, G., & Trumper, J. 1994, *Nature*, 368, 828

Boissier, S. & Prantzos, N. 2000, *MNRAS*, 312, 398

Boselli, A. 1994, *A&A*, 292, 1

Boselli, A., Boissier, S., Cortese, L., Gil de Paz, A., Buat, V., Iglesias-Paramo, J., Madore, B. F., Barlow, T., Bianchi, L., Byun, Y.-I., Donas, J., Forster, K., Friedman, P. G., Heckman, T. M., Jelinsky, P., Lee, Y.-W., Malina, R., Martin, D. C., Milliard, B., Morrissey, P., Neff, S., Rich, R. M., Schiminovich, D., Seibert, M., Siegmund, O., Small, T., Szalay, A. S., Welsh, B., & Wyder, T. K. 2005a, *ApJ*, 623, L13

Boselli, A., Boissier, S., Cortese, L., Gil de Paz, A., Seibert, M., Madore, B. F., & Martin, D. C. 2005b, *ApJ*, 1, submitted

Boselli, A., Casoli, F., & Lequeux, J. 1995a, *A&AS*, 110, 521

Boselli, A., Cortese, L., Deharveng, J. M., Gavazzi, G., Yi, K. S., de Paz, A. G., Seibert, M., Boissier, S., Donas, J., Lee, Y.-W., Madore, B. F., Martin, D. C., Rich, R. M., & Sohn, Y.-J. 2005c, *ApJ*, 629, L29

Boselli, A., Gavazzi, G., Combes, F., Lequeux, J., & Casoli, F. 1994, *A&A*, 285, 69

Boselli, A., Gavazzi, G., Donas, J., & Scoggio, M. 2001, *AJ*, 121, 753

Boselli, A., Gavazzi, G., Lequeux, J., Buat, V., Casoli, F., Dickey, J., & Donas, J. 1995b, *A&A*, 300, L13

—. 1997a, *A&A*, 327, 522

Boselli, A., Gavazzi, G., & Sanvito, G. 2003a, *A&A*, 402, 37

Boselli, A., Lequeux, J., & Gavazzi, G. 2002, *A&A*, 384, 33

Boselli, A., Lequeux, J., Sauvage, M., Boulade, O., Boulanger, F., Cesarsky, D., Dupraz, C., Madden, S., Viallefond, F., & Vigroux, L. 1998, *A&A*, 335, 53

Boselli, A., Sauvage, M., Lequeux, J., Donati, A., & Gavazzi, G. 2003b, *A&A*, 406, 867

Boselli, A., Tuffs, R. J., Gavazzi, G., Hippelein, H., & Pierini, D. 1997b, *A&AS*, 121, 507

Bower, R. & Balogh, M. 2004, in Clusters of Galaxies: Probes of Cosmological Structure and Galaxy Evolution

Bravo-Alfaro, H., Cayatte, V., van Gorkom, J. H., & Balkowski, C. 2000, *AJ*, 119, 580

—. 2001, *A&A*, 379, 347

Briel, U. G., Henry, J. P., & Boehringer, H. 1992, *A&A*, 259, L31

Briel, U. G., Henry, J. P., Lumb, D. H., Arnaud, M., Neumann, D., Aghanim, N., Gastaud, R., Mittaz, J. P. D., Sasseen, T. P., & Vestrand, W. T. 2001, *A&A*, 365, L60

Broeils, A. H. & Rhee, M.-H. 1997, *A&A*, 324, 877

Bruzual, A. G. & Charlot, S. 1993, *ApJ*, 405, 538

Bruzual, G. & Charlot, S. 2003, *MNRAS*, 344, 1000

Buat, V., Boselli, A., Gavazzi, G., & Bonfanti, C. 2002, *A&A*, 383, 801

Burstein, D. 1979, *ApJ*, 234, 435

Butcher, H. & Oemler, A. 1978, *ApJ*, 226, 559

—. 1984, *ApJ*, 285, 426

Byrd, G. & Valtonen, M. 1990, *ApJ*, 350, 89

Caldwell, N., Rose, J. A., & Dendy, K. 1999, *AJ*, 117, 140

Caldwell, N., Rose, J. A., Franx, M., & Leonardi, A. J. 1996, *AJ*, 111, 78

Caldwell, N., Rose, J. A., Sharples, R. M., Ellis, R. S., & Bower, R. G. 1993, *AJ*, 106, 473

Casoli, F., Boisse, P., Combes, F., & Dupraz, C. 1991, *A&A*, 249, 359

Cayatte, V., Kotanyi, C., Balkowski, C., & van Gorkom, J. H. 1994, *AJ*, 107, 1003

Cayatte, V., van Gorkom, J. H., Balkowski, C., & Kotanyi, C. 1990, *AJ*, 100, 604

Chemin, L., Cayatte, V., Balkowski, C., Amram, P., Carignan, C., Boselli, A., Adami, C., Marcellin, M., Garrido, O., Hernandez, O., & Boulesteix, J. 2005, *A&A*, 436, 469

Christlein, D. & Zabludoff, A. I. 2004, *ApJ*, 616, 192

Cole, S., Norberg, P., Baugh, C. M., Frenk, C. S., Bland-Hawthorn, J., Bridges, T., Cannon, R., Colless, M., Collins, C., Couch, W., Cross, N., Dalton, G., De Propris, R., Driver, S. P., Efstathiou, G., Ellis, R. S., Glazebrook, K., Jackson, C., Lahav, O., Lewis, I., Lumsden, S., Maddox, S., Madgwick, D., Peacock, J. A., Peterson, B. A., Sutherland, W., & Taylor, K. 2001, *MNRAS*, 326, 255

Colless, M. & Dunn, A. M. 1996, *ApJ*, 458, 435

Combes, F., Dupraz, C., Casoli, F., & Pagani, L. 1988, *A&A*, 203, L9

Condon, J. J., Condon, M. A., Gisler, G., & Puschell, J. J. 1982, *ApJ*, 252, 102

Conselice, C. J. 2002, *ApJ*, 573, L5

Conselice, C. J., Gallagher, J. S., & Wyse, R. F. G. 2001, *ApJ*, 559, 791

—. 2003a, *AJ*, 125, 66

Conselice, C. J., O’Neil, K., Gallagher, J. S., & Wyse, R. F. G. 2003b, *ApJ*, 591, 167

Cortese, L., Boselli, A., Buat, V., Gavazzi, G., Boissier, S., Gil de Paz, A., Seibert, M., Madore, B. F., & Martin, D. C. 2005a, ArXiv Astrophysics e-prints

Cortese, L., Boselli, A., Gavazzi, G., Iglesias-Paramo, J., Madore, B. F., Barlow, T., Bianchi, L., Byun, Y.-I., Donas, J., Forster, K., Friedman, P. G., Heckman, T. M., Jelinsky, P., Lee, Y.-W., Malina, R., Martin, D. C., Milliard, B., Morrissey, P., Neff, S., Rich, R. M., Schiminovich, D., Siegmund, O., Small, T., Szalay, A. S., Treyer, M. A., Welsh, B., & Wyder, T. K. 2005b, *ApJ*, 623, L17

Cortese, L., Gavazzi, G., Boselli, & Iglesias-Paramo, J. 2003, *A&A*, 410, L25

Cortese, L., Gavazzi, G., Boselli, A., Franzetti, P., Kennicutt, R., O’Neil, K., & Sakai, S. 2006, *A&A*, in press

Cortese, L., Gavazzi, G., Boselli, A., Iglesias-Paramo, J., & Carrasco, L. 2004, *A&A*, 425, 429

Cowie, L. L. & Songaila, A. 1977, *Nature*, 266, 501

Crowl, H. H., Kenney, J. D. P., van Gorkom, J. H., & Vollmer, B. 2005, *AJ*, 130, 65

Dale, D. A., Giovanelli, R., Haynes, M. P., Hardy, E., & Campusano, L. E. 2001, *AJ*, 121, 1886

Davies, R. D. & Lewis, B. M. 1973, *MNRAS*, 165, 231

de Lapparent, V., Geller, M. J., & Huchra, J. P. 1986, *ApJ*, 302, L1

De Propris, R., Colless, M., Driver, S. P., Couch, W., Peacock, J. A., Baldry, I. K., Baugh, C. M., Bland-Hawthorn, J., Bridges, T., Cannon, R., Cole, S., Collins, C., Cross, N., Dalton, G. B., Efstathiou, G., Ellis, R. S., Frenk, C. S., Glazebrook, K., Hawkins, E., Jackson, C., Lahav, O., Lewis, I., Lumsden, S., Maddox, S., Madgwick, D. S., Norberg, P., Percival, W., Peterson, B., Sutherland, W., & Taylor, K. 2003, *MNRAS*, 342, 725

De Propris, R., Colless, M., Peacock, J. A., Couch, W. J., Driver, S. P., Balogh, M. L., Baldry, I. K., Baugh, C. M., Bland-Hawthorn, J., Bridges, T., Cannon, R., Cole, S., Collins, C., Cross, N., Dalton, G., Efstathiou, G., Ellis, R. S., Frenk, C. S., Glazebrook, K., Hawkins, E., Jackson, C., Lahav, O., Lewis, I., Lumsden, S., Maddox, S., Madgwick, D., Norberg, P., Percival, W., Peterson, B. A., Sutherland, W., & Taylor, K. 2004, *MNRAS*, 351, 125

de Propris, R., Eisenhardt, P. R., Stanford, S. A., & Dickinson, M. 1998, *ApJ*, 503, L45

Desert, F.-X., Boulanger, F., & Puget, J. L. 1990, *A&A*, 237, 215

Diaferio, A., Kauffmann, G., Balogh, M. L., White, S. D. M., Schade, D., & Ellingson, E. 2001, *MNRAS*, 323, 999

Dickey, J. M. & Gavazzi, G. 1991, *ApJ*, 373, 347

Dopita, M. A., Kewley, L. J., Heisler, C. A., & Sutherland, R. S. 2000, *ApJ*, 542, 224

Doyon, R. & Joseph, R. D. 1989, *MNRAS*, 239, 347

Dressler, A. 1980, *ApJ*, 236, 351

—. 1984, *ARA&A*, 22, 185

—. 1986, *ApJ*, 301, 35

Dressler, A. 2004, in Clusters of Galaxies: Probes of Cosmological Structure and Galaxy Evolution, p207

Dressler, A., Oemler, A. J., Couch, W. J., Smail, I., Ellis, R. S., Barger, A., Butcher, H., Poggianti, B. M., & Sharples, R. M. 1997, *ApJ*, 490, 577

Dressler, A. & Sandage, A. 1983, *ApJ*, 265, 664

Dressler, A., Smail, I., Poggianti, B. M., Butcher, H., Couch, W. J., Ellis, R. S., & Oemler, A. J. 1999, *ApJS*, 122, 51

Driver, S. & De Propris, R. 2003, *Ap&SS*, 285, 175

Elmegreen, B. G. & Efremov, Y. N. 1997, *ApJ*, 480, 235

Elmegreen, D. M., Elmegreen, B. G., Chromey, F. R., & Fine, M. S. 2000, AJ, 120, 733

Elmegreen, D. M., Elmegreen, B. G., Frogel, J. A., Eskridge, P. B., Pogge, R. W., Gallagher, A., & Iams, J. 2002, AJ, 124, 777

Evrard, A. E. 1991, MNRAS, 248, 8P

Farouki, R. & Shapiro, S. L. 1980, ApJ, 241, 928

—. 1981, ApJ, 243, 32

Fasano, G., Poggianti, B. M., Couch, W. J., Bettoni, D., Kjærgaard, P., & Moles, M. 2000, ApJ, 542, 673

Franx, M. 2004, in Clusters of Galaxies: Probes of Cosmological Structure and Galaxy Evolution, 197–+

Fuchs, B. & von Linden, S. 1998, MNRAS, 294, 513

Fujita, Y. 1998, ApJ, 509, 587

—. 2004, PASJ, 56, 29

Fujita, Y. & Nagashima, M. 1999, ApJ, 516, 619

Gallego, J., Zamorano, J., Aragon-Salamanca, A., & Rego, M. 1995, ApJ, 455, L1

Gavazzi, G. 1987, ApJ, 320, 96

Gavazzi, G. 1988, in ASP Conf. Ser. 5: The Minnesota lectures on Clusters of Galaxies and Large-Scale Structure, 115–142

—. 1989, ApJ, 346, 59

—. 1993, ApJ, 419, 469

Gavazzi, G., Bonfanti, C., Sanvito, G., Boselli, A., & Scodéggi, M. 2002a, ApJ, 576, 135

Gavazzi, G. & Boselli, A. 1999, A&A, 343, 93

Gavazzi, G., Boselli, A., Cortese, L., Arosio, I., Gallazzi, A., Pedotti, P., & Carrasco, L. 2005a, A&A, in press

Gavazzi, G., Boselli, A., Donati, A., Franzetti, P., & Scodéggi, M. 2003a, A&A, 400, 451

Gavazzi, G., Boselli, A., & Kennicutt, R. 1991a, AJ, 101, 1207

Gavazzi, G., Boselli, A., Mayer, L., Iglesias-Paramo, J., Vílchez, J. M., & Carrasco, L. 2001a, ApJ, 563, L23

Gavazzi, G., Boselli, A., Pedotti, P., Gallazzi, A., & Carrasco, L. 2002b, *A&A*, 396, 449

Gavazzi, G., Boselli, A., Scoddeggi, M., Pierini, D., & Belsole, E. 1999, *MNRAS*, 304, 595

Gavazzi, G., Boselli, A., van Driel, W., & O’Neil, K. 2005b, *A&A*, 429, 439

Gavazzi, G., Boselli, A., Vílchez, J. M., Iglesias-Paramo, J., & Bonfanti, C. 2000a, *A&A*, 361, 1

Gavazzi, G., Catinella, B., Carrasco, L., Boselli, A., & Contursi, A. 1998, *AJ*, 115, 1745

Gavazzi, G., Contursi, A., Carrasco, L., Boselli, A., Kennicutt, R., Scoddeggi, M., & Jaffe, W. 1995, *A&A*, 304, 325

Gavazzi, G., Cortese, L., Boselli, A., Iglesias-Páramo, J., Vilchez, J. M., & Carrasco, L. 2003b, *ApJ*, 597, 210

Gavazzi, G., Franzetti, P., Scoddeggi, M., Boselli, A., & Pierini, D. 2000b, *A&A*, 361, 863

Gavazzi, G. & Jaffe, W. 1986, *ApJ*, 310, 53

—. 1987, *A&A*, 186, L1

Gavazzi, G., O’Neil, K., Boselli, A., & van Driel, W. 2005c, *A&A*, in press

Gavazzi, G., Pierini, D., & Boselli, A. 1996, *A&A*, 312, 397

Gavazzi, G. & Scoddeggi, M. 1996, *A&A*, 312, L29

Gavazzi, G., Scoddeggi, M., Boselli, A., & Trinchieri, G. 1991b, *ApJ*, 382, 19

Gavazzi, G., Zaccardo, A., Sanvito, G., Boselli, A., & Bonfanti, C. 2004, *A&A*, 417, 499

Gavazzi, G., Zibetti, S., Boselli, A., Franzetti, P., Scoddeggi, M., & Martocchi, S. 2001b, *A&A*, 372, 29

Geller, M. J. & Huchra, J. P. 1989, *Science*, 246, 897

Gioia, I. M., Gregorini, L., & Klein, U. 1982, *A&A*, 116, 164

Giovanelli, R. & Haynes, M. P. 1985, *ApJ*, 292, 404

Giovanelli, R., Haynes, M. P., & Kent, B. R. 2005a, *ArXiv Astrophysics e-prints*

Giovanelli, R., Haynes, M. P., Kent, B. R., Perillat, P., Saintonge, A., Brosch, N., Catinella, B., Hoffman, G. L., Stierwalt, S., Spekkens, K., Lerner, M. S., Masters, K. L., Momjian, E., Rosenberg, J. L., Springob, C. M., Boselli, A., Charmandaris, V., Darling, J. K., Davies, J., Lambas, D. G., Gavazzi, G., Giovanardi, C., Hardy, E., Hunt, L. K., Iovino, A., Karachentsev, I. D., Karachentseva, V. E., Koopmann, R. A., Marinoni, C., Minchin, R., Muller, E., Putman, M., Pantoja, C., Salzer, J. J., Scoddeggi, M., Skillman, E., Solanes, J. M., Valotto, C., van Driel, W., & van Zee, L. 2005b, *AJ*, 130, 2598

Girardi, M., Giuricin, G., Mardirossian, F., Mezzetti, M., & Boschin, W. 1998, *ApJ*, 505, 74

Gisler, G. R. 1980, *AJ*, 85, 623

Gnedin, O. Y. 2003, *ApJ*, 582, 141

Gomez, P. L., Nichol, R. C., Miller, C. J., Balogh, M. L., Goto, T., Zabludoff, A. I., Romer, A. K., Bernardi, M., Sheth, R., Hopkins, A. M., Castander, F. J., Connolly, A. J., Schneider, D. P., Brinkmann, J., Lamb, D. Q., SubbaRao, M., & York, D. G. 2003, *ApJ*, 584, 210

Goto, T., Okamura, S., Sekiguchi, M., Bernardi, M., Brinkmann, J., Gómez, P. L., Harvanek, M., Kleinman, S. J., Krzesinski, J., Long, D., Loveday, J., Miller, C. J., Neilsen, E. H., Newman, P. R., Nitta, A., Sheth, R. K., Snedden, S. A., & Yamauchi, C. 2003a, *PASJ*, 55, 757

Goto, T., Yamauchi, C., Fujita, Y., Okamura, S., Sekiguchi, M., Smail, I., Bernardi, M., & Gomez, P. L. 2003b, *MNRAS*, 346, 601

Gunn, J. E. & Gott, J. R. I. 1972, *ApJ*, 176, 1

Gursky, H., Solinger, A., Kellogg, E. M., Murray, S., Tananbaum, H., Giacconi, R., & Cavaliere, A. 1972, *ApJ*, 173, L99

Halliday, C., Milvang-Jensen, B., Poirier, S., Poggianti, B. M., Jablonka, P., Aragón-Salamanca, A., Saglia, R. P., De Lucia, G., Pelló, R., Simard, L., Clowe, D. I., Rudnick, G., Dalcanton, J. J., White, S. D. M., & Zaritsky, D. 2004, *A&A*, 427, 397

Haynes, M. P. & Giovanelli, R. 1984, *AJ*, 89, 758

Haynes, M. P., Giovanelli, R., & Chincarini, G. L. 1984, *ARA&A*, 22, 445

Haynes, M. P., Jore, K. P., Barrett, E. A., Broeils, A. H., & Murray, B. M. 2000, *AJ*, 120, 703

Henning, P. A., Sancisi, R., & McNamara, B. R. 1993, *A&A*, 268, 536

Henriksen, M. & Byrd, G. 1996, *ApJ*, 459, 82

Heyl, J., Colless, M., Ellis, R. S., & Broadhurst, T. 1997, *MNRAS*, 285, 613

Hinz, J. L., Rieke, G. H., & Caldwell, N. 2003, *AJ*, 126, 2622

Hoffman, G. L., Salpeter, E. E., Farhat, B., Roos, T., Williams, H., & Helou, G. 1996, *ApJS*, 105, 269

Hogg, D. W., Blanton, M. R., Eisenstein, D. J., Gunn, J. E., Schlegel, D. J., Zehavi, I., Bahcall, N. A., Brinkmann, J., Csabai, I., Schneider, D. P., Weinberg, D. H., & York, D. G. 2003, *ApJ*, 585, L5

Hollenbach, D. J., Werner, M. W., & Salpeter, E. E. 1971, *ApJ*, 163, 165

Huang, J.-S., Glazebrook, K., Cowie, L. L., & Tinney, C. 2003, *ApJ*, 584, 203

Hubble, E. & Humason, M. L. 1931, *ApJ*, 74, 43

Hummel, E., van der Hulst, J. M., Kennicutt, R. C., & Keel, W. C. 1990, *A&A*, 236, 333

Icke, V. 1985, *A&A*, 144, 115

Iglesias-Páramo, J., Boselli, A., Cortese, L., Vílchez, J. M., & Gavazzi, G. 2002, *A&A*, 384, 383

Iglesias-Páramo, J., Boselli, A., Gavazzi, G., Cortese, L., & Vílchez, J. M. 2003, *A&A*, 397, 421

Iglesias-Páramo, J., Boselli, A., Gavazzi, G., & Zaccardo, A. 2004, *A&A*, 421, 887

Iono, D., Yun, M. S., & Mihos, J. C. 2004, *ApJ*, 616, 199

Irwin, J. A. & Sarazin, C. L. 1996, *ApJ*, 471, 683

Jogee, S., Scoville, N., & Kenney, J. D. P. 2005, *ApJ*, 630, 837

Karachentseva, V. 1973, *Comm.Spec.Astrophys.Obs.*, 8, 1

Kashikawa, N., Sekiguchi, M., Doi, M., Komiya, Y., Okamura, S., Shimasaku, K., Yagi, M., & Yasuda, N. 1998, *ApJ*, 500, 750

Keel, W. C., Kennicutt, R. C., Hummel, E., & van der Hulst, J. M. 1985, *AJ*, 90, 708

Kenney, J. D. & Young, J. S. 1988a, *ApJS*, 66, 261

—. 1988b, *ApJ*, 326, 588

Kenney, J. D. P. & Koopmann, R. A. 1999, *AJ*, 117, 181

Kenney, J. D. P., Rubin, V. C., Planesas, P., & Young, J. S. 1995, *ApJ*, 438, 135

Kenney, J. D. P., van Gorkom, J. H., & Vollmer, B. 2004, *AJ*, 127, 3361

Kenney, J. D. P. & Yale, E. E. 2002, *ApJ*, 567, 865

Kenney, J. D. P. & Young, J. S. 1989, *ApJ*, 344, 171

Kennicutt, R. 1983a, *A&A*, 120, 219

Kennicutt, R. C. 1983b, *AJ*, 88, 483

—. 1998, *ARA&A*, 36, 189

Kennicutt, R. C., Roettiger, K. A., Keel, W. C., van der Hulst, J. M., & Hummel, E. 1987, *AJ*, 93, 1011

Klein, U. 1990, in ASSL Vol. 160: Windows on Galaxies, 157

Klein, U., Weiland, H., & Brinks, E. 1991, *A&A*, 246, 323

Knapen, J. H. 2005, *A&A*, 429, 141

Kobulnicky, H. A., Kennicutt, R. C., & Pizagno, J. L. 1999, *ApJ*, 514, 544

Kochanek, C. S., Pahre, M. A., Falco, E. E., Huchra, J. P., Mader, J., Jarrett, T. H., Chester, T., Cutri, R., & Schneider, S. E. 2001, *ApJ*, 560, 566

Kodama, T. & Smail, I. 2001, *MNRAS*, 326, 637

Kodama, T., Smail, I., Nakata, F., Okamura, S., & Bower, R. G. 2001, *ApJ*, 562, L9

Kodama, T., Tanaka, M., Tamura, T., Yahagi, H., Nagashima, M., Tanaka, I., Arimoto, N., Fumase, T., Iye, M., Karasawa, Y., Kashikawa, N., Kawasaki, W., Kitayama, T., Matsuhara, H., Nakata, F., Ohashi, T., Ohta, K., Okamoto, T., Okamura, S., Shimasaku, K., Suto, Y., Tamura, N., Umetsu, K., & Yamada, T. 2005, *PASJ*, 57, 309

Koopmann, R. A., Haynes, M. P., & Catinella, B. 2006, *AJ*, in press

Koopmann, R. A. & Kenney, J. D. P. 1998, *ApJ*, 497, L75

—. 2004a, *ApJ*, 613, 866

—. 2004b, *ApJ*, 613, 851

Lake, G., Katz, N., & Moore, B. 1998, *ApJ*, 495, 152

Larson, R. B., Tinsley, B. M., & Caldwell, C. N. 1980, *ApJ*, 237, 692

Lee, H., McCall, M. L., & Richer, M. G. 2003, *AJ*, 125, 2975

Lee, H., Richer, M. G., & McCall, M. L. 2000, *ApJ*, 530, L17

Lee, S. & Irwin, J. A. 1997, *ApJ*, 490, 247

Lequeux, J. 1971, *A&A*, 15, 42

Lewis, I., Balogh, M., De Propris, R., Couch, W., Bower, R., Offer, A., Bland-Hawthorn, J., Baldry, I. K., Baugh, C., Bridges, T., Cannon, R., Cole, S., Colless, M., Collins, C., Cross, N., Dalton, G., Driver, S. P., Efstathiou, G., Ellis, R. S., Frenk, C. S., Glazebrook, K., Hawkins, E., Jackson, C., Lahav, O., Lumsden, S., Maddox, S., Madgwick, D., Norberg, P., Peacock, J. A., Percival, W., Peterson, B. A., Sutherland, W., & Taylor, K. 2002, *MNRAS*, 334, 673

Lin, D. N. C. & Faber, S. M. 1983, *ApJ*, 266, L21

Madgwick, D. S., Lahav, O., Baldry, I. K., Baugh, C. M., Bland-Hawthorn, J., Bridges, T., Cannon, R., Cole, S., Colless, M., Collins, C., Couch, W., Dalton, G., De Propris, R., Driver, S. P., Efstathiou, G., Ellis, R. S., Frenk, C. S., Glazebrook, K., Jackson, C., Lewis, I., Lumsden, S., Maddox, S., Norberg, P., Peacock, J. A., Peterson, B. A., Sutherland, W., & Taylor, K. 2002, MNRAS, 333, 133

Makino, J. & Hut, P. 1997, ApJ, 481, 83

Marcolini, A., Brighenti, F., & D’Ercole, A. 2003, MNRAS, 345, 1329

Marzke, R. O., da Costa, L. N., Pellegrini, P. S., Willmer, C. N. A., & Geller, M. J. 1998, ApJ, 503, 617

McNamara, B. R., Sancisi, R., Henning, P. A., & Junor, W. 1994, AJ, 108, 844

Merritt, D. 1983, ApJ, 264, 24

—. 1984, ApJ, 276, 26

Metcalfe, L., Fadda, D., & Biviano, A. 2005, ArXiv Astrophysics e-prints

Mihos, J. C. 2004, in Clusters of Galaxies: Probes of Cosmological Structure and Galaxy Evolution, p278

Mihos, J. C., Richstone, D. O., & Bothun, G. D. 1992, ApJ, 400, 153

Miley, G. K., Perola, G. C., van der Kruit, P. C., & van der Laan, H. 1972, Nature, 237, 269

Miller, R. H. 1986, A&A, 167, 41

Mobasher, B. & Trentham, N. 1998, MNRAS, 293, 315

Mohr, J. J., Mathiesen, B., & Evrard, A. E. 1999, ApJ, 517, 627

Moore, B., Katz, N., Lake, G., Dressler, A., & Oemler, A. 1996, Nature, 379, 613

Moore, B., Lake, G., & Katz, N. 1998, ApJ, 495, 139

Moore, B., Lake, G., Quinn, T., & Stadel, J. 1999, MNRAS, 304, 465

Mori, M. & Burkert, A. 2000, ApJ, 538, 559

Moss, C. & Whittle, M. 2000, MNRAS, 317, 667

Moss, C., Whittle, M., & Pesce, J. E. 1998, MNRAS, 300, 205

Murakami, I. & Babul, A. 1999, MNRAS, 309, 161

Neistein, E., Maoz, D., Rix, H., & Tonry, J. L. 1999, AJ, 117, 2666

Nichol, R. C. 2004, in Clusters of Galaxies: Probes of Cosmological Structure and Galaxy Evolution, p24

Niklas, S., Klein, U., & Wielebinski, R. 1995, A&A, 293, 56

Nolan, L. A. 2004, in Clusters of Galaxies: Probes of Cosmological Structure and Galaxy Evolution

Nulsen, P. E. J. 1982, MNRAS, 198, 1007

Nulsen, P. E. J. & Carter, D. 1987, MNRAS, 225, 939

O'Connell, R. W. 1999, ARA&A, 37, 603

Okamoto, T. & Nagashima, M. 2001, ApJ, 547, 109

—. 2003, ApJ, 587, 500

Oosterloo, T. & van Gorkom, J. 2005, A&A, 437, L19

Osterbrock, D. E. 1989, Astrophysics of gaseous nebulae and active galactic nuclei (Research supported by the University of California, John Simon Guggenheim Memorial Foundation, University of Minnesota, et al. Mill Valley, CA, University Science Books, 1989, 422 p.)

Paolillo, M., Andreon, S., Longo, G., Puddu, E., Gal, R. R., Scaramella, R., Djorgovski, S. G., & de Carvalho, R. 2001, A&A, 367, 59

Patterson, R. J. & Thuan, T. X. 1992, ApJ, 400, L55

Phookun, B. & Mundy, L. G. 1995, ApJ, 453, 154

Pilyugin, L. S., Mollá, M., Ferrini, F., & Vílchez, J. M. 2002, A&A, 383, 14

Poggianti, B. M. & Barbaro, G. 1996, A&A, 314, 379

Poggianti, B. M., Bridges, T. J., Carter, D., Mobasher, B., Doi, M., Iye, M., Kashikawa, N., Komiyama, Y., Okamura, S., Sekiguchi, M., Shimasaku, K., Yagi, M., & Yasuda, N. 2001a, ApJ, 563, 118

Poggianti, B. M., Bridges, T. J., Komiyama, Y., Yagi, M., Carter, D., Mobasher, B., Okamura, S., & Kashikawa, N. 2004, ApJ, 601, 197

Poggianti, B. M., Bridges, T. J., Mobasher, B., Carter, D., Doi, M., Iye, M., Kashikawa, N., Komiyama, Y., Okamura, S., Sekiguchi, M., Shimasaku, K., Yagi, M., & Yasuda, N. 2001b, ApJ, 562, 689

Postman, M. & Geller, M. J. 1984, ApJ, 281, 95

Postman, M., Lubin, L. M., Gunn, J. E., Oke, J. B., Hoessel, J. G., Schneider, D. P., & Christensen, J. A. 1996, AJ, 111, 615

Quilis, V., Moore, B., & Bower, R. 2000, *Science*, 288, 1617

Rangarajan, F. V. N., White, D. A., Ebeling, H., & Fabian, A. C. 1995, *MNRAS*, 277, 1047

Rengarajan, T. N. & Iyengar, K. V. K. 1992, *MNRAS*, 259, 559

Rengarajan, T. N., Karnik, A. D., & Iyengar, K. V. K. 1997, *MNRAS*, 290, 1

Richstone, D. O. 1976, *ApJ*, 204, 642

Rines, K., Geller, M. J., Kurtz, M. J., & Diaferio, A. 2003, *AJ*, 126, 2152

Robinson, B. J. & Koehler, J. A. 1965, *Nature*, 208, 993

Rubin, V. C., Ford, W. K. J., & Whitmore, B. C. 1988, *ApJ*, 333, 522

Rubin, V. C., Waterman, A. H., & Kenney, J. D. P. 1999, *AJ*, 118, 236

Rybicki, G. B. & Lightman, A. P. 1979, *Radiative processes in astrophysics* (New York, Wiley-Interscience, 1979. 393 p.)

Sabatini, S., Davies, J., van Driel, W., Baes, M., Roberts, S., Smith, R., Linder, S., & O’Neil, K. 2005, *MNRAS*, 357, 819

Sakai, S., Kennicutt, R. C., van der Hulst, J. M., & Moss, C. 2002, *ApJ*, 578, 842

Salpeter, E. E. & Hoffman, G. L. 1996, *ApJ*, 465, 595

Sandage, A., Binggeli, B., & Tammann, G. A. 1985, *AJ*, 90, 1759

Sarazin, C. L. 1986, *Reviews of Modern Physics*, 58, 1

Sauty, S., Casoli, F., Boselli, A., Gerin, M., Lequeux, J., Braine, J., Gavazzi, G., Dickey, J., Kazes, I., & Fouque, P. 2003, *A&A*, 411, 381

Schechter, P. 1976, *ApJ*, 203, 297

Schindler, S., Binggeli, B., & Böhringer, H. 1999, *A&A*, 343, 420

Schulz, S. & Struck, C. 2001, *MNRAS*, 328, 185

Scodéglio, M., Gavazzi, G., Franzetti, P., Boselli, A., Zibetti, S., & Pierini, D. 2002a, *A&A*, 384, 812

—. 2002b, *A&A*, 384, 812

Sellwood, J. A. & Carlberg, R. G. 1984, *ApJ*, 282, 61

Skillman, E. D., Kennicutt, R. C., Shields, G. A., & Zaritsky, D. 1996, *ApJ*, 462, 147

Sofue, Y. & Wakamatsu, K. 1993, A&A, 273, 79

Soifer, B. T., Neugebauer, G., & Houck, J. R. 1987, ARA&A, 25, 187

Solanes, J. M., Manrique, A., García-Gómez, C., González-Casado, G., Giovanelli, R., & Haynes, M. P. 2001, ApJ, 548, 97

Solanes, J. M., Sanchis, T., Salvador-Solé, E., Giovanelli, R., & Haynes, M. P. 2002, AJ, 124, 2440

Somerville, R. S. & Primack, J. R. 1999, MNRAS, 310, 1087

Sparks, W. B., Ford, H. C., & Kinney, A. L. 1993, ApJ, 413, 531

Spitzer, L. J. & Baade, W. 1951, ApJ, 113, 413

Springel, V., White, S. D. M., Tormen, G., & Kauffmann, G. 2001, MNRAS, 328, 726

Springob, C. M., Haynes, M. P., & Giovanelli, R. 2005, ApJ, 621, 215

Stark, A. A., Knapp, G. R., Bally, J., Wilson, R. W., Penzias, A. A., & Rowe, H. E. 1986, ApJ, 310, 660

Stevens, I. R., Acreman, D. M., & Ponman, T. J. 1999, MNRAS, 310, 663

Struble, M. F. & Rood, H. J. 1991, ApJS, 77, 363

Sullivan, M., Treyer, M. A., Ellis, R. S., Bridges, T. J., Milliard, B., & Donas, J. 2000, MNRAS, 312, 442

Sun, M. & Vikhlinin, A. 2005, ApJ, 621, 718

Tanaka, M., Goto, T., Okamura, S., Shimasaku, K., & Brinkmann, J. 2004, AJ, 128, 2677

Thompson, L. A. 1981, ApJ, 244, L43

Thuan, T. X., Alimi, J., Gott, J. R. I., & Schneider, S. E. 1991, ApJ, 370, 25

Tosa, M. 1994, ApJ, 426, L81

Trentham, N. & Hodgkin, S. 2002, MNRAS, 333, 423

Trentham, N., Sampson, L., & Banerji, M. 2005, MNRAS, 357, 783

Treu, T. 2004, in Clusters of Galaxies: Probes of Cosmological Structure and Galaxy Evolution, 178–+

Treu, T., Ellis, R. S., Kneib, J.-P., Dressler, A., Smail, I., Czoske, O., Oemler, A., & Natarajan, P. 2003, ApJ, 591, 53

Tuffs, R. J., Popescu, C. C., Pierini, D., Völk, H. J., Hippelein, H., Leech, K., Metcalfe, L., Heinrichsen, I., & Xu, C. 2002, *ApJS*, 139, 37

Tully, R. B. & Shaya, E. J. 1984, *ApJ*, 281, 31

Völk, H. J. & Xu, C. 1994, *Infrared Physics Technology*, 35, 527

Valluri, M. 1993, *ApJ*, 408, 57

—. 1994, *ApJ*, 430, 101

Valluri, M. & Jog, C. J. 1990, *ApJ*, 357, 367

van den Bergh, S. 1976, *ApJ*, 206, 883

van Dokkum, P. G., Franx, M., Fabricant, D., Illingworth, G. D., & Kelson, D. D. 2000, *ApJ*, 541, 95

van Gorkom, J. H. 2004, in *Clusters of Galaxies: Probes of Cosmological Structure and Galaxy Evolution*, p306

van Zee, L., Barton, E. J., & Skillman, E. D. 2004a, *AJ*, 128, 2797

van Zee, L., Salzer, J. J., Haynes, M. P., O'Donoghue, A. A., & Balonek, T. J. 1998, *AJ*, 116, 2805

van Zee, L., Skillman, E. D., & Haynes, M. P. 2004b, *AJ*, 128, 121

Veilleux, S., Bland-Hawthorn, J., Cecil, G., Tully, R. B., & Miller, S. T. 1999, *ApJ*, 520, 111

Vikhlinin, A., Forman, W., & Jones, C. 1997, *ApJ*, 474, L7

Vilchez, J. M. 1995, *AJ*, 110, 1090

Vogt, N. P., Haynes, M. P., Giovanelli, R., & Herter, T. 2004, *AJ*, 127, 3300

Vollmer, B. 2003, *A&A*, 398, 525

Vollmer, B., Balkowski, C., Cayatte, V., van Driel, W., & Huchtmeyer, W. 2004a, *A&A*, 419, 35

Vollmer, B., Beck, R., Kenney, J. D. P., & van Gorkom, J. H. 2004b, *AJ*, 127, 3375

Vollmer, B., Braine, J., Balkowski, C., Cayatte, V., & Duschl, W. J. 2001a, *A&A*, 374, 824

Vollmer, B., Braine, J., Combes, F., & Sofue, Y. 2005, *A&A*, 441, 473

Vollmer, B., Cayatte, V., Balkowski, C., & Duschl, W. J. 2001b, *ApJ*, 561, 708

Vollmer, B., Cayatte, V., Boselli, A., Balkowski, C., & Duschl, W. J. 1999, *A&A*, 349, 411

Vollmer, B., Marcelin, M., Amram, P., Balkowski, C., Cayatte, V., & Garrido, O. 2000, A&A, 364, 532

Warmels, R. H. 1988, A&AS, 72, 427

White, D. A., Fabian, A. C., Forman, W., Jones, C., & Stern, C. 1991, ApJ, 375, 35

White, S. D. M., Briel, U. G., & Henry, J. P. 1993, MNRAS, 261, L8

Whitmore, B. C., Forbes, D. A., & Rubin, V. C. 1988, ApJ, 333, 542

Whitmore, B. C., Gilmore, D. M., & Jones, C. 1993, ApJ, 407, 489

Worthey, G. 1994, ApJS, 95, 107

Wyder, T. K., Treyer, M. A., Milliard, B., Schiminovich, D., Arnouts, S., Budavári, T., Barlow, T. A., Bianchi, L., Byun, Y.-I., Donas, J., Forster, K., Friedman, P. G., Heckman, T. M., Jelinsky, P. N., Lee, Y.-W., Madore, B. F., Malina, R. F., Martin, D. C., Morrissey, P., Neff, S. G., Rich, R. M., Siegmund, O. H. W., Small, T., Szalay, A. S., & Welsh, B. Y. 2005, ApJ, 619, L15

Yagi, M., Kashikawa, N., Sekiguchi, M., Doi, M., Yasuda, N., Shimasaku, K., & Okamura, S. 2002, AJ, 123, 87

Yee, H. K. C., Ellingson, E., & Carlberg, R. G. 1996, ApJS, 102, 269

Yoshida, M., Ohyama, Y., Iye, M., Aoki, K., Kashikawa, N., Sasaki, T., Shimasaku, K., Yagi, M., Okamura, S., Doi, M., Furusawa, H., Hamabe, M., Kimura, M., Komiyama, Y., Miyazaki, M., Miyazaki, S., Nakata, F., Ouchi, M., Sekiguchi, M., & Yasuda, N. 2004, AJ, 127, 90

Zwicky, F., Herzog, E., & Wild, P. 1968, Catalogue of galaxies and of clusters of galaxies (Pasadena: California Institute of Technology (CIT), 1961-1968)